STUDIES OF THE QUINONE BINDING SITES OF THE 'ESCHERICHIA COLI' TERMINAL OXIDASES, CYTOCHROMES BO_3 & BD

Stuart Fairbairn Hastings

A Thesis Submitted for the Degree of PhD
at the
University of St Andrews

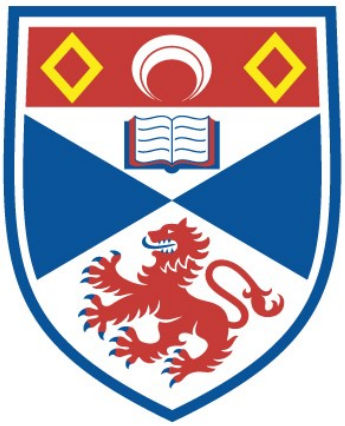

1997

STUDIES OF THE QUINONE BINDING SITES OF THE *ESCHERICHIA COLI* TERMINAL OXIDASES, CYTOCHROMES bo_3 & bd

Stuart Fairbairn Hastings

Ph.D.

Submitted 29th May 1997

Declaration

I, Stuart Fairbairn Hastings, hereby certify that this thesis, which is approximately 40,000 words in length, has been written by me, that it is the record of work carried out by me and that it has not been submitted in any previous application for a higher degree.

date 29/5/97 signature of candidate .....

I was admitted as a research student in October 1993 and as a candidate for the degree of Ph.D. in October 1994; the higher study for which this is a record was carried out in the University of St Andrews between 1993 and 1997.

date 29/5/97 signature of candidate .....

Certificate

I hereby certify that the candidate, Stuart F. Hastings, has fulfilled the conditions of the Resolution and Regulations appropriate for the degree of Ph.D. in the University of St. Andrews and that the candidate is qualified to submit this thesis in application for that degree.

Date 29/5/97 Signature of supervisor .....

Copyright Declaration

In submitting this thesis to the University of St.Andrews I understand that I am giving permission for it to be made available for use in accordance with the regulations of the University Library for the time being in force, subject to any copyright vested in the work not being affected thereby. I also understand that the title and abstract will be published and that a copy of the work be made and supplied to any bona fide library or research worker.

date 29/5/12... signature of candidate .....

Acknowledgements

I would like to thank firstly my supervisor Dr. John Ingledew for his help, guidance and understanding throughout both my undergraduate and postgraduate years at St. Andrews. In addition, thanks are due to the following people, Dr. Dominic Hunter and Alex Houston for the useful discussions and technical assistance respectively; Prof. Robert Gennis and and his research group at the University of Illinois for allowing me the opportunity to visit and learn useful skills, special thanks are due to Andromachi Katsonouri for her assistance with the mutagenesis experiments. Also Dr. Stephen Rigby and Dr. Peter Heathcote, for their invalubable expertise and help with the ENDOR and ESEEM experiments.

Finally, I wish to thank my family and friends who have supported and encouraged me throughout the last eight years, I could not have done this without them. This thesis is dedicated to my grandfather, Adam Fairbairn.

Abstract

The structure and function relationships involved in the binding of quinones to the terminal oxidases of *Escherichia coli*, cytochromes *bd* and bo_3, were investigated using redox potentiometery, site-directed mutagenesis and magnetic resonance techniques.

A stable semiquinone was identified as an intermediate of quinol oxidation by cytochrome *bd* in appropriately poised samples of both the membrane-bound and purified enzyme reconstituted with excess ubi- and menaquinone analogues. The effects of the inhibitors HOQNO and aurachin D on semiquinone formation were assessed.

The potentiometric behaviour of the semiquinone stabilised by membrane-bound and purified cytochrome bo_3 reconstituted with excess quinone analogues was characterised. The effects of two cytochrome bo_3 subunit II mutations and the inhibitor tridecylstigmatellin were studied. The data presented is consistent with the presence of one quinone binding site.

The hyperfine splittings present in the ESR spectrum of the cytochrome bo_3 semiquinone were resolved by ENDOR spectroscopy. The resultant electronic structure of the bound semiquinone and the nature of the hydrogen bonding to the protein is described. ESEEM spectroscopy was used to identify a nitrogen nucleus hydrogen bonded to the semiquinone. A model of this quinone binding site and a possible location is presented.

CONTENTS

List of Figures

List of Tables

Abbreviations

A	hyperfine coupling constant
AMPSO	3-[(1,1-dimethyl-2-hydroxyethyl)amino]-2-hydroxy-propane sulphonic acid
bis-tris-propane	bis(2-hydroxyethyl)-2-aminoethane sulphonic acid
cyd	cytochrome *bd* operon
cyo	cytochrome bo_3 operon
DPPH	1,1-diphenyl-2-picrylhdrazyl
DQ	duroquinone
E_1	midpoint potential of quinone/semiquinone couple
E_2	midpoint potential of semiquinone/quinol couple
E_h	ambient redox potential
E_m	midpoint potential
ENDOR	electron nuclear double resonance
ESEEM	electron spin echo envelope modulation
ESR	electron spin resonance
hfc	hyperfine coupling
HOQNO	2-n-heptyl-4-hydroxyquinoline *N* oxide
MQ	menaquinone/phylloquinone/vitamin K_1
mT	milli Telsa
NQR	nuclear quadrapolar resonance
pD	-log10 [deuterium ions]
PQ	plastoquinone
Q	quinone
$Q^{\cdot-}$	semiquinone

Q_{bd}	quinone binding site of the cytochrome *bd* complex
Q_{bo}	quinone binding site of the cytochrome bo_3 complex
QH-	semiquinone anion
QH·	protonated semiquinone
QH_2	quinol
SOMO	singly occupied molecular orbital
TDS	tridecylstigmatellin
TMPD	tetramethylphenylenediamine
TSS	transformation and storage solution
UQ	ubiquinone
USE	unique site elimination

1.0 INTRODUCTION

1.1 Scope of Review

Quinone binding sites are found in many photosynthetic and respiratory chains that use quinones as electron carriers. They often act as transformers between one-electron and two-electron processes. With the exception of one mini-review (Rich, 1996) there have been no recent reviews that deal specifically with quinone binding sites. Therefore a large portion of this introduction is devoted to recent advances in determining the structure and functional relationships involved in the interaction of quinones with proteins. The quinone binding sites associated with the *E. coli* terminal oxidases, the subjects of this study, are dealt with in individual sections and in relation to these enzyme complexes.

The extensive reviews of the cytochrome bo_3 complex (Ingledew & Poole, 1984; Poole & Ingledew, 1987; Anraku & Gennis, 1987) are brought up to date and with particular emphasis directed at its position in the haem-copper respiratory oxidase superfamily. This relationship has added importance with the recent publication of the crystal structures of two cytochrome *c* oxidases and these are compared and contrasted with the cytochrome bo_3 complex (Iwata *et al.*, 1995; Tsukihara *et al.*, 1996).

The cytochrome *bd* complex was the subject of a recent review by Borisov, 1996. This placed particular emphasis on the ligand binding properties of the oxidase therefore a repetition of this material is not required. Instead, recent literature on the structure and function of cytochrome *bd* from *E. coli* is reviewed.

1.2 General Introduction

All life on earth, be it animal, plant, prokaryotic or eukaryotic is sustained by the efficient use of energy to drive the primary cellular processes. Lying at the heart of this energy transduction is a group of predominantly membrane-bound enzyme complexes containing redox active metal centres, separated spatially and thermodynamically and linked by mobile electron carriers, to form a respiratory chain. The passage of low potential electrons from the primary energy source along this chain is coupled to the translocation of protons across the membrane thus generating a proton electrochemical gradient, $\Delta\mu H^+$, which forms the basis of Mitchell's chemiosmotic theory. This gradient or proton-motive force is used to drive cellular processes such as ATP synthesis and the active transport of metabolites.

Respiratory chains vary greatly in their length and composition. The mitochondrial respiratory chain is perhaps the most studied and best understood. It consists of more than twenty discrete components grouped together into four enzyme complexes (I to IV). Bacterial respiratory chains tend to be more varied but with components normally simpler than their mitochondrial counterparts. This variation is largely the result of bacteria being able to grow on a number of different substrates and in different environments. In response to this bacterial respiratory chains are often branched or capable of branching in order to maximise the efficiency of use of the substrates and oxidants available.

Present in all respiratory chains are a group of highly non-polar electron carriers known as quinones. These relatively simple

molecules act as the major mobile link between the respiratory chain components and due to their hydrophobic nature are found in between the membranes lipid bilayer. Each respiratory chain complex has specific sites which can bind and either reduce or oxidise quinone and which should share common structural features. *E. coli* is no exception and is the bacterium of choice in this study because of its ease of growth and genetic manipulation but primarily because of the wealth of information available on it from studies into energy transduction by other researchers.

1.3 The Respiratory Chain of *Escherichia coli.*

Escherichia coli is a gram-negative bacterium which can draw on a large repertoire of enzyme complexes to make up its respiratory chain depending on its growth conditions (Ingledew & Poole, 1984; Poole & Ingledew, 1987). Commonly found living in the anaerobic environment of the gastro-intestinal tract it is equally capable of subsistence in aerobic conditions exploiting the available reduced substrates and altering the respiratory chain in response to environmental changes. It should also be noted that *E. coli* can also use fermentable carbon sources in substrate phosphorylation reactions, therefore a functional respiratory chain is not an obligatory requirement for growth.

At its simplest the aerobic respiratory chain of *E. coli* would consist of a primary dehydrogenase linked via a mobile electron carrier, which under aerobic conditions is ubiquinol-8, to an oxidase complex. Practically, the respiratory chain is branched, a common feature of bacterial respiratory systems, with several dehydrogenases and two terminal oxidases. The anaerobic

respiratory chain is terminated by fumarate and nitrate reductases and also several other less utilised reductases, figure 1.1.

The two terminal oxidases, cytochrome bo_3 and cytochrome *bd*, are the major topics of this research project. Each will be dealt with individually and in greater detail later in the text. It would be useful however, at this point to give a brief introduction to both oxidases.

1.4 The Terminal Oxidases of *Escherichia coli.*

Cytochrome bo_3 and cytochrome *bd* both catalyse the direct oxidation of ubiquinol-8 within the bacterial membrane and the reduction of dioxygen to water (Anraku & Gennis 1987; Poole,1988). This is achieved by transferring electrons from ubiquinol through a number of metal centres to the site of dioxygen reduction on the cytoplasmic side of the membrane. Turnover of either oxidase leads to the establishment of a proton electrochemical gradient across the membrane. Cytochrome bo_3 in addition to this proton translocation, unlike cytochrome *bd*, is an active proton pump giving an overall stoichiometery of $4H^+/2e^-$, figure 1.2.

Synthesis of cytochrome bo_3 is induced under conditions of high aeration and conversely cytochrome *bd* synthesis is induced by low aeration (Rice & Hempfling, 1978; Kranz & Gennis, 1983). The affinity of cytochrome *bd* for dioxygen is much greater than that of cytochrome bo_3 and maintains efficient energy conservation under microaerobic conditions and possibly has an additional role in the protection of oxygen sensitive anaerobic enzymes (Anraku & Gennis, 1987; D'Mello *et al.*, 1995; 1996). Therefore, by regulating

Figure 1.1 The respiratory chain of *E. coli*

The major dehydrogenase complexes are displayed on the left and the major oxidase complexes on the right. The quinones menaquinone-8 and ubiquinone-8 act as the mobile electron-transporting link between the two. Ubiquinone predominates under aerobic growth conditions with menaquinone levels increasing towards anaerobosis. Each complex may contain a number of individual redox components (e.g. cytochromes, flavins or iron-sulphur centres). Levels of each complex within the *E. coli* membrane are determined by growth conditions.

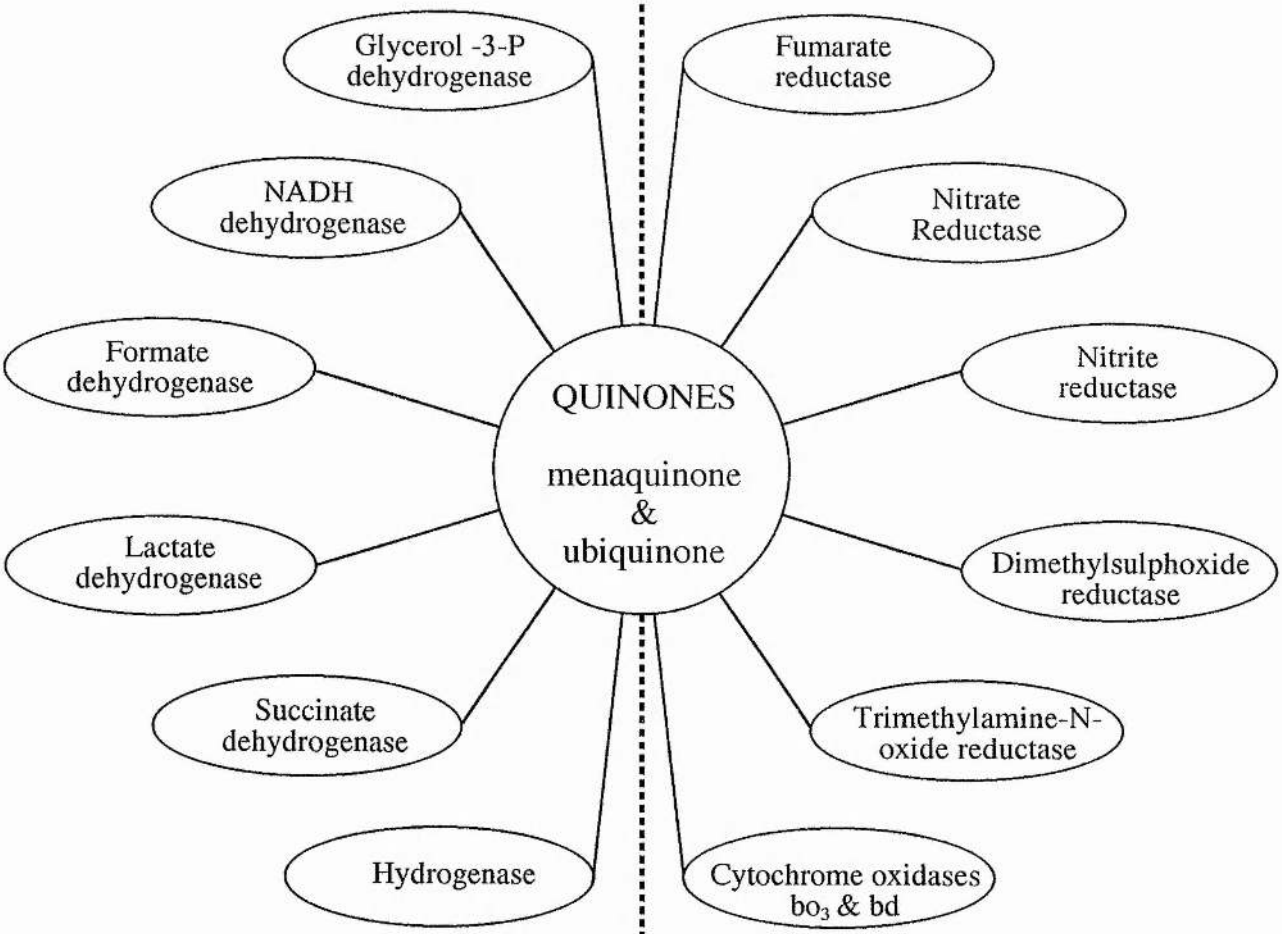
QUINONES
menaquinone
&
ubiquinone
Glycerol -3-P dehydrogenase
NADH dehydrogenase
Formate dehydrogenase
Lactate dehydrogenase
Succinate dehydrogenase
Hydrogenase
Fumarate reductase
Nitrate Reductase
Nitrite reductase
Dimethylsulphoxide reductase
Trimethylamine-N-oxide reductase
Cytochrome oxidases bo_3 & bd

Figure 1.2 The terminal oxidases of *E. coli*

Both cytochromes *bd* and bo_3 oxidise ubiquinol and transfer the released electrons through a set of metal centres to the oxygen binding site where oxygen is reduced to water. (a) Electron transfer through cytochrome *bd* proceeds from ubiquinol → haem b_{558} → haem b_{595} → haem *d* → H_2O. (b) Electron transfer through cytochrome bo_3 proceeds from ubiquinol → haem b_{562} → haem o:Cu_B → H_2O. Both oxidation reactions release two protons into the matrix. Cytochrome bo_3 also actively pumps two protons. The subunits indicated are represented according to projected structures from hydropathy profiles (Green *et al.*, 1988.)

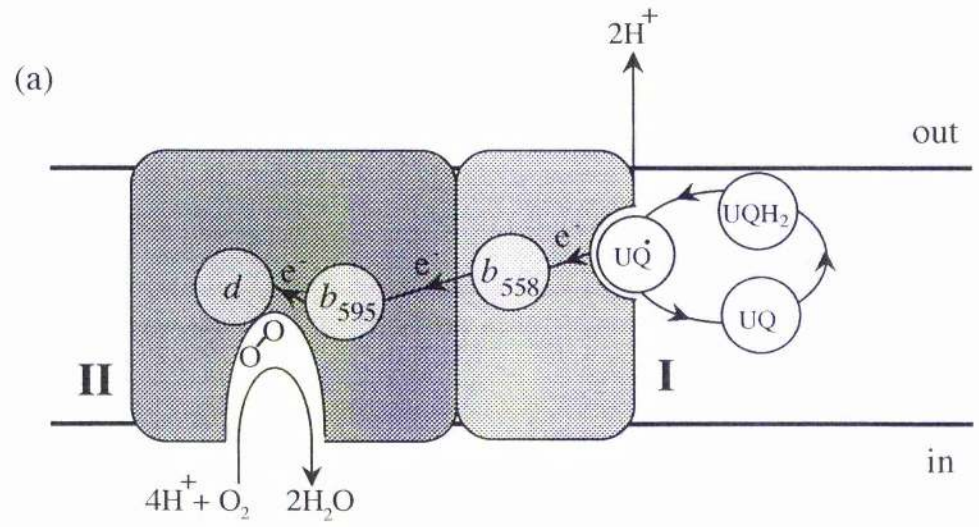
(a)
2H+
out
UQH2
UQ
UQ
e-
e-
e-
d
b595
b558
O
O
II
I
in
4H+ + O2
2H2O

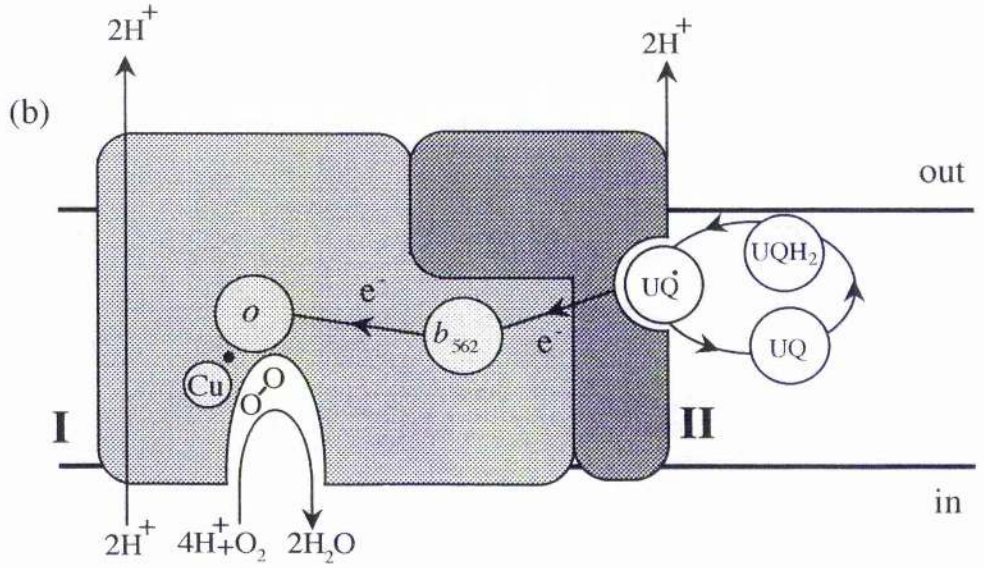
(b)
2H+
2H+
out
UQH2
UQ
UQ
e-
e-
o
b562
Cu
O
O
I
II
in
2H+
4H+ + O2
2H2O

the levels of each oxidase, *E. coli* has the ability to grow under a broad range of oxygen tensions. Each oxidase will be reviewed individually in the forthcoming sections.

1.5 Quinones and Quinone Binding Sites.

Biological quinones are substituted *p*-benzoquinones or *p*-napthoquinones with a long hydrophobic side chain of repeating isoprenoid units. There are three basic types, ubiquinone found in mitochondria and aerobically grown bacteria, menaquinone found in anaerobically grown bacteria (Figure 1.3) and plastoquinone found in chloroplasts. Each undergoes a $2H^+/2e^-$ reduction to the corresponding quinol. Electron spin resonance spectroscopy (ESR)[1] has shown that this reduction proceeds through a semiquinone intermediate (Rich, 1982).

The low fractional turnover of quinone relative to other respiratory chain components led to it being assigned to a side pathway. However, Kröger & Klingenberg, 1973 realised that the large excess of quinone in comparison to other respiratory chain components was sufficient to designate quinones as having an integral part in the respiratory pathway, acting as a mobile membrane-bound carrier of reducing equivalents between dehydrogenases and adjacent respiratory complexes. Subsequently, Mitchell, 1976, formulated a more complex role for quinones in association with the cytochrome bc_1 (complex III or ubiquinone:cytochrome *c* oxidoreductase) in the "protonmotive Q-

[1]The term Electron Spin Resonance (ESR) by convention is preferred when applied to unpaired electrons in free radical systems eg. semiquinones. When dealing with unpaired electrons in metal centeres the term Electron Paramagnetic Resonance (EPR) is applied.

Figure 1.3 The structures of ubi-quinone-8 and menaquinone-8.

(a) Ubiquinone and (b) menaquinone are substituted *p*-benzoquinones and *p*-napthoquinones respectively. Each has a large hydrophobic side chain at C-3 of repeating isoprenoid units, R, ($R=-CH_2-CH=C(CH_3)-CH_2)_nH$. The number of isoprenoid units (*n*) varies with and within species, in *E. coli* $n=8$ in mammalian mitochondria $n=10$.

(a)

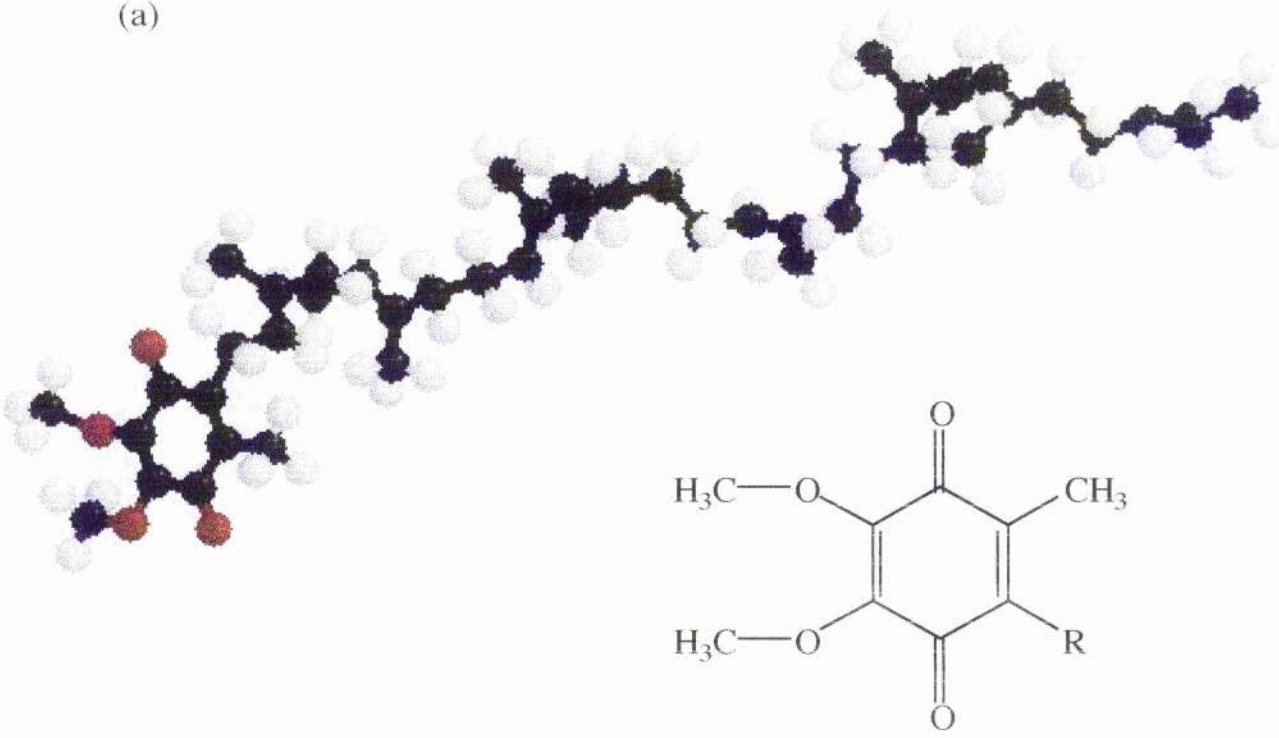

(b)

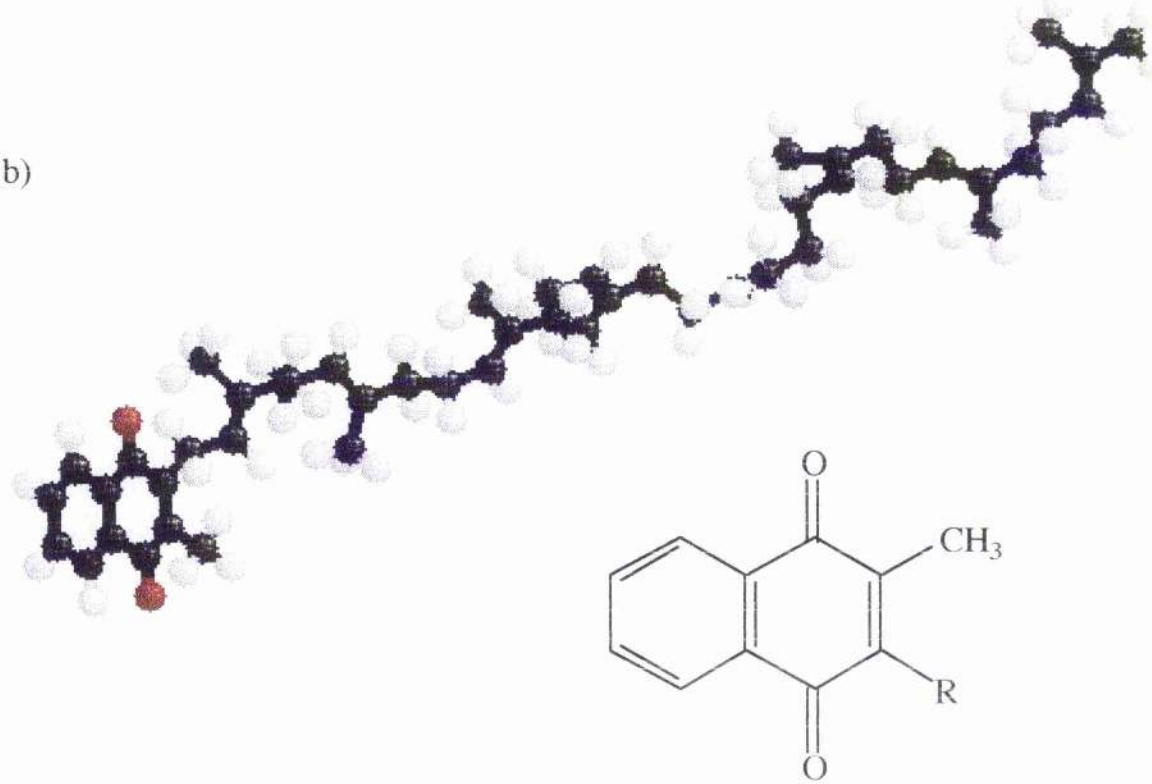

cycle" where vectorial movement of ubiquinone and ubiquinol across the membrane leads to the generation of a proton gradient for use in energy transduction at certain coupling sites of the respiratory chain (for recent review see Brandt & Trumpower, 1994).

The respiratory chain of *E. coli* is much simpler lacking the cytochrome bc_1 complex, a cytochrome *c* and consequently a cytochrome c oxidase. This simplification is achieved by the presence of the ubiquinol oxidases, cytochrome bo_3 and cytochrome *bd*, which results in a situation that can be explained by evoking a simple quinol loop where quinone is reduced by a dehydrogenase and oxidised by a terminal cytochrome oxidase. The penalty for the simplification is the translocation of fewer protons which results in the production of less ATP.

Quinone binding sites fulfil a fundamental role in respiratory systems and as a result are therefore the sites of action of numerous pesticides, herbicides and antibiotics (reviewed in Hoefnagel *et al.*, 1996; Rich, 1996). In addition abnormalities in quinone binding sites of human mitochondrial respiratory complexes can lead to the establishment of a disease state. One example of such a mitochondrial disorder, or collectively a mitochondrial myopathy, is Leber's Hereditary Optic Neuropathy (LHON), maternally inherited and clinically characterised by a rapid loss of central vision occurring predominantly in juvenile males (Delgi Esposti *et al.*, 1994). LHON is caused by a point mutation in mitochondrial DNA which results in the substitution of certain amino acid residues at the quinone binding site of NADH dehydrogenase (Complex I).

These substitutions destabilise the ubisemiquinone intermediate formed in quinone reduction, thus impairing electron transport and ultimately cellular respiration. The destabilised semiquinone is also thought to contribute further to mitochondrial damage by reacting directly with molecular oxygen and produce harmful free radicals. Ubiquinone has also been reported recently to have several functions in mammalian organisms outwith the respiratory chain and is known to have antioxidant properties in the reduced quinol form, (for review see Ernster & Dallner, 1995).

Quinone binding sites fall into three categories, acceptor (reduction) sites, donor (oxidation) sites, or pair-splitting sites (see Table 1.1). At acceptor sites a quinone molecule receives two electrons from its immediate donor, often a metal centre, in two one electron transfers which proceed through a semiquinone, converting it to the quinol form. The opposite occurs at a donor site where a quinol molecule is oxidised in two one-electron transfers again proceeding through the semiquinone state, with both electrons going to the same acceptor. At a pair splitting site, electron transfer from a quinol occurs in two one-electron steps but these go to two discrete acceptors, separated both spatially and thermodynamically.

The reduction and oxidation reactions of quinones that occur at acceptor and donor sites proceed through the free radical semiquinone state. Most free biological semiquinones are highly unstable with stability constants at neutral pH of approximately 1×10^{-10} (Mitchell, 1976). Therefore, quinone redox reactions would be unlikely to occur unless the semiquinone state is stabilised. Donor and acceptor quinone binding sites serve this purpose by confining the semiquinone species and conferring thermodynamic

stability upon it to allow electron transfer to proceed. This is achieved at these sites by the equalising of the midpoint potentials of the quinone/semiquinone and semiquinone/quinol one-electron couples a through tighter binding of semiquinone state (Mitchell, 1976).

Pair splitting sites do not require a stable semiquinone intermediate as the midpoint potential of the semiquinone/quinol couple is usually comparable to that of the acceptor (eg an Fe-S centre) allowing one electron to be transferred efficiently. The resulting semiquinone is short lived as the remaining electron is quickly transferred to the other acceptor leading to a more favourable lower energy state.

Mitochondria have acceptor type Q-sites associated with NADH dehydrogenase, succinate dehydrogenase (complex II) and cytochrome bc_1 (Complex III). The Q_n site of NADH dehydrogenase may stabilise two semiquinone species and functions as the acceptor of reducing equivalents from NADH via the redox centres of the complex which is proposed to include an integral bound ubiquinone (Suzuki & King, 1983; Kotylar *et al.,* 1990; Weiss *et al.,* 1991).

The Q_s site of succinate dehydrogenase is another site at which two semiquinones are stabilised and accepts reducing equivalents from succinate dehydrogenase. This site is readily distinguishable from other mitochondrial Q-sites by virtue of its sensitivity to thienoyl-3,3,3-trifluoroacetone and its rapid spin relaxation

Table 1.1 Types of quinone binding site

Site	Enzyme	Donor	Acceptor
Acceptor-type			
Q_n	NADH dehydrogenase	NADH	quinone
Q_s	succinate dehydrogenase	succinate	quinone
Q_n	cytochrome bc_1	ubiquinol	ubiquinone
Q_A	photosynthetic reaction centre	bacteriopheophytin	ubiquinone
Q_B	photosynthetic reaction centre	ubiquinol	ubiquinone
Donor-type			
Q_{bo}	cytochrome bo_3	ubiquinol	oxygen
Q_{bd}	cytochrome *bd*	ubi/menaquinol	oxygen
Q_B	fumarate reductase	menaquinol	fumarate
Pair-Splitting-type			
Q_p	cytochrome bc_1	ubiquinol	cytochrome *c*

(Ingledew & Ohnishi, 1977; Salerno & Ohnishi, 1980, Yankovskaya *et al.*, 1996).

Cytochrome bc_1 has one acceptor type Q-site and one pair-splitting site (Crofts *et al.*, 1992). The acceptor site Q_n (Q_i or Q_c) is situated near the matrix side of the mitochondrial membrane close to haem b_{562} (b_H) which is the immediate electron donor. This site has been extensively studied in both mitochondria and the corresponding bacterial complex (Salerno *et al.*, 1990; 1980; De Vries *et al.*, 1980; Robertson *et al.*, 1984). This site displays sensitivity to antimycin with the ESR semiquinone radical signal being quenched on the addition of this inhibitor (De Vries *et al.*, 1982). Strong hyperfine interactions with exchangeable protons hydrogen bonded to the quinone oxygens were observed using Electron Nuclear Double Resonance (ENDOR) and it is thought these protons play a critical part in semiquinone stabilisation (Salerno *et al.*, 1990). Site-directed mutagenesis studies of the *Rhodobacter sphaeroides* and *Rhodobacter capsulatus* complex on residues selected on the basis of them being at or near missense mutations resulting in inhibitor resistance identified four residues that may be involved in quinone binding (ala52, his217, lys251 and arg252). These affected electron transfer from cytochrome b_H to Q_n but it could not be ascertained whether any residue was essential for quinone binding (Hacker *et al.*, 1993; Gray *et al.*, 1994) except mutations of his217. Replacement of this residue with a positive charge, such as arginine resulted in a semiquinone with higher stability compared to wild-type. Substitution by a residue with a negatively charged side-chain e.g. aspartate or an aliphatic residue e.g. leucine conversely destabilised the semiquinone at Q_n.

The remaining Q-site of cytochrome bc_1, Q_p, is a pair splitting site located close to the cytoplasmic side of the mitochondrial membrane and oxidises ubiquinol with each electron being directed to two different acceptors, the Rieske iron-sulphur protein and haem $b_{566}(b_L)$. These acceptors are separated not only by their location but also by their thermodynamic properties. The 300-400mV difference in redox potentials effectively obviates the necessity for the type of semiquinone stabilisation seen at Q_n. Both the iron-sulphur protein and cytochrome *b* contribute amino acid residues shown to be involved in quinone binding. However, during turnover conditions and in the presence of antimycin a transient ubisemiquinone radical can be observed by ESR spectroscopy. It has been proposed that Q_p binds two quinone molecules and a corresponding Q-cycle model taking account of this has been suggested (Ding *et al.,* 1992). The two ubiquinone binding domains have differing affinities for quinone, one strongly binding ubiquinone and one binding weakly. Mutations in the *Rb. capsulatus* enzyme have identified a phenylalanine and glycine residue as forming part of these Q-sites (Ding *et al.,* 1995A; 1995B), with a threonine residue implicated in the *Rb. sphaeroides* enzyme (Mather *et al.,* 1996).

Mitochondria have no homologous donor type Q-sites to those which operate in the *E. coli* cytochrome bo_3 and cytochrome *bd* complexes. The Q-sites of these ubiquinol oxidases are discussed individually in the forthcoming sections. The remaining well resolved donor-type Q-site which stabilises a semiquinone intermediate is that associated with the fumarate reductase of *E. coli* (Simpkin & Ingledew, unpublished results). Fumarate reductase is

very similar to succinate dehydrogenase in terms of the constituent co-factors, subunit compositon and predicted secondary structure (Unden & Cole, 1983). The complex acts as both a fumarate reductase and a succinate dehydrogenase, is selective for menaquinol and is proposed to have two quinone binding sites, Q_A and Q_B, similar in function to the Q_A and Q_B sites of the photosynthetic reaction centres (see later in text). One of these sites is thought to be in close association to the 3Fe-4S centre of the complex (Cecchini *et al.,* 1995). Several mutants have been identified which affect menaquinol oxidation. In particular when frdC-glu29 is mutated to asp, leu, lys or phe both quinol oxidation and reduction are affected. The mutation *frd*C-his82 to asp, leu, tyr or gln leads to a large decrease in quinol oxidation while the reverse reaction is variably affected. The positive charge on his82 is proposed to be required to stabilise the semiquinone intermediate whereas the negative charge on glu29 is needed for deprotonation of menaquinol (Westenberg *et al.,* 1990; 1993). Several effective inhibitors of both mitochondrial succinate dehydrogenase and *E. coli* fumarate reductase based on 2-substituted-4,6-dinitrophenols have been synthesised which give particularly potent inhibition when the latter enzyme is operating as a menaquinol oxidase (Yankovskaya *et al.,* 1996). The data indicated that two Q-sites were present consistent with the theory that one (Q_A) contained a tightly bound quinone which cycled between the quinone and semiquinone forms and mediated single electron transfer between the enzyme and the dissociable quinone at Q_B.(Westenberg *et al.*, 1993).

The crystallographic structures of two acceptor-type Q-sites at <3Å are known (Allen *et al.,* 1987; Deisenhofer & Michel, 1989;

Feher *et al.*, 1989). They are the Q_A and Q_B sites of the photosynthetic reaction centers from *Rb. sphaeroides* and *Rhodopseudomonas viridis*. These complexes catalyse the light-driven separation of charge across the bacterial membrane and consist of three subunits, H, M, L, and several co-factors namely bacteriochlorophylls, bacteriopheophytins, one non-haem iron atom and two quinones. These quinones termed primary and secondary are designated Q_A and Q_B respectively and lie either side of the Fe(II) atom. The primary quinone undergoes a one electron reduction by bacteriopheophytin but quickly transfers this to Q_B in ~ 100μs. A second electron transfer step doubly reduces Q_B from Q_B^- to Q_B^{2-} which is then protonated prior to the release of quinol. The vectorial electron transfer between Q_A and Q_B must be due to the differences in protein environment which makes Q_A of lower redox potential to Q_B. The major difference between the sites in the two bacterial types is that in *Rsp. viridis* menaquinone is the primary quinone. This replacement can be accounted for by the position of the iron atom which is located closer to Q_B in *Rsp. viridis*. The resultant change in electronic interactions of Fe(II) with Q_B will have an effect on the differences in redox potential of menaquinone and ubiquinone.

In *Rb. sphaeroides* R-26 the quinone in the Q_A site is tightly bound in a highly hydrophobic pocket near the cytoplasmic side of the membrane (see Figure 1.4). The plane of the quinone ring forms an angle of around 60° with the plane of the membrane. The carbonyl oxygens form hydrogen bonds to the peptide NH of ala M260 and are within H-bonding distance to thr M222. A sterically unhindered conformation of the quinone is also possible where it

Figure 1.4 The structure of the Q_A and Q_B sites from the photosynthetic reaction centre of *Rb. Sphaeroides*, R-26.

(a) The quinone occupying Q_A is H-bonded via the carbonyl oxygens to ala M260 and thr M222 (bond distances 1.55Å and 1.78Å, respectively.) with an alternative H-bond possible to his M219. The quinone at the Q_B site is H-bonded to the Nδ of his L190 and ser L223. (b) As (a) viewed along the plane of the quinone ring.

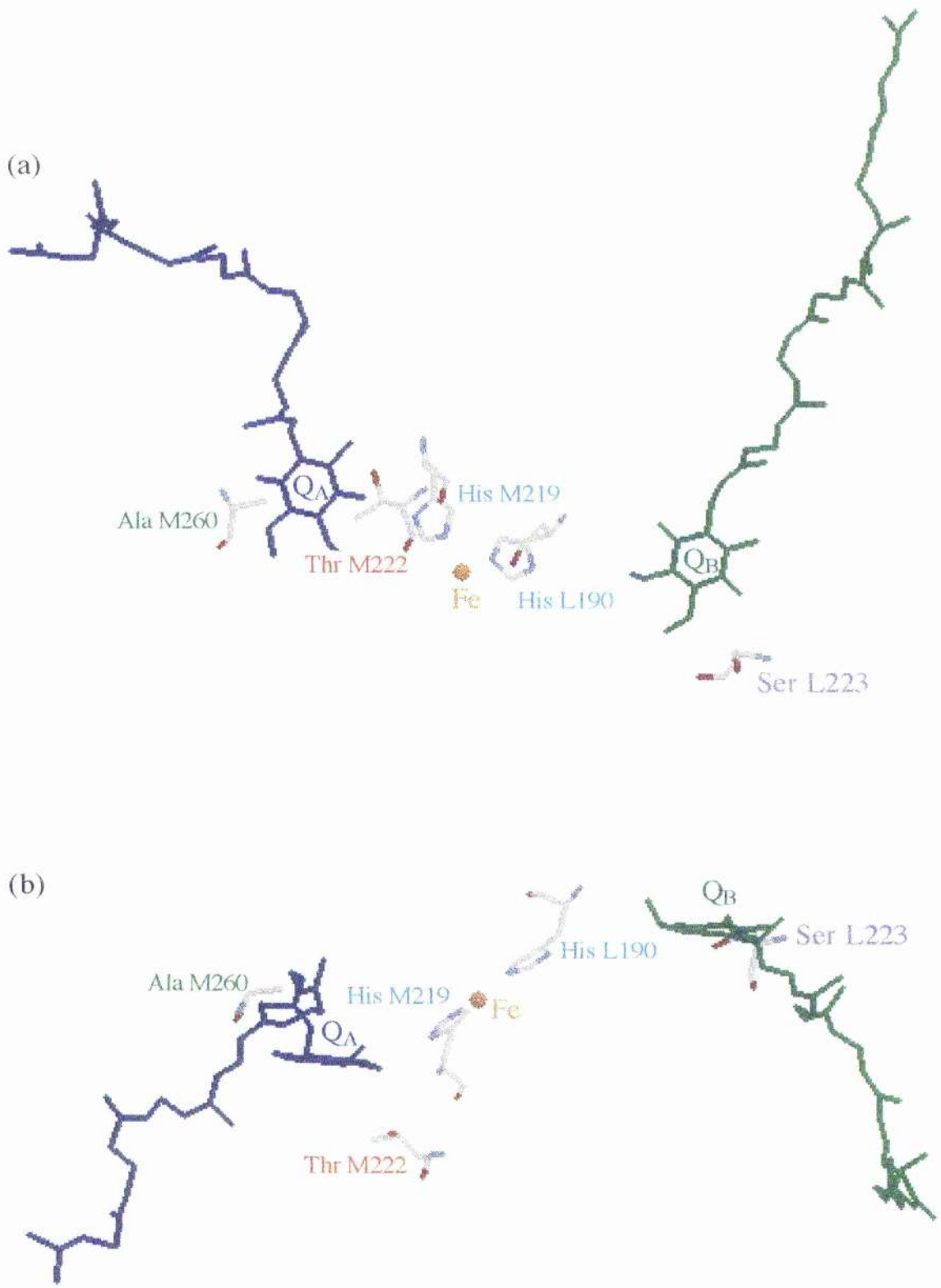
(a)
Ala M260
Q_A
Thr M222
His M219
Fe
His L190
Q_B
Ser L223
(b)
Ala M260
His M219
Q_A
Fe
His L190
Q_B
Ser L223
Thr M222

Figure 1.5 The structure of the Q_A and Q_B sites from the photosynthetic reaction centre of *Rsp. viridis.*

(a) The quinone in Q_A (a menaquinone) is H-bonded via the carbonyl oxygens to NH of ala M258 and Nδ of his M217. Q_B is only partially filled as crystallised and is shown occupied with a Q-1 analogue. The carbonyl oxygens form one H-bond to Nδ of his L190 and a bifurcated bond to NH of gly L225 and Oγ of ser L223. (b) As (a) viewed along the plane of the quinone ring.

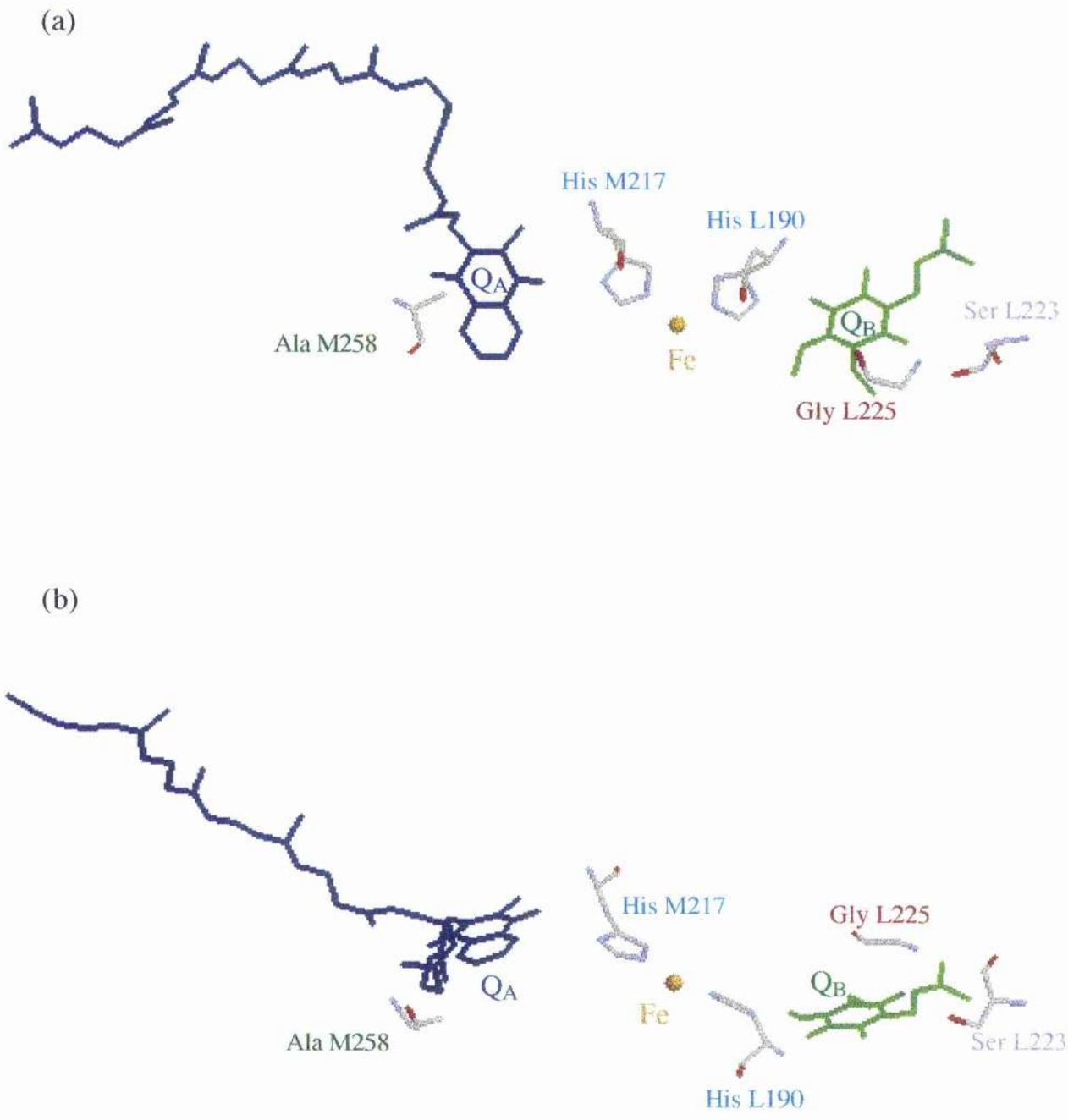
(a)
His M217
His L190
Q_A
Q_B
Ser L223
Ala M258
Fe
Gly L225
(b)
His M217
Gly L225
Q_A
Q_B
Fe
Ser L223
Ala M258
His L190

could H-bond to the his M219 which is a ligand of the Fe(II). The secondary quinone Q_B is also located near the cytoplasmic side of the membrane and forms a similar angle of 60° to the membrane normal. The carbonyl oxygens form H-bonds to ser L223 and the Nδ of his L190, another Fe(II) ligand (Allen *et al.*, 1987; 1988; Feher *et al*; 1989).

In *Rsp. viridis* the primary quinone is a menaquinone but structurally the sites are very similar (Figure 1.5). Q_A again is in a highly hydrophobic pocket with the carbonyl oxygens H-bonded to NH of ala M258 and Nδ of his M217 (ala M260 and his M219 in *Rb. sphaeroides* respectively). Q_B forms H-bonds via the carbonyl oxygens, one to the Nδ of his L190 and the other a bifrucated H-bond to NH of gly L225 and Oγ of ser L223. (Deisenhofer & Michel, 1989; Feher *et al.*, 1989; Albert *et al.*, 1994).

The binding sites of many cofactors and prosthetic groups often involve characteristic protein folds which have highly conserved residues in their primary sequence enabling similar sites in other proteins to be predicted. Despite the sequences of many quinone binding proteins being available and with the elucidation of the photosynthetic reaction centre crystal structures in addition to the studies on the aforementioned Q-sites and several others no general structural motif for quinone binding sites has been established. However, there are likely to be several physical features common to all quinone binding sites. All sites are hydrophobic allowing access to the hydrophobic quinone from the membrane phase. The most important factor in quinone binding is the availability of groups on the protein capable of forming hydrogen

bonds to the quinone molecule. In addition, quinone binding sites that inter-convert between the quinone and quinol forms require access to the aqueous medium to allow for the relevant protonation steps to occur (Rich, 1996). This could occur directly or by a hydrophilic channel. The absence of access to water restricts the function of the quinone binding site allowing it only to cycle between the quinone and semiquinone forms (Feher *et al.*, 1989).

The specificity of a site for a particular quinone is most likely a consequence of the midpoint redox potential of the quinone being compatible for electron transfer to occur to and from the immediate acceptor or donor. Napthoquinones tend have lower E_m's than benzoquinones (ubiquinone, E_{m7}=+70mV, menaquinone, E_{m7}= -74mV) although these can be greatly influenced by the protein environment of a bound quinone. An extreme case is the A_1 site of photosystem 1 at which the E_{m7} of the native menaquinone is decreased by 700mV (Rigby et al., 1996).

The length of the isoprenoid quinone tail varies with and within species. Mammalian mitochondrial quinones have 10 isoprenoid units with many bacteria, eg *E. coli*, favouring 8. Quinone hydrophobicity increases with increasing tail length rendering them more 'membrane soluble'. Chain length in most cases has little influence on the reactions at quinone binding sites although it may be important in the correct positioning of the head group in the site (Warnke *et al.*, 1994).

1.6 Organisation and Regulation of Expression of the Genes Encoding Cytochrome bo_3 and cytochrome *bd*.

Cytochrome bo_3 and cytochrome *bd* are the gene products of the *cyo* and *cyd* operons respectively. The *cyo* operon contains 5 genes, *cyo A, B, C, D* and *E* which are located at 10.2 minutes on the *E. coli* chromosome map, between 458-464 Kbp on the physical map. The *cyd* operon has just two genes *cydA* and *B* and maps to 16.6 minutes at a physical location of 785-788Kbp (Calhoun *et al.*, 1991). In addition to this a third gene *cydC*, essential for the assembly of the cytochrome *bd* complex has been identified and mapped to 19.2 minutes at a physical location of 938-943Kbp's(Georgiou *et al.*, 1987; Poole *et al.*, 1989).

Both operons have been cloned and sequenced (Green *et al.*, 1984; Green *et al.*, 1988; Au & Gennis, 1987; Chepuri *et al.*, 1990). Mutants lacking in either or both of the operons have been isolated. Either oxidase can support aerobic growth however mutants which carried both *cyo*$^-$ and *cyd*$^-$ alleles could not, although they grew normally under anaerobic conditions in the presence of nitrate. Reintroduction of the wild type *cyd*$^+$ allele into this double deficient strain restored the ability of the mutant to grow anaerobically. Similarly when either operon was subcloned onto a multi copy plasmid and introduced to a *cyo*$^-$*cyd*$^-$ mutant strain the ability to grow aerobically was restored. This has been exploited to generate mutants which over-express either oxidase and a number of such strains are employed throughout this work.

Expression of the *cyo*and *cyd* operons is regulated at transcription by the *fnr* and *arcA* gene products (Cotter *et al.*, 1990;

Cotter & Gunsalus, 1992). The FNR and ArcA proteins are known to be transcriptional activators in a number of anaerobic respiratory enzymes (Iuchi & Lin, 1988).

Using a gene fusion between the *cyo* and *cyd* operons and the reporter gene *lacZ* the individual and combined effects of each of the fnr and arcA gene products were evaluated in response to changes in oxygen tension (Cotter *et al.,* 1990; Cotter & Gunsalus, 1992). this was achieved using Δ*arcA*, Δ*fnr* and Δ*arcA*Δ*fnr* double mutant strains on the *cyo-lacZ* and *cyd-lacZ* gene fusion constructs.

Wild-type strains typically showed the highest expression of *cyo-lacZ* under aerobosis. The same strain grown anaerobically displayed ~150-fold lower expression. Conversely expression of *cyd-lacZ* was ~3-fold greater under anaerobosis than under aerobosis. In the Δ*arcA* or Δ*fnr* strains under anaerobic conditions *cyo-lacZ* expression was de-repressed but not to the same extent as in the aerobically grown Δ*fnr* strain however the expression was an additional four times greater under anaerobosis. The Δ*arcA* strain elicited a 60-65% decrease in *cyd-lacZ* expression under aerobosis or anaerobosis but the ratio of aerobic to anaerobic expression was unchanged. The double mutation Δ*fnr*Δ*arcA* strain produced an 88fold de-repression of *cyo-lacZ* expression compared to 30 and 67fold in the Δ*fnr* and Δ*arcA* strains respectively under anaerobosis. The double mutant strain did not significantly effect the levels of expression of *cyd-lacZ.*

From this it was concluded that FNR and ArcA are independent repressors of the *cyo* operon. ArcA is an activator of expression of the *cyd* operon under either anaerobosis or aerobosis.

FNR represses *cyd* expression during anaerobic but not aerobic conditions. The latter occurs only in the presence of the ArcA protein and in contrast to the *cyo* operon FNR and ArcA do not act independently (Tseng *et al.,* 1996).

1.7 The Cytochrome *bd* Complex.

Cytochrome *bd* is known to be distributed widely in gram-negative bacteria, (Kranz & Gennis, 1985, Borisov, 1996). It has also been identified in several gram-positive bacteria particularly from the *Bacillus* genus (Hicks et al., 1991; Kostyrko et al., 1991; Sakamoto et al., 1996). It is often considered to be unique amongst respiratory oxidases as it shows no apparent structural or sequence homologies with the large super-family of haem-copper respiratory oxidases. However, cytochrome *bd* and the copper containing quinol oxidases share a common feature in that they contain a quinol oxidation site close to a hexaco-ordinate haem *b*. Cytochrome *bd* is often found alongside the cytochrome *o* containing oxidases as an alternative oxidase as in *E. coli*. The *E. coli* enzyme remains the best characterised non-haem-copper respiratory oxidase, however recently there have been several publications concerning the homologous complex associated with *Azotobacter vinelandii* a free-living nitrogen-fixing bacterium. Sequence alignments of *E. coli cyd*A and *A.vinelandii cyd*A resulted in a 69% complete sequence identity, this rose to 83% when conservative substitutions were made. Similarly a 68% sequence identity was found on alignment of *E. coli cyd*B and *A.vinelandii cyd*B (Kelly *et al.,* 1990; Moshiri *et al.,* 1991). This very high sequence identity is in agreement with studies which have shown immunological and spectral similarities between the two *bd*-type oxidases (Kranz & Gennis, 1984,1985;

Kolonay *et al.,* 1994). Recently, a second cytochrome *bd*-type oxidase was isolated from an Δ*cyo* Δ*cydE. coli* strain complemented by genes from *B.firmus* OF4 (Sturr *et al.*, 1996). This second complex, encoded by the *app* locus shares significant sequence, spectral and structural similarities to the *cyd* encoded cytochrome *bd* but the significance of this new oxidase under normal growth conditions is not known.

The *cyd* operon of *E. coli* in common with *A.vinelandii* encodes two subunits, I and II. A fully functional cytochrome *bd* complex has one copy of each subunit (Miller *et al.,* 1988). Subunit I and II have molecular weights of 58,000 and 43,000 respectively. Both subunits have been shown by hydropathy profiles combined with β-galactosidase and alkaline phosphatase fusions to have several trans-membrane spanning helical segments. Subunit I has seven such helices and subunit II has eight (Green *et al.,* 1988; Georgiou *et al.,* 1988; Newton *et al.,* 1991).

Subunit I is the location of the low-spin hexaco-ordinate haem b_{558} (Green *et al.,* 1986). The site of quinol oxidation is proposed to be in the region of a large periplasmic domain between trans-membrane helices five and six, known as the 'Q-loop'(Dueweke & Gennis, 1990, 1991). Both haem b_{558} and the quinol oxidation site are thought to be in close association with one another. This haem being the first metal centre reduced by quinol has an approximate midpoint potential at pH7.0 (E_{m7}) of +250mV (Reid & Ingledew, 1979). Site directed mutagenesis studies on the six histidines of subunit I revealed only one as being an axial ligand of haem b_{558}. This residue, his-186, is located on the periplasmic side of trans-membrane helix four (Fang *et al.,* 1989). Recently, a second axial

ligand has been proposed to be a methionine residue in subunit I based on near-infrared magnetic circular dichroism studies and confirmed by further site-directed mutagenesis studies as met393 (Spinner *et al.*, 1995; Kaysser *et al.*, 1995). The plane of haem b_{558} lies perpendicular to the plane of the membrane as deduced by EPR studies on oriented multi-layer preparations of cytochrome *bd* containing membranes (Ingledew *et al.*, 1992).

One other histidine of subunit I was also found to act as a haem axial ligand. Mutagenesis of his19 caused the elimination of binding of both the haem groups of subunit II. None of the histidines of subunit II, four in total, were found to be haem axial ligands (Fang *et al.*, 1989). His19 is therefore required for the correct assembly of the complex (Sun *et al.*, 1996). Subunit I can be assembled in the membrane when expressed in the absence of subunit II. Subunit II assembly is on the other hand dependent on the presence of subunit I. In the absence of haem a stable apo-protein is still formed and assembled in the membrane (Newton & Gennis, 1991).

The two haems of subunit II, cytochrome b_{595}, formerly cytochrome a_1, and cytochrome *d* are high-spin, the latter being a chlorin co-factor (Lorence *et al.*, 1986) with E_{m7} values of +160mV and +260mV respectively (Lorence *et al.*, 1984). It has been proposed that haem *d* and haem b_{595} form a haem-haem oxygen reducing centre similar to the haem-copper binuclear centre of the oxidase super-family given evidence that certain ligands seem to bind to both haems (Hill *et al.*, 1993). Whether this has implications for oxygen reduction is not yet known although haem *d* is still considered the primary oxygen binding haem with b_{595} the immediate electron donor (Sun *et al.*, 1995).

1.8 Quinone Binding Associated With The Cytochrome *bd* Complex.

The quinone binding site associated with the cytochrome *bd* complex (Q_{bd}) has thus far been studied largely through proteolysis, antibody binding and inhibitor binding techniques. Proteolysis of either the purified enzyme or of the enzyme reconstituted into proteoliposomes by trypsin or chymotrypsin results in the preferential cleavage of subunit I into two fragments of similar size. In the native conformation subunit II appears to be rather impervious to proteolysis. Significantly, this cleavage selectively inhibits ubiquinol-8 oxidase activity and that of its homologue ubiquinol-1 while not affecting the oxidase activity of the artificial reductant N,N,N',N'-tetramethyl -*p*- phenylenediamine (TMPD). This apparently localises the site of quinol oxidation to subunit I, previously shown to be the location of the low-spin ferri-haem, cytochrome b_{558} and the site of TMPD oxidation to a distinct site associated with subunit II. Proteolysis of the enzyme reconstituted into proteoliposomes revealed that only those proteoliposomes with the active site for quinol oxidation on the outside were cleaved by trypsin indicating that in the native environment Q_{bd} is located near the periplasmic side of the membrane. (Lorence *et al.,* 1988; Dueweke & Gennis, 1991). The structure of the complex and the electrochemical behaviour of haem prosthetic groups were not in any way disrupted by proteolysis.

The use of a radio-labelled, photoreactive azido-ubiquinone derivative to locate Q_{bd}, an approach successfully used in cytochrome bc_1 of mitochondria, also indicated that subunit I is the location of this Q-site. (Yu *et al.,* 1985; Yang *et al.,* 1986). Again,

Figure 1.6 The proposed topographical model of subunit I (*cydA*) from *E. coli*, cytochrome *bd*.

The model is based on Kyte-Doolittle hydropathy profiles in combination with gene fusion experiments. The 'Q-loop' is located between trans-membrane helices V & VI. The boxed region indicates the epitope of antibodies which affect quinol oxidation. The sites of cleavage of trypsin and chymotrypsin are indicated. His186 and met393 are the axial ligands of haem b_{558}.

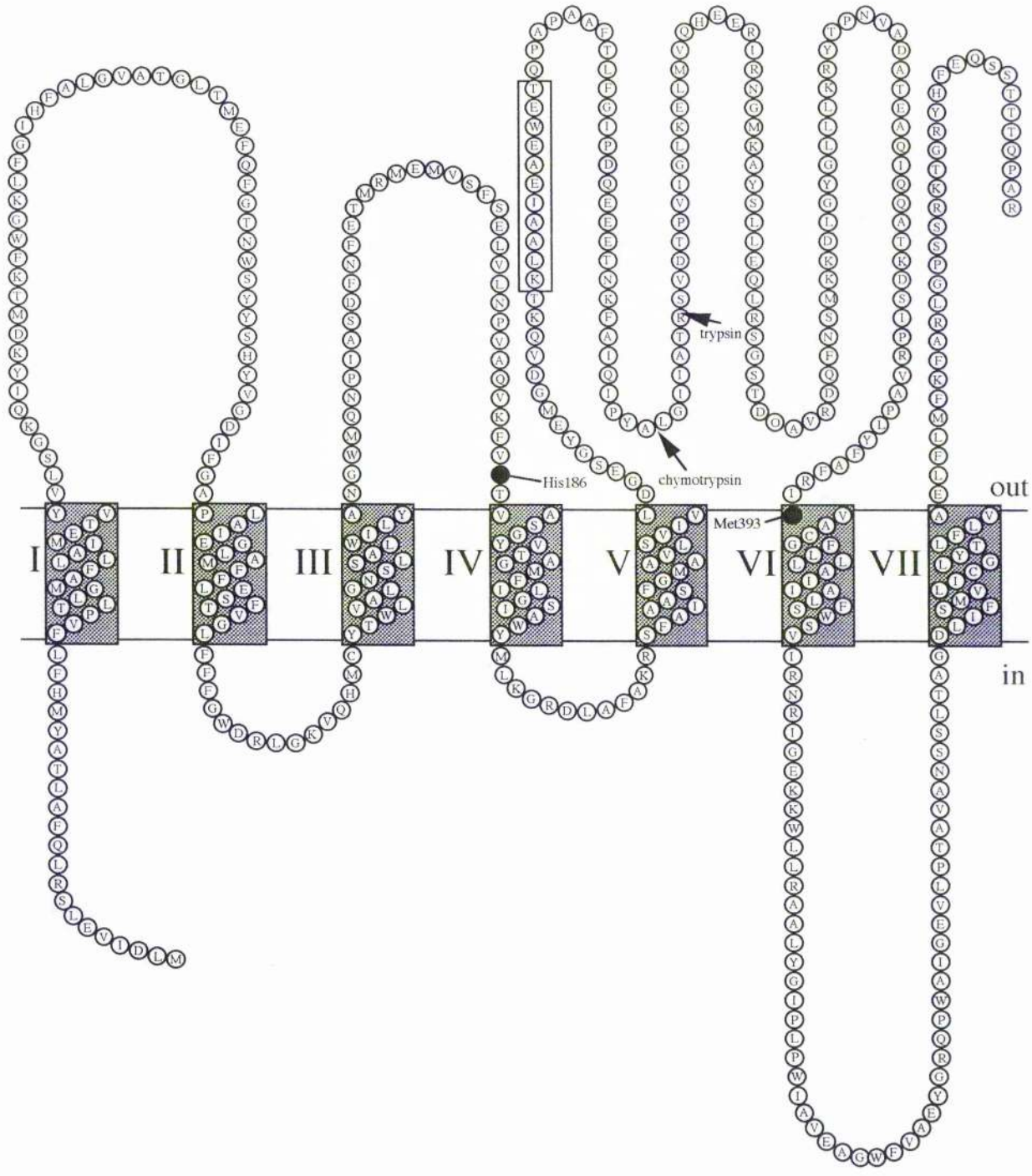
I
II
III
IV
V
VI
VII
out
in
His186
chymotrypsin
trypsin
Met393

the rate of the azido-ubiquinone derivative binding correlated with the loss of ubiquinol oxidase activity but had no effect on TMPD oxidase activity.

Polyclonal and monoclonal antibodies directed against the complex served further to characterise Q_{bd} (Kranz & Gennis, 1984; Dueweke & Gennis, 1990). Two monoclonal antibodies, A14-5 and A16-1 were particularly effective in inhibiting ubiquinol oxidase activity with no observed effect on TMPD oxidase activity. The reverse was found when anti-subunit II antibodies were employed. The epitopes of A14-5 and A16-1 have been mapped to a single 11 amino acid sequence on subunit I which lies in a large hydrophilic loop between the putative trans-membrane helices V and VI, as shown in figure 1.6. This section, termed the Q-loop, is thought to lie in close proximity in the tertiary structure to his186, identified as an axial ligand of cytochrome b_{558} (Fang *et al.*, 1989) and also contains the cleavage sites for trypsin and chymotrypsin. Recently an artificial protease, (S)-1-[p-(bromoacetamido)benzyl]-EDTA, has been used to hydrolyse peptide bonds in close proximity (up to 12Å) to specific cysteines added at points of interest on subunit I and II, thus providing information on the three-dimensional folding pattern of the complex. From these studies it was demonstrated that leu39 of subunit II is near ala255 of subunit I in the 'Q-loop' of the complex (Ghaim *et al.*, 1995).

Inhibitors known to act in other quinone utilising systems, for example HOQNO, have been shown to be effective on cytochrome *bd* (Kita *et al.*, 1984). The non-specific nature of these inhibitors yielded little structural information on Q_{bd}. The recent

identification of an inhibitor specific to cytochrome *bd* thought to act at Q_{bd} namely aurachin D raises the prospect of generating inhibitor resistant mutants, a technique exploited in other Q-site containing systems (Meunier *et al* , 1995).

1.9 The Cytochrome bo_3 Complex.

Cytochrome *o*-type oxidases are probably the most widely distributed of all bacterial oxidases and commonly they terminate one of two or more respiratory chains, as in *E. coli* (Poole & Ingledew, 1987; Poole; 1988; Suprin *et al.*, 1994) The cytochrome bo_3 complex of *E. coli* is a member of the haem-copper respiratory oxidase super-family and its relationship in this context is considered later in the text.

As isolated, the cytochrome bo_3 complex contains four subunits encoded by the *cyo* operon (Nakamura *et al.,* 1990; Chepuri *et al.,* 1990). Subunits I, II and III have corresponding molecular weights of 75,000, 35,000 and 23,000 are encoded by *cyo*B, A, C respectively. All have substantial sequence homology with the related subunits of other haem-copper respiratory oxidases. The function of the *cyo*D and *cyo*E gene products as with subunit III is unknown and it is not altogether certain whether these encode actual subunits. They have molecular weights of 12,000 and 32,000 respectively and contain regions of putative trans-membrane helices, three for the *cyo*D gene product, probably subunit IV and seven for the *cyo*E gene product. Deletion of these genes result in the production of an inactive complex and therefore it is possible that these gene products have a structural or an assembly role in the complex (Chepuri & Gennis, 1990). Thus *cyo*E is thought to encode

a protohaem IX farensyltransferase for assembly of haem *o* (Saiki *et al.*, 1992; 1993) and recently, a role in assisting the binding of Cu_B to subunit I has been assigned to subunit IV(Saiki *et al.*, 1996).

Subunit I is the location of both the haem-copper binuclear centre and the low-spin haem *b* and it is proposed to have fifteen transmembrane helices. This haem *b* has an approximate mid-point potential (E_{m7}) of 220mV (Salerno *et al.*, 1990). The binuclear centre, the site of dioxygen reduction is a high-spin pentaco-ordinate haem *o* closely associated with a Cu_B atom. The distance between the two metal centres is thought to be ~4Å, this being close enough to allow spin coupling to occur when in the Cu(II) state (Salerno *et al.*, 1990; Ingledew & Bacon, 1991). EPR and Fourier Transform Infra-red Spectroscopy studies have indicated that two metal centres are bridged by an unknown ligand when in the fully oxidised Fe^{3+} Cu^{2+} form. This ligand is replaced by the binding of cyanide or rearranged on the binding of other exogenous ligands (Tsubaki *et al.*, 1993; Moody *et al.*, 1993; Calhoun *et al.*, 1994). As regards dioxygen reduction it is thought that Cu_B plays an important role in the preferential binding and reduction of dioxygen as a mutation in subunit I, his333ala results in a very low oxidase activity and also leads to the formation of a stable bound carbon monoxide form (Mogi *et al.*, 1995).

The ligands of the Cu_B and haem *o* are highly conserved within the haem-copper respiratory oxidase super-family and have been identified by site directed mutagenesis of specific histidine residues within subunit I. His333, his334 and his419 are assigned as being the Cu_B ligands whilst his284 has been tentatively assigned as a haem *o* ligand (Minagawa *et al.*, 1992). Recently, a highly

conserved methionine residue of subunit I, met110 in the *E. coli* oxidase, previously proposed to be a Cu_B ligand has been ruled out as having such a role by mutation of this residue. the met110 appears to be non-essential to enzyme integrity and is not involved at the binuclear centre (Calhoun *et al.,* 1995).

The remaining metal centre is the hexaco-ordinate low-spin haem *b*, previously termed b_{562} but now accepted as being $b_{563.5}$. The role of this haem is thought to be similar to that of haem b_{558} of the cytochrome *bd* complex acting as the initial acceptor of electrons from ubiquinol. Further mutagenesis studies have identified his106 and his421 as being the axial ligands of this haem (Lemieux *et al.,* 1992).

Cytochrome bo_3 is a proton pump, a common feature of the haem copper oxidases. Certain mutations within an intra-helical loop between helices II and III and in helix IV of subunit I have resulted in a loss of proton translocation activity, specifically asp135asn. In addition two further non-conservative mutations also affected proton translocation, asn124 and asn142. Second site-directed mutations were conducted in the asp135asn mutant where acidic group substitutions at pro139 and asn142 resulted in the restoration of proton translocation. These residues could therefore form part of the proton uptake pathway via the intra-helical loop forming an α-helical structure (Garcia-Horsman *et al.,* 1995). Mutation of glu286 in helix IV also causes a significant decrease in proton uptake (Svensson-Ek *et al.*, 1996)

Subunit II of the complex is encoded by the *cyo*A gene and has two transmembrane helices. It contains no metal centres unlike its

homologue in the cytochrome *c* oxidases due to the replacement of the substrate, ubiquinol for cytochrome *c*. This subunit is thought to be the location of or form part of the ubiquinol oxidation site and is discussed in this context in greater detail in the next section.

1.10 Cytochrome bo_3 in Relation to the Haem-Copper Respiratory Oxidase Superfamily.

The cytochrome bo_3 complex of *Escherichia coli* is a member of the haem-copper respiratory oxidase superfamily (for reviews see Gennis, 1991; Musser *et al.,* 1993; Garcia-Horsman *et al.,* 1994; Calhoun *et al.,* 1994). It shares significant sequence and structural homology with other superfamily members and has the unique bi-metallic active site consisting of a high-spin haem in close association with a copper atom. Within the superfamily run two main branches separated according to their substrate preferences. Many bacterial respiratory oxidases, including cytochrome bo_3, utilise intrinsic membrane-bound quinol, be it menaquinol, ubiquinol or similar. Soluble cytochrome *c* is the substrate of the mitochondrial cytochrome *c* oxidase, a cytochrome aa_3-type oxidase and of many bacteria which contain several different respiratory oxidases (figure 1.7).

On account of this the cytochrome bo_3 complex is inextricably linked to the cytochrome *c* oxidases and as a result it is necessary to draw comparisons between the two. This is especially true in view of the recent publication of the crystallographic structure of the cytochrome *c* oxidase from *Paracoccus denitrificans* and bovine heart cytochrome *c* oxidase, which is discussed later (Iwata *et al.,* 1995; Tsukihara *et al.,* 1996).

Figure 1.7 A comparison of cytochrome *c* oxidases and the cytochrome bo_3 complex from *E. coli.*

(a) Electron transfer through cytochrome bo_3 proceeds from the electron donor - ubiquinol → haem b_{562} → haem o:Cu_B → H_2O. (b) in cytochrome *c* oxidase reduced cytochrome *c* is the electron donor with electron transfer proceeding through Cu_A → *a* → a_3:Cu_B → H_2O. Both oxidation reactions release two protons and actively pump two protons into the matrix. The subunits indicated are represented according to the crystal structures and projected structures of cytochrome *c* oxidase and cytochrome bo_3 respectively (Iwata *et al.*; 1995; Gohke *et al.*, 1997).

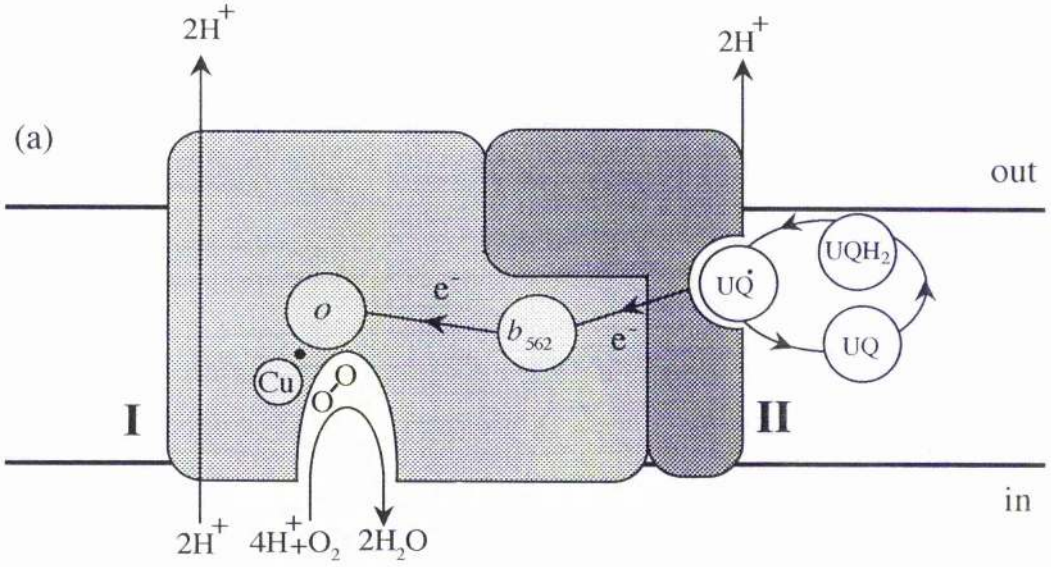
(a)
2H+
2H+
out
UQH2
UQ·
UQ
e-
o
b562
e-
Cu
O
O
I
II
in
2H+
4H+ + O2
2H2O

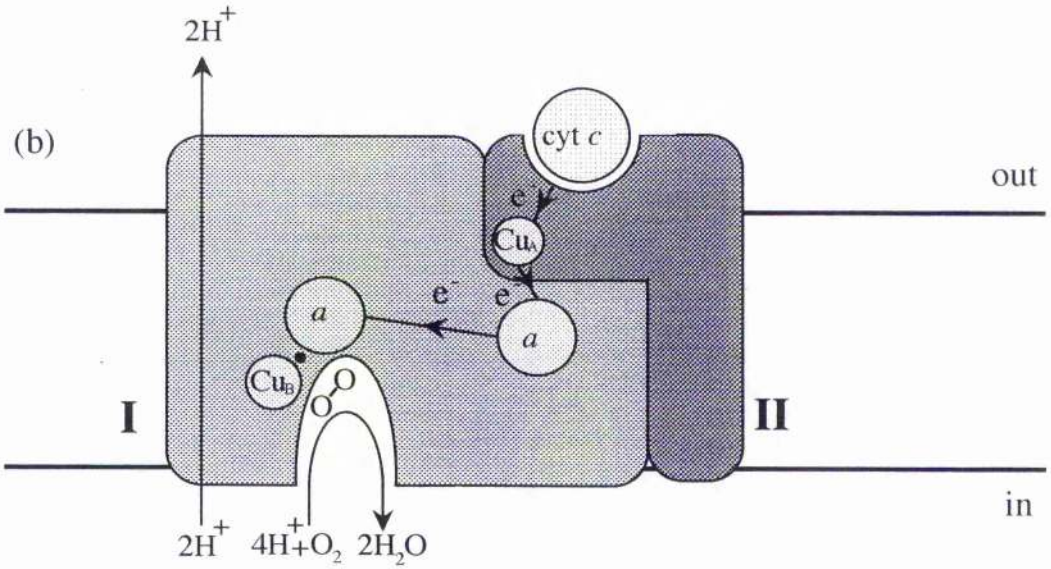
(b)
2H+
cyt c
out
e-
CuA
e-
e-
a
a
CuB
O
O
I
II
in
2H+
4H+ + O2
2H2O

The *cyo* operon encoding all of the subunits of cytochrome bo_3 has been shown to share a high proportion of sequence homology with other haem-copper respiratory oxidases. As previously mentioned, the gene products of *cyo*A, *cyo*B and *cyo*C are subunits II, I and III respectively. Each has a homologue within the other oxidases of the superfamily although some oxidases may have several more subunits. For example, the mammalian cytochrome *c* oxidase contains in addition to the mitochondria encoded subunits I, II and III up to a further ten nuclear encoded subunits. The former three are the only subunits required for enzyme function.

The metal centres of these oxidases reside in the same subunits. Subunit I contains the haem-copper binuclear centre as well as the low-spin haem. Comparison of the amino acid sequence of subunit I of cytochrome bo_3 with the cytochrome *c* oxidase of *P.denitrificans* reveals a 37% sequence identity (Chepuri *et al.,* 1990). Comparison to other cytochrome *c* oxidases reveals even greater identity particularly with residues implicated, by site-directed mutagenesis, as being ligands for the metal centres (Minagawa *et al.,* 1992; Lemieux *et al.,* 1992). In addition, hydropathy profiles and gene fusions indicate substantial structural similarity to the cytochrome *c* oxidases (Chepuri *et al.,* 1990; Chepuri & Gennis, 1990).

The crystallographic structure of cytochrome *c* oxidases of *P.denitrificans* and bovine heart have been solved at 2.8Å (Iwata *et al.,* 1995; Tsukihara *et al.,* 1995, 1996; Ostermeier *et al.,* 1996). The *P. denitrificans* enzyme crystallised as a four subunit complex. while the bovine heart enzyme crystallised as a thirteen subunit dimer. A comparison of the arrangement of the core subunits (I, II

& III) between the two was very similar and is likely to be close to that of cytochrome bo_3. Figure 1.8 shows the structure of the cytochrome *c* oxidase core subunits. In subunit I the helices are arranged in three semi-circular arcs, forming three pores two of which are occupied by the haem *a* and a_3. The large polar domain of subunit II is arranged so that the Cu_A site is directly above the metal centres of subunit I. The helices of subunit III are arranged in a V-shape and this is only loosely associated with subunit I. Despite the elucidation of these structures the mechanisms of dioxygen reduction and proton pumping remain unclear. Possible channels for the movement of protons, dioxygen and water were tentatively assigned (Iwata *et al.*, 1995).

As mentioned previously subunit II of the cytochrome *c* oxidases is the location of the Cu_A metal centre and the site of cytochrome *c* binding, see figure 1.8. The lack of Cu_A and the different substrate in cytochrome bo_3 perhaps provides the insight to suspect that this subunit would have little significant sequence identity when compared to the cytochrome *c* oxidases. This is indeed the case with both the bovine heart and *P.denitrificans* cytochrome *c* oxidase and cytochrome bo_3 sharing only 10% identity in this subunit with the highly conserved ligands of Cu_A in the cytochrome *c* oxidases being absent from cytochrome bo_3 as well as the residues implicated in cytochrome *c* binding. A comparison of the crystal structures of the two cytochrome *c* oxidases and the structure of the C-terminal domain of cytochrome bo_3, subunit II, known as the *cyo*A fragment has shown that the overall structure is similar (Van der Oost *et al.*, 1993; Wilmanns *et al.*, 1995) with each respective subunit possessing two

Figure 1.8 The crystal structure of subunits I, II & III from bovine heart cytochrome *c* oxidase at 2.8Å.

Subunits I, II and III are displayed in yellow, magenta and blue respectively. Copper atoms are shown in blue, iron atoms in magenta with the surrounding haem groups in red and blue representing *a* and a_3 respectively.

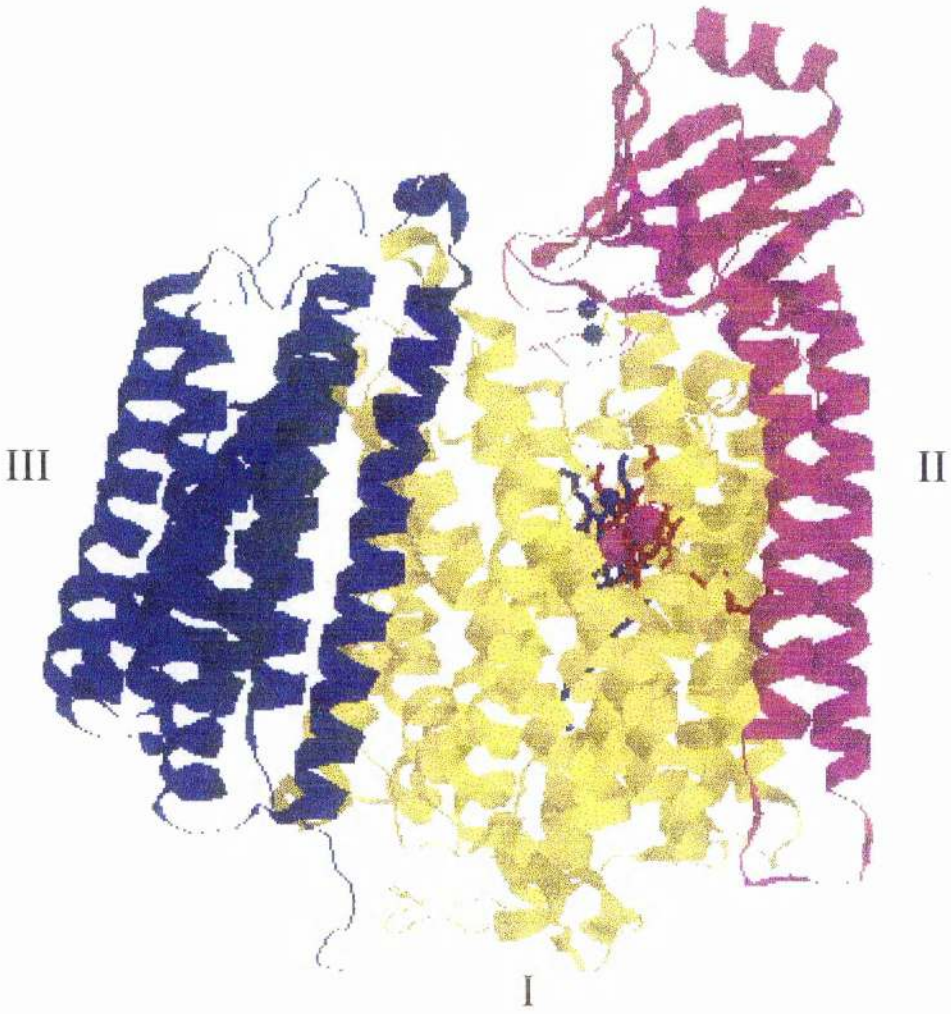
III
II
I

Figure 1.9 A comparison of the crystal structures of the *cyo*A fragment from *E. coli* cytochrome bo_3 subunit II and the corresponding domain from bovine heart cytochrome *c* oxidase.

(a) The *cyo*A fragment from *E. coli*, cytochrome bo_3 subunit II. (b) The corresponding C-terminal region of bovine heart cytochrome *c* oxidase subunit II. α-helices are shown in magenta, β-sheets in green, turns in grey and Cu_A atoms in red.

(a)

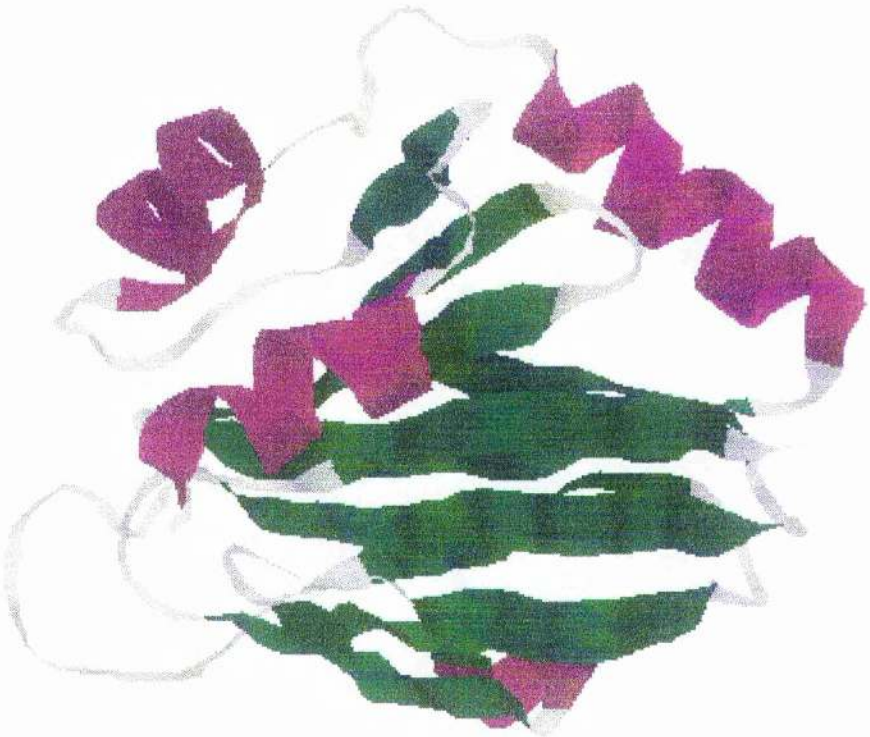

(b)

transmembrane helices and a large hydrophilic carboxy-terminal domain containing the cupredoxin fold, a β-barrel common to the small blue copper protein family (Saraste, 1991; Van der Oost *et al.*, 1992; Wittung *et al.*, 1994). The crystal structures of the bovine heart cytochrome *c* oxidase subunit II hydrophillic domain and the C-terminal fragment of subunit II from cytochrome bo_3 are displayed in Figure 1.9. By a relatively small number of mutations in subunit II, both a blue copper-type site and a Cu_A site can be restored without any large perturbation in tertiary structure. This has been achieved in both the *cyo*A fragment and in the native enzyme. The mutant enzyme can complement aerobic growth in GO105 (a strain lacking a functional oxidase) but does not have any cytochrome *c* oxidase activity with the quinol oxidase activity being indistinguishable from the wild-type enzyme (Rumbley, 1994). The crystal structure of the Cu_A containing *cyo*A fragment has also been resolved and yields purple crystals hence the fragment is termed purple *cyo*A.

The elucidation of the structure of both cytochrome *c* oxidases and the *cyo*A fragment is of enormous importance to this project given that subunit II has been implicated in quinone binding (Welter *et al.*, 1994). Figure 1.10 shows a topographical representation of subunit II. A study employing a photoreactive radio-labelled azido-ubiquinone derivative identified subunit II as being at least partly involved in ubiquinol-8 binding. The majority of labelling appeared on subunit II but some was also detected on subunit I. Subunit II has therefore been the target of extensive site-directed mutagenesis and to date a total of 29 residues have been mutated based on sequence alignments of all the known haem-copper quinol oxidases and

Figure 1.10 The proposed topographical model of subunit II (*cyo*A) from *E. coli* cytochrome bo_3.

The model is based on Kyte-Doolittle hydropathy profiles in combination with gene fusion experiments. The position of trp136 is indicated.

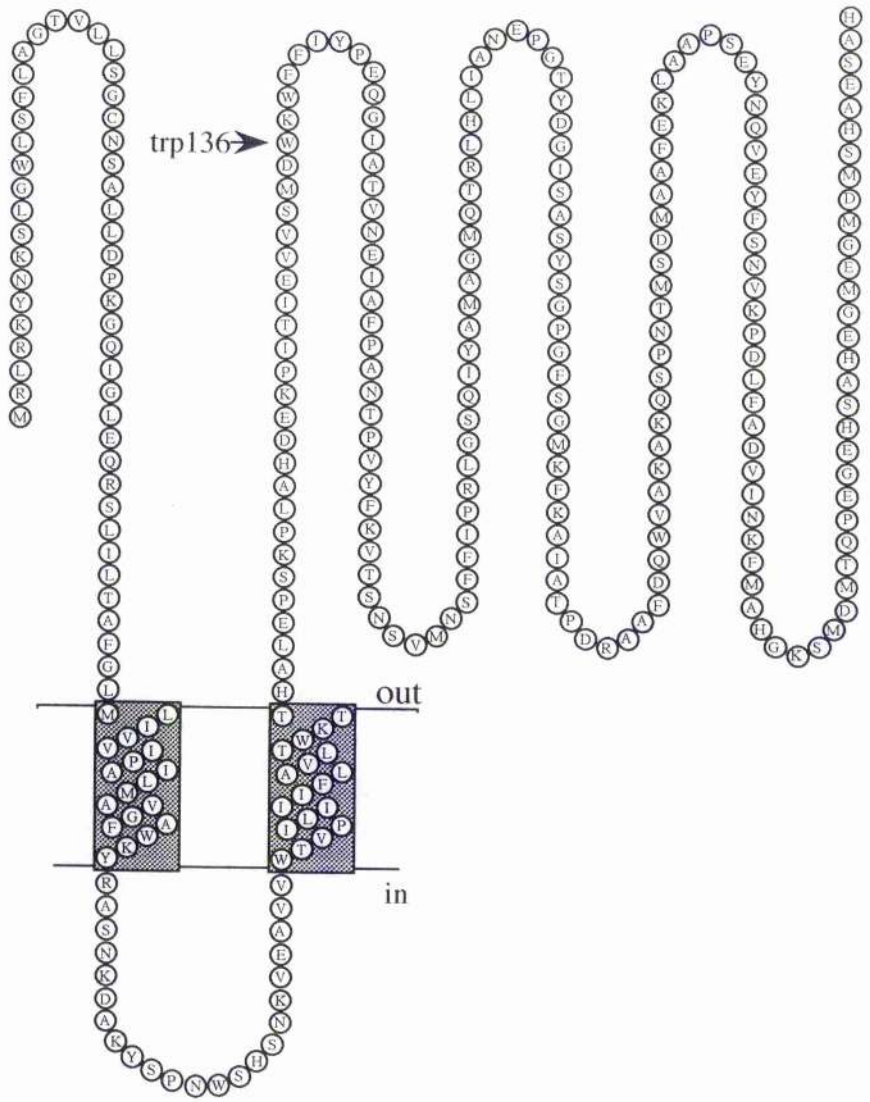
trp136
out
in

several cytochrome *c* oxidases (Ma, 1995). Two mutations glu89ala and glu89gln result in enzymes which cannot complement aerobic growth in GO105 but these have normal K_m values for ubiquinol-1, hence their involvement in quinone binding can be ruled out. Only the trp136ala mutation produced an enzyme with an unusually high K_m for ubiquinol-1 oxidation. This was 242μM compared to 38μM for wild-type. The position of this residue in the crystal structure is close to that of the absent Cu_A site and this is an obvious candidate for a quinone binding participant residue (Wilmanns *et al.*, 1995).

1.11 Quinone Binding Associated With The Cytochrome *bo*$_3$ Complex.

The cytochrome *bo*$_3$ complex, being a quinol oxidase and a member of the superfamily of haem-copper respiratory oxidases shares many sequence and structural similarities with prokaryotic respiratory oxidases and the mitochondrial cytochrome *c* oxidases. As mentioned in the previous section the major difference between the quinol oxidases and the cytochrome *c* oxidases is the choice of reductant, ubiquinol-8 in preference to soluble ferri-cytochrome *c*. Also the Cu_A site in subunit II of the quinol oxidases is absent as are the amino acid residues implicated as being Cu_A ligands or part of the cytochrome *c* binding site.

The difference in reductants with regards to shape, size and type clearly require binding domains with very different properties. The cytochrome *c* binding site lies on a large hydrophilic region on the outer surface of the protein. The ubiquinol-8 binding site (Q_{bo}) would be expected to be in a small hydrophobic region lying near to the membrane surface because of the hydrophobic nature of the

molecule. The photo-affinity labelling study strongly implicated subunit II as being involved at least partly in binding quinone. The binding of reduced quinone to this site and its subsequent oxidation proceeds through a stabilised semiquinone intermediate, in two one electron stages. This is confirmed by the identification of a highly stable bound ubisemiquinone radical associated with purified cytochrome bo_3 by ESR (Ingledew *et al.*, 1995; but see also Sato-Watanabe *et al.*, 1995). Such stabilisation of the semiquinone state is a fundamental requirement of this form of oxidation. A site which can stabilise the intermediate semiquinone is necessitated by the low stability of free ubisemiquinone. Significant amounts of semiquinone were observed even at pH7.0 with the stability of the radical increasing with pH. The midpoint potential at pH7.0, E_{m7}, of the quinone/quinol two electron couple, of +70mV, was found to be compatible to that of the low-spin ferri-haem (E_{m7}=+220mV) further indicating its role as the immediate electron acceptor. The ESR spectrum of the ubisemiquinone radical, with a line width of approximately 0.9mT, was of an unusual type due to the presence of partially resolved hyperfine splittings at 0.3mT.

The pathway of electron transfer from ubiquinol is not clear although binding studies with *p*-benzoquinones and substituted phenols at Q_{bo}, suggest that exogenous ligands are recognised asymmetrically leading to the electron transfer in sequential one electron steps to the low-spin ferri-haem (Sato-Watanabe *et al.*, 1994a) either by spatially different pathways or through an intermediate electron carrier suggested to be a second bound ubiquinol-8 molecule which acts in a similar manner to the Q_A site of the photosynthetic reaction centre. The latter proposal is

supported by evidence that a stoichiometric amount of a tightly bound ubiquinol-8 co-purifies with the complex (Sato-Watanabe *et al.,* 1994b) which has been interpreted as being at a second quinone binding site, distinct from the previously reported quinol oxidation site, Q_L (Ingledew *et al.*, 1995). This second site termed Q_H is proposed to be close to both the quinol oxidation site and the low-spin ferri-haem at a position near the periplasmic area of subunit I or on the interface of subunit I and the large hydrophilic periplasmic domain of subunit II. Whether semiquinone stabilisation occurs at this site is not apparent although Sato-Watanabe *et al.*, 1995, suggest that the characteristic ESR semiquinone signal is derived from their high-affinity, Q_H site and that none is derived from the quinol oxidation site which is thermodynamically very unlikely.

Puustinen and co-workers have also identified a bound molecule of ubiquinone, the amount of which varies in different enzyme preparations depending on the detergent used to extract the complex . Enzymes extracted in the presence of Triton X-100 typically show a low level of bound ubiquinone whilst those in n-dodecyl-β-D-maltoside or sucrose monolaurate show typically near stoichiometric amounts. The role suggested for this ubiquinone molecule is analogous to that of Cu_A, based on observations that when present the enzyme reacts with dioxygen with multi-phasic kinetics similar to cytochrome *c* oxidases. When the ubiquinone molecule is absent a mono-phasic reaction with dioxygen occurs whilst the multi-phasic kinetics can be restored on incubation with ubiquinone (Puustinen *et al.*, 1996). An alternative two Q-site model has also been proposed which postulates a ubiquinol-loop

mechanism similar to that in cytochrome bc_1 operates in cytochrome bo_3 (Musser *et al* 1993;). This is based on inhibitor binding studies under steady-state turnover conditions which indicate two ubiquinone binding sites, both in dynamic equilibrium with the quinone pool. Although two quinone binding site models are not without precedent simpler single site models can be submitted.

1.12 Research Objectives of This Thesis

The experimental aims of this thesis were to run parallel studies on the quinone binding sites associated with cytochromes bo_3 and *bd* in order to determine the structure and function relationships pertaining to the oxidation of quinol. This was conducted as follows:

1. The identification of the semiquinone intermediate of quinol oxidation by cytochromes bo_3 and *bd* using ESR spectroscopy.

2. The characterisation of the potentiometric behaviour of the semiquinones using (a) purified oxidase with different quinone analogues and (b) the membrane-bound complex with endogenous quinone (cytochrome bo_3 only).

3. The monitoring of the effect of inhibitors of quinol oxidation using ESR spectroscopy.

4. The assignment of the origin of the partially resolved hyperfine splittings in the ESR spectrum of the cytochrome bo_3 semiquinone. To establish the existence of similar splittings in the cytochrome *bd* semiquinone.

5. The characterisation of the electronic structure of the bound semiquinone from both oxidases using ENDOR spectroscopy.

6. The determination of the nature of protein-quinone interactions using Electron Spin Echo Envelope Modulation (ESEEM) spectroscopy (cytochrome bo_3 only).

7. The identification of amino acid residues involved in quinone binding and semiquinone stabilisation by site-directed mutagenesis (cytochrome bo_3 only).

2.0 MATERIALS & METHODS

2.1 Bacterial strains

Table 2.1 lists the *E. coli* strains used in this work. FUN4/pNG2 was the major source of cytochrome *bd* (Fang, *et al.*, 1989). This strain has a point mutation in *cyo* and had the *cyd* operon present on a multicopy plasmid containing the gene for tetracycline resistance. Strain RG145/pRG101 was used in the studies of the membrane-bound cytochrome bo_3 complex, which had a point mutation in *cyd* and the *cyo* operon present on a multicopy plasmid containing the genes for tetracycline and ampicillin resistance (Au & Gennis, 1987). Purified cytochrome bo_3 was obtained from strain GO105 with the plasmid pJRHisA, this expressed a genetically modified enzyme with a C-terminal histidine 'tag' in subunit II and contained the gene for ampicillin resistance (Rumbley, 1995).

All strains of the organism were stored in 75% Luria broth, 25% glycerol (v/v), pH7.2 at -70°C and sub-cultured onto LB agar plates containing the appropriate antibiotic when required.

2.2 Media and cell growth conditions

Single colonies of the bacteria were taken from the plate using a sterile transfer loop and used to inoculate 5ml of the appropriate growth medium supplemented with an antibiotic if required. The cultures were grown for 18-20 hours at 37°C and used to inoculate 100ml of growth medium and grown as before, a portion of these cultures then inoculated 500ml of growth medium in 2 litres shaker flasks. If larger volumes of cells were required the 500ml cultures were used for the inocultation of a fermentor (New Brunswick

Table 2.1 Strains of *E. coli* used in this work

Strain	Plasmid	Genotype	Reference /source
FUN4	pNG2 (cyd^+)	*F^- rspL gal(?) memA401 nadA cydA2 cyo recA srl SU^+*	Fang *et al.*, 1989
RG145	pRG101 (cyo^+)	*F^- rspL thi gal nadA cydA2 cyo lon100 sr1300:: Tn10 recA*	Au & Gennis, 1987
GO105	pJRHisA (cyo^+)	*Δ(cyd AB')455 zbg-2200::Km^R cyo recA srl300 ::Tn10*	Rumbley, 1995
BL21(DE3)	pET.E2	*F' traD36 $proA^+$ $proB^+$ lacIq lacZΔM15/rec1 endA1 gyrA96 (Nalr) thi hsdR17 supE44 relA1 Δ(lac-proAB)mrcA*	Oost *et al.*, 1992
DH5α		*F' endA1 hsdR17(rK^-mK^+) supE44 thi-l recA1 gyrA (Nalr) relA1 Δ(lacZYA-argF)u169(m80lacZΔM15)*	Pharmacia
NM522		*F' D(lac-pro) $lacI^q$z DM15 $proAB^+$*	Pharmacia

Fermentors) with a working volume of 10 litres. *E. coli* strains RG145 and GO105 were grown in conditions of high aeration. FUN4 was grown with low aeration. These conditions reflect the oxygen tensions which give maximum expression of each oxidase. Both RG145 and FUN4 were grown to late log phase and harvested. GO105/pJRHisA was grown to early to mid-log phase to minimise the expression of a protease which cleaves the histidine tag.

2.2.1 LB agar plates

LB agar plates contained the following in 1 litre :- 10g, tryptone; 5g, yeast extract; 5g, NaCl; 15g, agar and 1ml, 1M NaOH. If appropriate, antibiotics were added as follows : ampicillin, 100μg/ml; tetracycline, 10μg/ml. Plates were poured and dried for 1 hour at 37°C, sealed and stored at 4°C.

2.2.2 Minimal media M63 plates

These plates were used for complementation assays of GO105 and contained the following in 1 litre, 15g, bacto-agar; 100mL of stock M63 salts (10× stock: 30g, KH_2PO_4; 70g, K_2HPO_4; 20g, $(NH_4)_2SO_4$; 5mg $FeSO_4$ in 1 litre) supplemented with 1mM, $MgSO_4$; 1mM, thiamine; 0.00125%, nicotinic acid; 0.3%, DL-lactate; 0.3%, succinamide.

2.2.3 Luria broth

This medium contained the following per litre :- 10g tryptone, 5g, yeast extract; 5g NaCl and 1ml, 1M NaOH. Cytochrome bo_3 expressing strains were supplemented with both 5mg, $CuSO_4$ and 2mg, $FeCl_3$. Cytochrome *bd* expressing strains were supplemented

with 2mg, $FeCl_3$ only. A 15%(v/v) solution of glycerol in Luria broth was used to maintain stock cultures.

2.2.4 Rich glucose medium

This medium was used for most fermentor growths and contained the following per litre. 3g, KH_2PO_4; 5g, K_2HPO_4; 5g, D-glucose; 2g, tryptone; 2g, yeast extract; 0.5g, acid hydrolysed casein; 1g, $(NH_4)_2SO_4$; 2mg, $FeCl_3$; 5mg, $CuSO_4$ (if appropriate); 1ml trace elements solution (see section 2.2.6). After autoclaving the media was supplemented with the following :- 0.05g thiamine, 0.05g nicotinic acid; 0.1ml, 0.5M $MgSO_4$ and the appropriate antibiotic as in section 2.2.1.

2.2.5 ^{15}N media

This growth medium was used to grow RG145 in order to produce ^{15}N labelled cytochrome *bo*$_3$ and was prepared essentially according to Feng *et al.*, 1991 and contained the following per litre :- 5.46g, KH_2PO_4; 11.4g, K_2HPO_4; 1.5g, NaCl; 2mg, $FeCl_3$; 5mg, $CuSO_4$. The pH was adjusted to 7.2 if required. After autoclaving 3.35mg, δ-aminolevulinic acid; 0.2mg, thiamine; 1.0g, ^{15}N-labelled $(NH_4)_2SO_4$; 0.204g, $MgCl_2$; 0.2g, ampicillin and 4.0g, D-glucose were added from filter sterilised solutions.

2.2.6 Transformation and storage solution (TSS)

Transformation of plasmid DNA into *E. coli* was achieved using TSS (Chung, 1989). This was based on standard LB medium containing 10% PEG (mw 8000), 5% (v/v) DMSO and 50mM $MgCl_2$, pH7.0.

2.2.7 Trace elements solution

This solution was adapted from that described by Cohen & Rickenberg, 1956 and contained the following: 3mM, $FeCl_3$; 2mM, $MnCl_2$; 1.2mM $CoSO_4$, 4.5mM boric acid, 15mM $ZnCl_2$ with the pH adjusted to 7.0.

2.2.8 Harvesting of cell cultures

Cell cultures under 2 litres were harvested by centrifugation at 9000×g for 15mins at 4°C using a Sorvall RC-5B Superspeed centrifuge (Dupont). Larger volumes were harvested using a cross flow membrane system (Millipore, UK). In both cases the cells were washed twice in 5mM Tris/HCl, pH7.2 and centrifuged as before. The whole cells were finally resuspended in 2mM, $MgSO_4$; 50mM, BES; pH7.4, and frozen in 'pea form' by adding the cell suspension dropwise into liquid nitrogen using a pipette and stored at -20°C until required.

2.3 Preparation of *E. coli* membranes

For studies of the *in situ* cytochrome *bd* and bo_3 complexes membranes of *E. coli* strains FUN4 and RG145 were prepared as follows. Approximately 100g (wet weight) of cells were thawed and resuspended to 250ml in 50mM BES pH 7.4, 5mM $MgSO_4$ containing 1mM leupeptin, 2mg lysozyme, 2mg pancreatic DNase (type I), 2mM benzamide and 1mM phenylmethylsulphonyl flouride. The suspension was passed through a French pressure cell (American Instrument Company, Silver Spring, Maryland, U.S.A.) at 1.0 x 10^8 Pa. Large cell debris and residual whole cells were

removed by centrifuging the lysate at 10000×g for 10 minutes at 4°C.

The membrane fragments were treated essentially as described by Matsushita *et al.*, 1984. Firstly, with a 5M urea wash in 50mM potassium phosphate, pH7.5 (RG145 membranes only) then following ultracentrifugation at 150000×g for 1hr at 4°C (Beckman ultracentrifuge) with sodium cholate (6% for RG145 membranes, 0.6% for FUN4 membranes) in the same buffer and then finally in 50mM potassium phosphate, pH7.5 alone. The membrane pellets were resuspended by homogenisation in a minimal volume of an appropriate buffer and frozen in 'pea form' and stored under liquid nitrogen until required. The prepared membranes typically had a protein content of ~30-40mg/ml.

2.4 Purification of the cytochrome bo_3 complex

Cytochrome bo_3 was isolated using a method adapted from Puustinen *et al.*, 1996. Membrane fragments of *E. coli* strain GO105/pJRHisA were sedimented from approximately 50g of cells by French Pressure Cell treatment as described in section 2.3. pJRHisA expresses a genetically modified cytochrome bo_3 complex which has a C-terminal histidine tag on subunit II (Rumbley, 1995). This enables the isolation of a homogenous preparation of the complex in a one step procedure, using a metal chelate affinity column and elution with a high imidazole solution.

Membrane fragments were washed with 5mM imidazole, 300mM NaCl, 20mM Tris-HCl, pH7.8 and centrifuged at 150000g as before. The washed membranes were resuspended in 5mM imidazole, 300mM NaCl, 20mM Tris-HCl, pH7.8 and the

cytochrome bo_3 complex solublised using either 1% (w/v) *n*-dodecyl-β-D-maltoside (dodecylmaltoside) or 1% triton X-100 and 1% *n*-octyl-β-D-glucopyranoside (octylglucoside). This suspension was stirred at 4°C for approximately 45 minutes and centrifuged as before. The supernatant was retained and applied to a Ni-NTA agarose column (Quiagen), bed volume 25ml, which had been equilibrated with 5 column volumes of 0.05% dodecylmaltoside or 0.1% triton X-100 in 5mM imidazole, 300mM NaCl, 20mM Tris-HCl, pH7.8. The column was washed with 4 bed volumes of the equilibration buffer then the detergent exchanged with 0.05% sarkosyl, 5mM imidazole, 300mM NaCl, 20mM Tris-HCl, pH7.8. The cytochrome bo_3 complex was then eluted with 1 bed volume of 0.05% sarkosyl, 300mM imidazole, 300mM NaCl, 20mM Tris-HCl, pH7.8.

The high concentrations of imidazole and NaCl were removed by dialysis against 5 litres, 0.05% sarkosyl, 20mM Tris-HCl, pH7.8 for 2 days. Concentration of the complex was carried out using either an Amicon Centriprep-10 or, for smaller volumes, Amicon Centricon-10 to approximately 250μM. The preparation was then frozen in 100μl aliquots and stored at under liquid nitrogen until required.

2.5 Purification of the cytochrome *bd* complex

Cholate treated FUN4 membrane fragments prepared as described in section 2.3 were extracted with 1% triton X-100 and 1% octylglucoside in 50mM potassium phosphate, pH7.5 and centrifuged at 150000×g for 1hr at 4°C to solublise the cytochrome *bd* complex. The supernatant was retained, concentrated using

Centriprep-10 membranes and stored under liquid nitrogen until required. The resultant preparation was sufficiently pure for redox titrations and had an approximate specific haem content of 7.5nmol/mg protein which represents around 80% purity.

The complex was purified further for preparation of samples of concentrated semiquinone. The brown supernatant from the detergent extraction was placed on a column of DEAE Sepharose CL-6B (bed volume 25ml) equilibrated with 0.1% Triton X-100 in 5mM Tris-HCl, pH8.0. The column was washed with 2 bed volumes of the equilibration buffer and the detergent exchanged to 0.05% sarkosyl. Two bed volumes of this detergent in 5mM Tris-HCl, pH8.0 were passed through the column. The cytochrome *bd* complex was eluted in one step with 300mM NaCl, 0.05% sarkosyl, 5mM Tris-HCl, pH8.0 and desalted by dialysis against 2 litres of 0.05% sarkosyl, 5mM Tris-HCl, pH8.0 and concentrated as before using Centriprep-10 membranes.

2.6 Removal of loosely associated quinones

Approximately 500nmols of purified oxidase was diluted to 25mls in 50mM tris/HCl, 0.05% sarkosyl, pH7.8 and precipitated in 70% ammonium sulphate. The precipitate was pelleted by centrifugation at 100000×g for 1 hour and resuspended in 10mls 50mM tris/HCl, 0.05% sarkosyl, pH7.8 and dialysed against 2 litres of the same buffer for 24 hours at 4°C. The oxidase solution was then concentrated by centrifugation to approximately 200μM using an Amicon centriprep-10.

2.7 Purification of the *cyo*A fragment

E. coli strain BL21(DE3), containing the plasmid pET.E2 was used as the source of the *cyo*A fragment. The strain was grown and the *cyo*A fragment was purified essentially according to Oost *et al.*, 1992 with the omission of the FPLC purification step. The *cyo*A fragment was concentrated using Centriprep-3 membranes and quantified using an extinction coefficient of 23.6 $mM^{-1}cm^{-1}$ at 278nm (Oost *et al*, 1992).

2.8 Redox potentiometery

Potentiometric titrations were performed according to Dutton, 1978 as adapted for quinone investigations (Ingledew *et al.*, 1995). The dye system was chosen so that it would give minimum free radical interference with quinone-like mediators avoided or kept to a minimum concentration compared with the quinone under investigation to decrease the probability of them binding to the site. Control titrations were conducted to monitor any radical species originating from the redox mediators with the inclusion of bovine serum albumin at $30mgml^{-1}$.

The stock enzyme was diluted in 200mM of the appropriate buffer as indicated with 0.1% octylglucoside. The redox mediators were varied but the general mix contained (the approximate midpoint potentials are indicated); phenazine methosulphate (E_{m7}=+80mV); toludine blue (E_{m7}=+34mV); duroquinone (E_{m7} =+10mV); resorufin (E_{m7}=-50mV); indigo disulphonate (E_{m7}=-145mV); anthraquinone-2,5-disulphonate (E_{m7}=-175mV); anthraquinone-2-sulphonate (E_{m7}=-218mV); hexaamine ruthenium (II) chloride (E_{m7}=-214mV) were added to a final concentration of

50μM except phenazine methosulphate which was at final a concentration of 0.05μM; 2mM EDTA, 100μM sodium citrate, 75μM sodium pyrophosphate with 50μM ferrous sulphate was also present as an additional mediator.

The ubiquinone or menaquinone analogues were were added to give a final concentration of 1mM and in some sets of titrations HOQNO (2-heptyl-4-hydroxyquinoline-N-oxide), aurachin D or tridecylstigmatellin were added at the concentrations indicated.

The ambient redox potential (E_h) was adjusted by the addition of potassium ferricyanide and sodium dithionite and measured using a combination platinum / (Ag/AgCl) reference electrode purchased from Russell pH Ltd. (Auchtermuchty, Fife, UK). Redox titrations were conducted anaerobically, the redox titration vessel continuously flushed with N_2 that had been passed through a Nil-Ox O_2-scrubbing apparatus (Jencons Scientific, Hemel Hempstead, Herts., UK). Before each redox titration the redox electrode was calibrated using powdered quinhydrone in 50mM BES, 2mM EDTA, pH7.0, which gave an E_h value of +297mV. The pH was checked before and after the titration and adjusted if necessary with the addition of HCl or NaOH.

2.9 ESR sample preparation

Samples for ESR analysis were poised, transferred to quartz ESR tubes 3mm internal diameter and quick frozen by immersion in an isopentane-methylcyclohexane (1:4, v/v) freezing mixture and stored under liquid nitrogen until required.

2.10 Quantitation of semiquinone and derivation of theoretical curves

The semiquinone signals were quantitated by double integration of the signal against a 10μM 1,1-diphenyl-2-picrylhydrazyl free radical standard and a 1mM $CuSO_4$ standard. The oxidation of quinol occurs by two one-electron transfer steps through a semiquinone intermediate. Each electron transfer, or half-reaction has a redox potential represented by E_1 and E_2. E_1 is defined as the potential of the quinone/semiquinone couple and E_2 as the potential of the semiquinone/quinol couple. The maximum concentration of semiquinone is observed at E_m, the mid-point of the n=2 couple ($E_m = {}^1/_2(E_1+E_2)$. The expression for the semiquinone radical concentration as a function of E_h is:-

$$[SQ] = C_{site}[(1+10^{(E_h-E_1)/59}+10^{(E_2-E_h)/59})]^{-1}$$

This equation is derived from the Nernst equation as shown below:-

$$Q \Leftarrow E_1 \Rightarrow SQ \Leftarrow E_2 \Rightarrow QH_2$$

The expression for E_1, (where ox=oxidised and sq=semiquinone) is thus:

$$E_h = E_1 + 59 \log ox/sq$$

$$E_h - E_1 = 59 \log ox/sq$$

A unitary concentration of quinone forms is assumed; therefore ox=1-sq

$$10^{(E_h-E_1)/59} = ox/sq = 1\text{-}sq/sq$$

$$sq10^{(E_h-E_1)/59} = 1\text{-}sq$$

$$sq10^{(E_h-E_1)/59} + sq = 1$$

$$10^{(E_h-E_1)/59} + 1 = 1/sq$$

$$sq = \frac{1}{1 + 10^{(E_h-E_1)/59}} \qquad \text{(for } E_1 \text{ only)}$$

The expression for E_2, (where red=reduced) is thus:

$$E_h = E_2 + 59 \log red/sq$$

$$E_h - E_2 = 59 \log red/sq$$

Again a unitary concentration of quinone forms is assumed; therefore red=1-sq

$$10^{(E_h-E_2)/59} = sq/red = sq/1-sq$$

$$10^{(E_h-E_2)/59} - sq10^{(E_h-E_2)/59} = sq$$

$$10^{(E_h-E_2)/59}/sq - 10^{(E_h-E_2)/59} = 1$$

$$10^{(E_h-E_2)/59}/sq = 1 + 10^{(E_h-E_2)/59}$$

$$sq = 10^{(E_h-E_2)/59}/1 + 10^{(E_h-E_2)/59} \qquad \text{(for } E_2 \text{ only)}$$

The total semiquinone concentration, SQ, is a product of fractions therefore:

$$SQ = sq(\text{from } E_1) \times sq(\text{from } E_2))$$

$$\text{Fraction of SQ} = 10^{(E_h-E_2)/59}/[1 + 10^{(E_h-E_2)/59}][1 + 10^{(E_h-E_1)/59}]$$

The total semiquinone concentration is dependant on the number of quinone binding sites, C_{site}, therefore:

$$SQ = C_{site} 10^{(E_h - E_2)/59} / [1 + 10^{(E_h - E_2)/59}][1 + 10^{(E_h - E_1)/59}]$$

$$SQ = C_{site} [1 + 10^{(E_h - E_1)/59} + 10^{(E_h - E_2)/59}]^{-1}$$

This equation is used to obtain theoretical lines modelling the variation in semiquinone concentration (represented as site occupancy) with changing pH and E_h. Small adjustments are made to E_1 and E_2 to optimise the fit to the data, using a spread-sheet (CA-Cricket graph III, version 1.0, for Macintosh, Computer Associates International, Inc., NY, USA.) (Ingledew *et al.*, 1995). It should be noted that these are not statistical best-fit curves but are simulated theoretical lines fitted by eye. The sensitivity of the fit is such that a 20% change in the maximum amplitude of the simulation results in a 10mV separation of E_1 and E_2.

2.11 Deuterium exchange of oxidase complexes

Both purified and membrane-bound oxidase samples were exchanged into deuterium oxide before generation of the semiquinone described in section 2.12. Approximately 0.5g of *E. coli* membrane fragments were resuspended and washed three times in 10ml of 200mM AMPSO, pD=9.0 and centrifuged after each wash for 1hr, 150000g at 4°C. pD values were determined using a pH meter and the following relationship: $pD = pH_{(meter\ measurement)} + 0.4$ (Glasnoe *et al.*, 1966).

To deuterium exchange the purified oxidase complex around 500µl of concentrated oxidase (~250µM) was diluted in 5ml of 200mM AMPSO, pD=9.0 and reconcentrated using Centriprep-10 membranes. This procedure was repeated twice and the oxidase concentrated to approximately 200µM.

2.12 Preparation of concentrated semiquinone samples

2.12.1 Membrane-bound complex samples

Approximately 1g of *E. coli* membranes prepared in section 2.3, were resuspened in 100mL of 200mM AMPSO, pH9.0 and centrifuged for 5 hours at 100000×g, 4°C. The membranes were then packed into a 1ml disposable syringe and a quantity (~300μL) injected into the ends of 3mm internal diameter ESR tubes. The tubes were placed in a swing-out bucket centrifuge for 2 hours at 5000×g, 4°C, until the membranes were well packed at the bottom of the tube. The samples were then placed in an anaerobic jar and left overnight at 4°C, then quick frozen and stored under liquid nitrogen until required.

2.12.2 Purified complex samples

Approximately 250μl of oxidase (~200mM) in 200mM AMPSO, pH9.0 which had the loosely bound quinones removed as outlined in section 2.6 was placed in an ESR tube and mixed with the appropriate quinone to a final concentration of 1mM. The samples were reduced using a small amount of sodium dithionite, quick frozen and the amount of semiquinone formation monitored by ESR until a maximal amount of semiquinone was achieved.

2.12.3 *In vitro* semiquinone radicals

Semiquinone anion radicals were produced by the stoichiometric reduction by sodium borohydride of alkaline solutions of the quinone in isopropanol under a stream of argon in an ESR tube and immediately quick frozen and stored under liquid

nitrogen. Deuterated samples were prepared in isopropanol deuterated at the hydroxyl group (isopropan(*ol-d*)).

2.13 Sequence alignments of subunit II of haem-copper type quinol oxidases and cytochrome *c* oxidases

All quinol and cytochrome *c* oxidase sequences used in this alignment were extracted from the Swiss-Prot Database. Sequence alignments were carried out using the PILEUP program of the GCG package (Devereux *et al.*, 1984). and the profile alignment option of the CLUSTALV program (Higins *et al.*, 1992) to introduce more divergent sequences followed by manual adjustment where necessary.

2.14 Site-directed mutagenesis of subunit II of cytochrome bo_3

The unique site elimination (USE) method of site directed mutagenesis was used to produce the lys118leu mutation in cytochrome bo_3 subunit II (Deng & Nickoloff, 1992). A USE kit manufactured by Pharmacia, Biotech. was used for this purpose.

2.14.1 Synthesis of K118L primer

Two primers were synthesised, a mutagenic primer for the mutation K118L and a USE primer to eliminate the unique EcoRI site in *cyo*C in the cloning vector pJRHisA and are shown below. The mutated bases are underlined. A HindIII site was introduced into the K118L to facilitate screening.

K118L primer

5'-gct ctt gag cc<u>a</u> agc <u>ttg</u> ccg ctg gca-3'

USE primer

5'-gaa atc tat gaa ttc cat cac ctg att gtt-3'

Both primers were synthesised at the Oligo Synthesis Genetic Engineering Facility, School of Chemical Sciences, University of Illinois at Urbana-Champaign, USA. The primers were phosphorylated as described by manufacturers kit (Pharmacia Biotech).

2.14.2 Mutagenesis of *cyo*A

The plasmid pJRHisA DNA was prepared by the standard protocol of Manniatis *et al.*, 1982 The plasmid was melted and the USE primer, mutagenic primer annealed and incubated with T4 DNA polymerase and T4 DNA ligase and deoxynucleotides as described in the USE manufacturers kit (Pharmacia Biotech). The plasmid was digested with the selection restriction enzyme (EcoRI) according to the manufacturers instructions (New England Biolabs, USA).

2.14.3 Transformation of pJRHisA into host strain

The restricted plasmid was transformed into *E. coli* strain NM522 using Transformation and Storage Solution (TSS) (Chung, 1989) and grown overnight in LB medium

2.14.4 Secondary restriction digest of pJRhisA

Plasmids were prepared from the transformed NM522, restricted a second time with EcoRI to increase the efficiency of selection and transformed into DH5α using TSS. Cells were plated

out on LB plates and grown overnight. Single colonies were picked and grown in 5ml LB media.

2.14.5 Screening of possible K118L mutant colonies.

The secondary restricted plasmid DNA was prepared from DH5α and restricted with HindIII, this site had been introduced into the mutagenic primer. Possible mutants indicated by the restriction pattern on an agarose gel were submitted for sequencing.

2.14.6 Sequencing of K118L

The K118L mutant was sequenced using a Triple Helix Sequencer, (Applied Biosystems) at the Genetic Engineering Facility, School of Chemical Sciences, University of Illinois at Urbana-Champaign,USA. Mutant plasmid was then transformed into GO105 for aerobic complementation assays.

2.14.7 Complementation assay for aerobic growth

The ability of the K118L mutant to compliment aerobic growth in an *E. coli* strain (GO105) lacking a functional oxidase was determined by transforming the mutant plasmid into GO105, growing the mutant on minimal media M63 plates anaerobicaly overnight. Single colonies were picked, plated onto minimal media M63 plates and tested for their ability to grow aerobically.

2.15 Electron spin resonance spectroscopy (ESR)

ESR spectra were obtained using an X-band Bruker ER200D electron paramagnetic resonance spectrometer linked to a Bruker

ESP3320 Data System (Bruker Analytische Messtechnik MBH, Silberstreifen, D-7512, Rheinstetten 4, Germany). Temperature regulation above liquid nitrogen temperature was achieved using a liquid nitrogen Variable Temperature Unit (Oxford Instruments, Osney Mead, Oxford, UK). Temperature regulation below liquid nitrogen temperature was achieved with a liquid helium transfer line and variable temperature cryostat (Oxford Instuments).

2.16 Electron nuclear double resonance spectroscopy (ENDOR)

ENDOR spectra were recorded using an X-band ESP300 spectrometer (Bruker) associated with a Bruker EN 003 ENDOR interface, Wavetek 3000-446 radiofrequency synthesiser, EN 370 power amplifier and EN 801 ENDOR cavity (Rigby *et al.*, 1994a). All spectra were recorded at 60K using an Oxford Instruments continuous flow cryostat. ESR and ENDOR conditions used are indictated in the figure legends. The precision of the hfc determination or the variation in hfc determination between the samples was ±0.1MHz. The spectra are presented as the first derivative. The hfc's are measured from zero crossover points, except for $A_{||}$ features where the peak maximums / minimums are used.

2.17 Electron spin echo envelope modulation spectroscopy (ESEEM)

ESEEM spectra were recorded on a Bruker ESP380E X-band pulsed spectrometer which was equipped with a variable Q,

dielectric resonator (Bruker model 1052 DLQ-H 8907). For a s=1/2, g=2.002 system, the maximum microwave magnetic field (generated by a 1KW travelling wave tube amplifier was approximately 0.6mT within the 10mm homogenous region of the resonator. All ESEEM spectra were acquired at 4K with a cavity quality factor, (Q) of about 100 which corresponds to a minimum dead time of approximately 100ns. Where shown, three pulse 1D ESEEM spectra were acquired with the phase cycled stimulated echo sequence (π-/2-τ-π/2-T-π/2) with π/2=16ns where τ is held constant and T is varied. The echo was recorded with the Bruker integrator ESP380-IN1078 with a variable gate width. Data analysis was performed using Bruker WINEPR software.

2.18 Optical spectroscopy

Optical spectra were obtained using a split beam spectrophotometer constructed in the workshop of the Irvine Building, School of Biological and Medical Sciences at the University of St. Andrews linked to a PC fitted with a data handling system developed at the Glynn Research Institute, Bodmin, Cornwall, UK. The spectrometer could be adapted so as to allow spectra to be recorded at 77K as well as room temperature.

2.19 Decylubiquinol oxidase assays

Decylubiquinol oxidase activities were measures at 30°C using a Clark-type oxygen electrode (Rank Brothers). The reaction vessel had a working volume of 2.5ml. 50mM TES, pH7.0 was used as a buffer. Oxidase concentrations were approximately 2μM. Decylubiquinone was reduced with the addition of a small amount

of sodium borohydride. The reactions were inititated with the addition of decylubiquinol (200μM final)

2.20 Analytical Methods

All protein determinations were performed according to Lowry *et al.*, 1951 with the inclusion of 1% sodium dodecyl sulphate. All reactions were conducted at 37°C, using bovine serum albumin as a standard. The concentration of cytochromes bo_3 and *bd* was determined using the absorbtion coefficients $E_{560\text{-}580}$ of 18.7 and 14.8$mM^{-1}cm^{-1}$ respectively for the low spin *b* haem from the reduced minus oxidised optical difference spectrum (Kita *et al*, 1984a,b)

2.22 Materials

E. coli strain BL21(DE3)/pET.E2 was a gift of Dr. M. Saraste, EMBL, Heidelberg, Germany. DH5α and NM522 were obtained from Pharmacia. All other strains and *cyo*A mutant W136A were a kind gift of Prof. R.B. Gennis, University of Illinois at Urbana-Champaign, Illinois, USA.

Decylubiquinone, ubiquinone-1, vitamin K_1 and menadione were obtained from Sigma as were octylgluoside, triton X-100 and dodecylmaltoside, HOQNO, DPPH, deuterium oxide and isopropan(*ol-d*). Yeast extract, tryptone, and acid-hydrolysed casein were obtained from Merck. Aurachin D and tridecylstigmatellin were a kind gift of Dr. P. Rich, formerly of Glynn Research Institute, Bodmin, Cornwall, UK.

USE mutagenesis kits and Phosphorylation kits were obtained from Pharmacia Biotech. Restriction enzymes and other molecular

biology reagents were obtained form New England Biolabs, USA. All other laboratory reagents including redox dye mediators were obtained form Sigma or Aldrich Chemical Company.

3.0 SEMIQUINONE STABILISATION BY CYTOCHROME bo_3

3.1 Introduction

Chapter 1.9 reviewed the recent literature concerning the elucidation of the structure and functional relationships in cytochrome bo_3 and chapter 1.10 focused on the current understanding of quinone binding to the complex. The principle aim of this chapter is to describe experiments designed to probe further the thermodynamics of quinol oxidation and to provide conclusive evidence on the nature of quinone binding and the resultant implications for the catalytic mechanism of the enzyme.

Ingledew *et al.*, 1995, in a study using ESR spectroscopy described the presence of a ubisemiquinone radical intermediate associated with the cytochrome bo_3 complex during potentiometric titrations and thermodynamic behaviour of the species. The results were deemed consistent with there being one quinone binding site and that being the site of quinol oxidation. In addition the ESR spectrum of the semiquinone had partially resolved hyperfine splittings at 0.4mT which were unassigned.

Sato-Watanabe *et al.*, 1994b observed that when the cytochrome bo_3 complex was extracted using dodecylmaltoside, a stoichiometric amount of ubiquinone-8 co-purified with the complex. Extraction with octylglucoside and triton X-100 resulted in a preparation with little or no bound quinone. Based on inhibitor binding studies the quinone molecule was proposed to bind in a second high-affinity site separate from the ubiquinol oxidation site. A further ESR study of this bound quinone gave a semiquinone species similar to that described by Ingledew *et al.*, 1995 (the enzyme in this study was prepared using octylglucoside/triton X-

100 extraction and reconstituted with excess ubiquinone analogue) in terms of the thermodynamic properties and the lineshape of the ESR spectrum of the semiquinone (Sato-Watanabe *et al.*, 1995). They concluded that there would appear to be no ESR active semiquinone at the site of ubiquinol oxidation under the conditions of the potentiometric titrations conducted in both studies.

The aims of the present chapter are five-fold. The first was to reconcile the findings of Ingledew *et al.*, and Sato-Watanabe *et al.*, in the light of the ambiguity in quinone binding due to the choice of extraction detergent. To this end potentiometric titrations of the membrane-bound cytochrome bo_3 complex with endogenous ubiquinone-8 and of the octylglucoside/triton X-100 and dodecylmaltoside preparations with and without excess quinone were conducted.

The second was to probe the structure of the quinone binding site giving rise to the ESR spectrum using ubiquinone and menaquinone analogues and other substituted benzoquinones and assessing the effect on the lineshape of the ESR spectrum of the semiquinone. Deuterium exchange and ^{15}N labelling studies were conducted in an attempt to identify the species giving rise to the hyperfine splittings of the semiquinone ESR spectrum.

The third was to assess the effect of the inhibitors HOQNO and tridecylstigmatellin on semiquinone formation during potentiometric titrations. Both inhibitors are known to act at sites of quinone binding and inhibit ubiquinol oxidation (Kita *et al.*, 1984a; Meunier *et al.*, 1995).

The fourth aim, in view of the availability of a crystal structure of the *cyo*A fragment (Wilmanns *et al.*, 1995) and given that subunit II has been implicated in quinone binding to the complex (Welter *et al.*, 1994) was to assess this hydrophilic portion of subunit II , using ESR, for the presence of any quinone binding and subsequent semiquinone stabilisation ability.

Finally, the semiquinone radicals of two subunit II mutants, K118L and W136A were studied using ESR. Despite the sequences of many quinone binding proteins being known including the crystal structures of two there is no overall structural motif to identify an amino acid residue as being part of a quinone binding site. The sequences of all the known haem-copper quinol oxidases were aligned with three cytochrome *c* oxidases. Differences between the two sub-groups were probed by site-directed mutagenesis and the resultant mutant, K118L together with W136A were studied using ubiquinol oxidase assays, redox potentiometery and ESR.

3.2 Results & Discussion

3.2.1 ESR spectra of semiquinone species associated with the cytochrome bo_3 complex.

Quinol oxidation or reduction proceeds through two one-electron transfer steps with a semiquinone produced as a reaction intermediate. Quinone binding sites which stabilise a semiquinone do so by roughly equalising the midpoint potentials of the two one electron couples, E_1 ($Q/Q^{\cdot -}$) and E_2 ($Q^{\cdot -}/QH_2$). The stability constant of free semiquinone at pH7.0 is approximately 1×10^{-10} therefore in order for the quinol oxidation (or quinone reduction) reaction to proceed a high degree of kinetic and thermodynamic stabilisation mediated by the protein is required. The binding of the semiquinone must be around 1×10^{5} times as tight to achieve a stability constant of 1 (Mitchell, 1975; 1976). By restricting the semiquinone species to a specific site the protein also prevents the establishment of unproductive or damaging reactions given the high reactivity of the species.

Biological ubisemiquinones in respiring mitochondria were first detected by ESR in 1970 with signal at g=2.003 tentatively assigned to the species (Bäckström *et al.*, 1970; Hamilton *et al.*, 1970). Since then many more stable semiquinones have been identified and characterised by ESR in a wide range of photosynthetic and respiratory systems. The semiquinone species associated with the cytochrome bo_3 complex was first identified by Ingledew *et al.*, 1995 in a preparation of the enzyme extracted with octylglucoside/triton X-100 that had been reconstituted using an excess of ubiquinol-1. The semiquinone species formed had a line

Figure 3.1 ESR spectra of the ubi-semiquinone radical stabilised by the cytochrome bo_3 complex in *E. coli* strain RG145 membranes.

The zero cross over point is approximately g=2.004, the line width of the radical is 0.945mT. (a) Signal derived from cytochrome bo_3 present in RG145 membranes washed with 200mM bis-tris-propane pH9.0 then overnight anaerobic incubation at 4°C. (b) As (a) but membranes washed twice with buffer in D_2O, pD9.0. (c) Difference spectrum (a) minus (b). The membranes contained approximately 30mg protein ml^{-1} . EPR conditions were as follows : Temperature, 100K; modulation frequency, 100kHz; modulation amplitude, 0.1mT, microwave frequency, 9.45GHz; microwave power 0.2mW.Average of 50 scans.

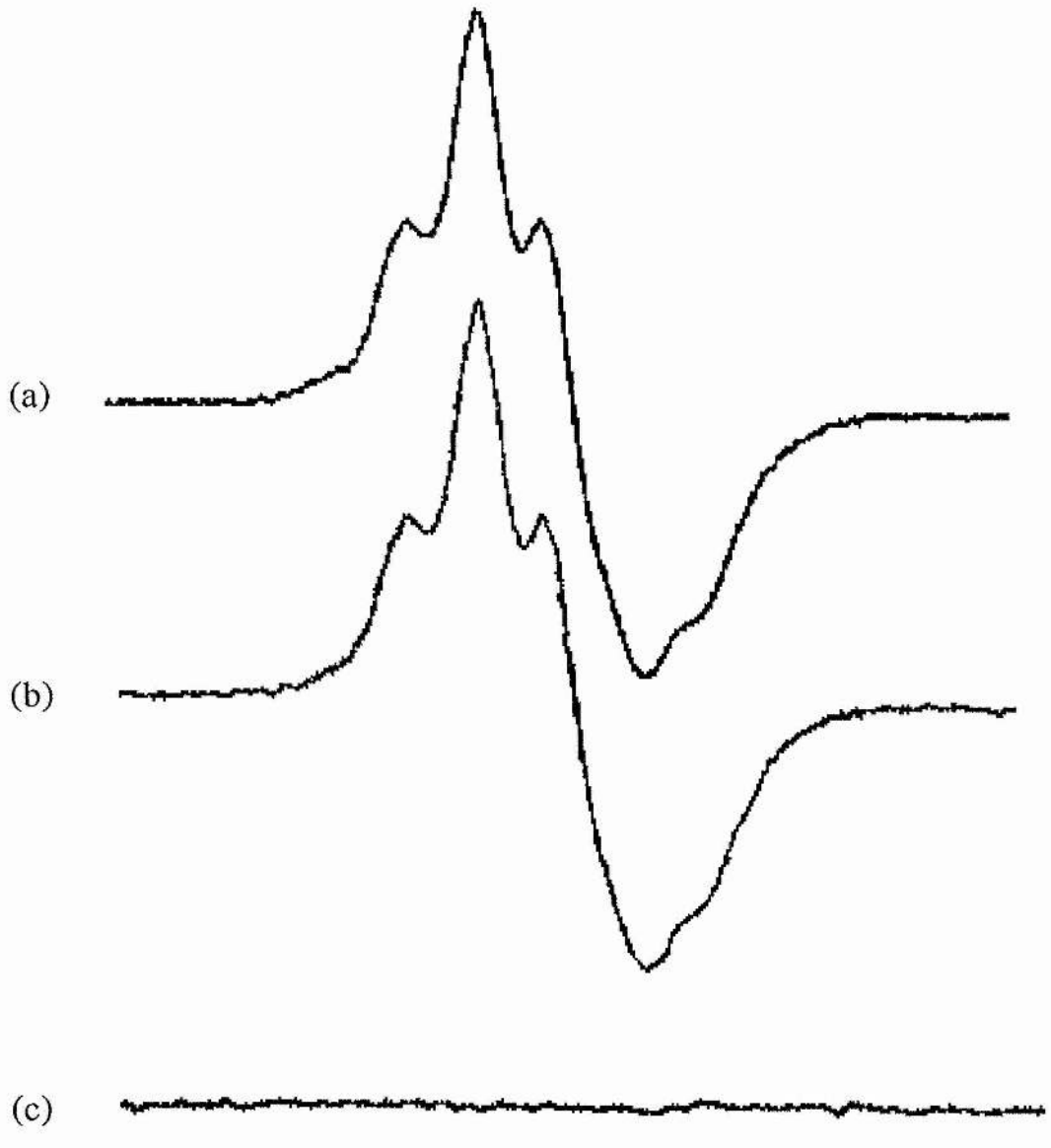
(a)
(b)
(c)
1mT

width of approximately 0.9mT and was unusual by virtue of its partially resolved hyperfine splittings of 0.4mT. Such splittings arise from the interaction of the unpaired electron with surrounding nuclei or other unpaired electrons. The influence of the surrounding protein environment on a semiquinone is well documented. Hydrophobic and hydrophilic interactions along with hydrogen bonding between semiquinone and protein are major contributors to the perturbation of the ESR spectrum.

Efforts to assign the interactions leading to the hyperfine splittings were unsuccessful largely due to the low concentration of semiquinone observed during potentiometric titrations. A new method of poising the semiquinone was developed in the present study to increase the concentration of the radical (outlined in chapter 2.12). This lead to a much improved signal to noise ratio with the hyperfine splittings better defined. Figure 3.1(a) shows the semiquinone derived from the cytochrome bo_3 complex in RG145 membranes (a *cyd*$^-$ strain) under the conditions indicated. The quinone being stabilised is the endogenous ubiquinone-8. The line width of the ESR signal is 0.945mT (peak centre to trough centre). When the membranes are exchanged into deuterium oxide (>99%) there is little change to the lineshape of the spectrum as demonstrated by the difference spectrum (a) minus (b). Therefore either protons do not contribute significantly to the spectrum or the position of the site in the complex is such that it does not allow the efficient exchange of protons with the aqueous medium.

Figure 3.2(a) shows the spectra obtained form octylglucoside/triton X-100 extracted cytochrome bo_3.with an

Figure 3.2 ESR spectra of the ubisemiquinone radical stabilised by the purified cytochrome bo_3 complex.

(a) Signal derived from octylglucoside/triton X-100 extracted cytochrome bo_3 (~250μM) in 200mM bis-tris-propane, pH9.0 reconstituted with excess (1mM) ubiquinone-2 analogue, decylubiquinone and reduced using sodium dithionite. (b) As (a) but exchanged with buffer in D_2O, pD9.0. (c) Difference spectrum (a) minus (b). ESR conditions same as in figure 3.1.

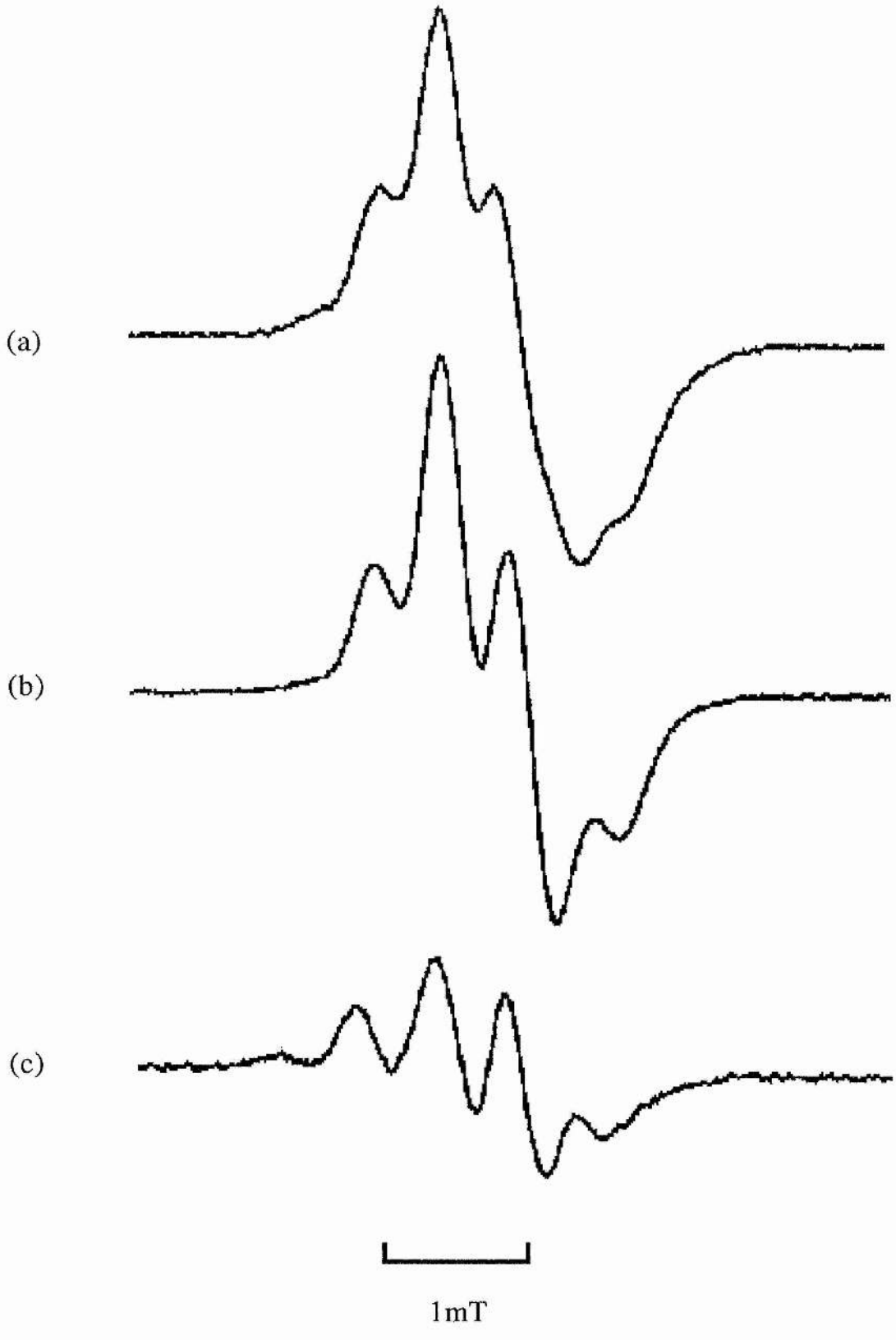
(a)
(b)
(c)
1mT

excess of the ubiquinone-2 analogue, decylubiquinone. Samples extracted in this way and then precipitated in ammonium sulphate should have little or no native quinones bound (Sato-Watanabe *et al.*, 1995b; Puustinen *et al.*, 1996). The sample was prepared as described in chapter 2.12.2 and gives a similar spectrum to figure 3.1(a). When this cytochrome bo_3 preparation was exchanged into D_2O the hyperfine splitting on the upfield side of the spectrum became more resolved providing a clear difference between the two as in 3.2(c). This effect indicates the presence of exchangeable protons at the site, not accessible in the membrane-bound complex but these are not a major factor in the hyperfine splittings. The hyperfine splitting becomes better resolved as a result of the removal of the line broadening effects of protons. Hydrogen bonding to the semiquinone broadens the radicals spectrum by the incorporation of additional hyperfine structure arising from the bond. These effects are lessened in a deuterated solvent due to the smaller magnetic moment of the deuterium nuclei (Hales & Case, 1981).

The semiquinone radical species derived from the endogenous ubiquinone-8 and the ubiquinone-2 analogue, decylubiquinone are essentially the same. Therefore, despite the large change in tail length of the two quinones, the influence of this group upon quinone binding would appear to be minimal. This is consistent with a study of the influence of tail length on cytochrome bo_3 quinol oxidase activities (Sakamoto *et al.*, 1996) but in contrast to the findings of a similar study of the Q_A and Q_B sites from the photosynthetic reaction centres which claimed a specific role for the tail structure in quinone binding (Warncke *et al.*, 1994).

The complexity of the ESR spectrum may have been the result of an interaction with a nitrogen nucleus. ^{14}N has a spin of 1 and an interaction of a semiquinone with a nucleus of this type would be expected to produce a complex splitting pattern. Any hyperfine interaction arising from coupling to ^{14}N could be indicated by a change in the ESR spectrum of semiquinone when the protein is labelled with the stable isotope, ^{15}N, which has a spin of $^1/_2$. Figure 3.3 shows the ESR spectrum of the semiquinone species associated with the ^{15}N labelled cytochrome *bo*$_3$ complex. The resulting spectrum is very similar to the 'normal' ^{14}N semiquinone and it is therefore unlikely to be a nitrogen nucleus causing the hyperfine structure of the Q_{bo} radical.

Gaining further information on the structure of this quinone binding site may be achieved by binding a different quinone to the site and observing the effects, if any, on the ESR spectrum of the semiquinone. One choice would be a napthoquinone e.g. vitamin K_1. The cytochrome *bo*$_3$ complex is thought to be more specific for ubiquinone as this is the predominant quinone under aerobic growth conditions (Ingledew & Poole, 1984). The quinol oxidase activities of the two types of quinone are however comparable (Kita *et al.*, 1984a). The difference between the structures of menaquinone and ubiquinone is the replacement of the methoxy groups at C-5 and C-6 with an aromatic ring structure (see below). The introduction of bulky ethoxy at these positions had most effect on the quinol oxidase activity of the enzyme when introduced at C6 (Sakamoto *et al.*, 1996). The methoxy groups would appear to have a role in quinone binding. Figure 3.4, shows the ESR spectrum of the menasemiquinone species bound to cytochrome *bo*$_3$ along with the

Figure 3.3 ESR spectrum of the ubi-semiquinone radical stabilised by the ^{15}N labelled cytochrome bo_3 complex.

ESR spectrum derived from membranes of *E. coli* strain RG145 grown on minimal media supplemented with $(^{15}NH_4)_2SO_4$. Membranes were washed with 200mM bis-tris-propane pH9.0 and then incubated anaerobically overnight at 4°C. ESR conditions same as in figure 3.1.

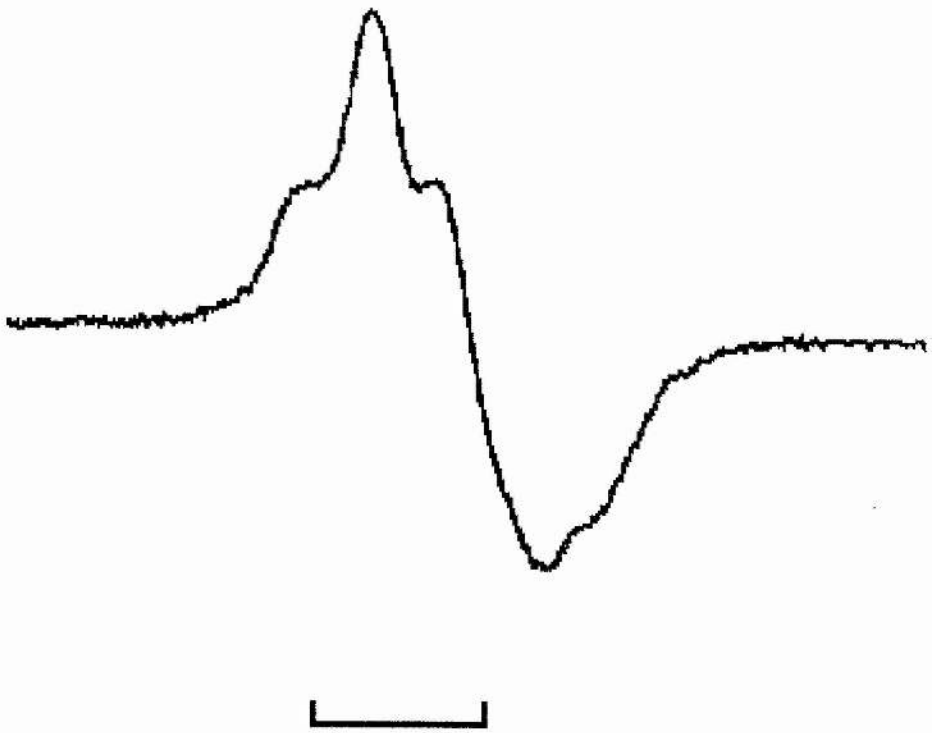
1mT

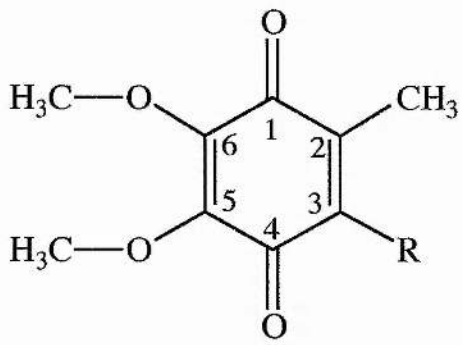

ubiquinone

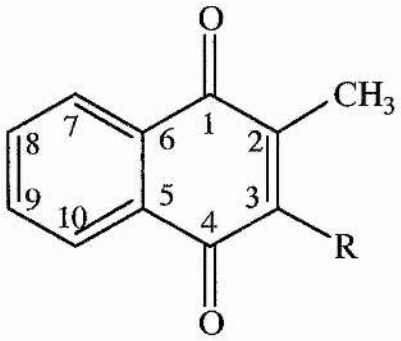

menaquinone

ubisemiquinone spectrum. As indicated by the difference spectrum (a) minus (b) the two are dissimilar particularly in the upfield region of the spectrum. This difference is most probably due to the rearrangement of the electronic structure in the quinone which exerts a slight effect on the hyperfine interactions. Although of possible importance in quinone recognition the methoxy groups do not contribute significantly to the ESR spectrum of the semiquinone species.

3.2.2 Thermodynamics of semiquinone stabilisation

3.2.2.1 Membrane-bound cytochrome bo_3 with endogenous ubiquinol-8.

Ingledew *et al.*, 1995 and later Sato-Watanabe *et al.*, 1995 reported the potentiometric behaviour of the semiquinone species associated with the cytochrome bo_3 complex using the purified enzyme reconstituted with excess ubiquinone-1. The redox behaviour of the semiquinone associated with the membrane-bound enzyme has not been characterised nor the semiquinone reported. Figure 3.1 showed the ESR spectrum of the endogenous semiquinone. This semiquinone was observed in potentiometric

Figure 3.4 A comparison of the ESR spectra of ubisemiquinone and mena-semiquinone species stabilised by the purified cytochrome bo_3 complex.

(a) Signal derived from octylglucoside/triton X-100 extracted cytochrome bo_3 (~250μM) in 200mM bis-tris-propane, pH9.0 reconstituted with excess (1mM) ubiquinone-2 analogue, decylubiquinone and reduced using sodium dithionite. (b) As (a) but reconstituted with excess (1mM) menaquinone-2 analogue, vitamin K_1. (c) Difference spectrum (a) minus (b). ESR conditions same as in figure 3.1.

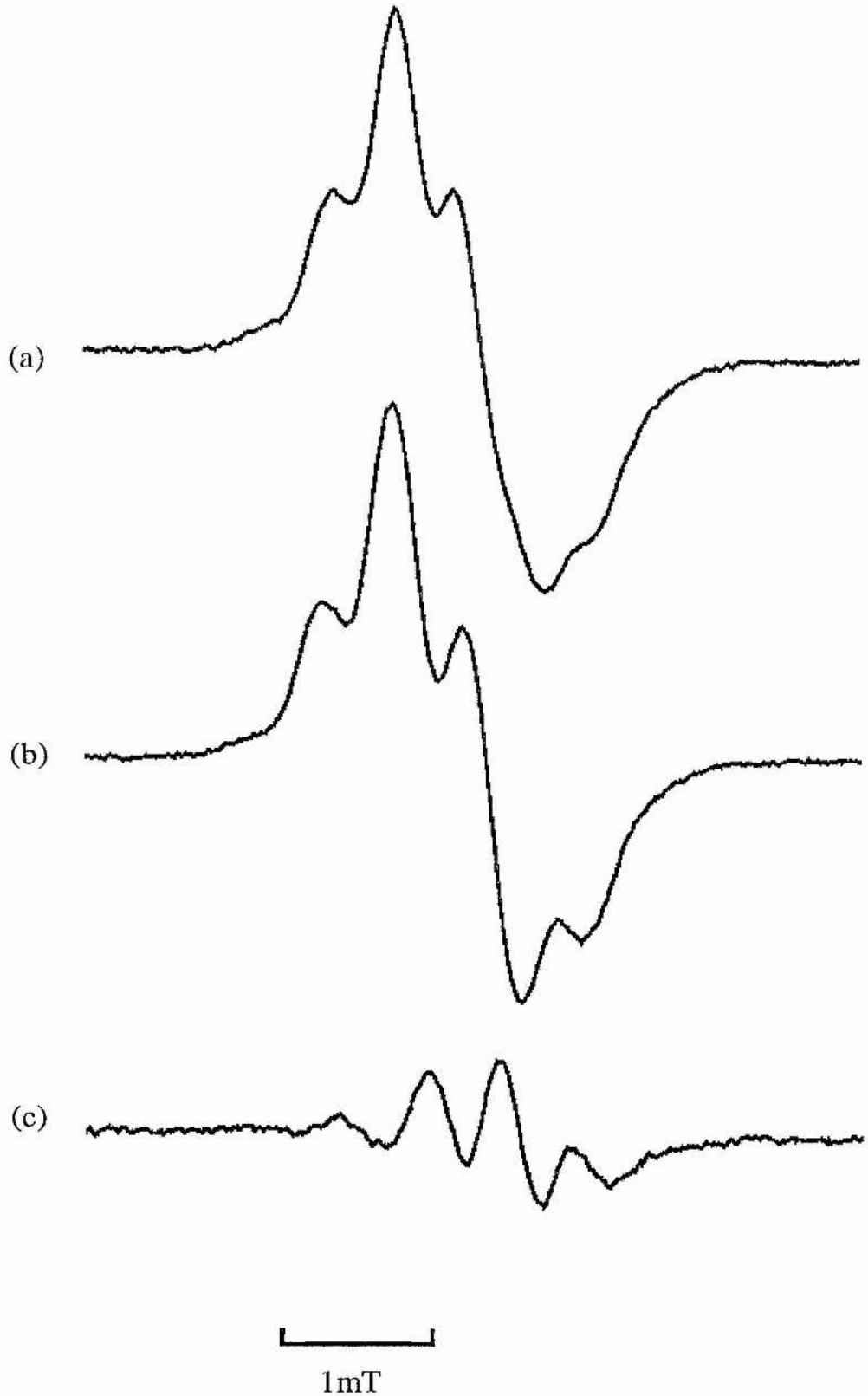
(a)
(b)
(c)
1mT

titrations of *E. coli* strain RG145 membrane suspensions. Figure 3.5 demonstrates the variation in the occupancy of the quinone binding site by the semiquinone in response to changes in the ambient redox potential, E_h, over the pH range 7.5 - 9.5. The semiquinone titrates in general as a bell-shaped curve, the rise in semiquinone concentration as E_h is increased corresponds to the oxidation of quinol to semiquinone and the subsequent decrease past the maximum is attributed to the oxidation of semiquinone to quinone. These two one-electron transfer steps have mid-point potentials of E_2 and E_1 respectively. The maximal semiquinone concentration occurs at E_m, the mid-point potential of the quinol/quinone two-electron couple ($E_m=^1/_2[E_1+E_2]$).

$$QH_2 \Leftarrow E_2 \Rightarrow Q^{\cdot -} \Leftarrow E_1 \Rightarrow Q$$

The results were modelled using a derivation of the Nernst equation as described in chapter 2.10. The theoretical curves were obtained by varying E_1 and E_2 to optimise the data fit as indicated (Ingledew *et al.*, 1995).

As shown by figure 3.6 the maximal occupancy of the quinone binding site by semiquinone is also dependent on pH. The radical appears to be more stable at alkaline pH. The maximum amount of semiquinone formed at pH9.5 is four times that at pH7.5. This is a feature of all known sites of semiquinone stabilisation and is due to the anionic form of the semiquinone being stabilised.

A plot of E_1, E_2 and E_m vs pH (figure 3.7) shows the pH dependencies of these couples. The state diagram below indicates the

possible redox and protonation states of the bound quinone likely to be important over the pH range

$$\begin{array}{ccc} QH_2 & & \\ \uparrow\downarrow pK2 & & \\ QH^- & \Leftarrow E_2 \Rightarrow & QH\cdot \\ & & \uparrow\downarrow pK1 \\ & & Q\cdot^- \Leftarrow E_1 \Rightarrow Q \end{array}$$

(adapted from Ingledew *et al.*, 1995)

studied. As described by Salerno *et al.*, 1990, the equilibrium between these states can be represented by four parameters, pK_1, pK_2, $E_{1'}$ and $E_{2'}$. The two one electron potentials E_1 and E_2 can be written in terms of these:-

$$E_1=E_{1'}+59\log(1+10^{pK1-pH})$$

$$\text{and } E_2=E_{2'}+59\log[(1+10^{pK2-pH})/(1+10^{pK1-pH})]$$

Thus, a pH below both pKs will result in E_1, E_2 and E_m all having a -60mV/pH dependence. At a pH above both pKs, E_1 will be pH independent, E_2 will have a -60mV/pH dependence and E_m will have a -30mV/pH dependence. In the region between the pKs, if $pK_1<pK_2$ E_1 will be pH independent, E_2 will have a -120mV/pH dependency and E_m will have a -120mV/pH dependence. If this situation is reversed and $pK_1>pK_2$, E_2 will be pH independent, E_1 will have a -60mV/pH dependency and E_m will have a -30mV/pH dependence.

The theoretical fits shown in figure 3.7 are derived using the following parameters:- $E_{1'}$=40.75mV, $E_{2'}$=-76.5mV, pK_1=8.9 and pK_2=11.2. The -60mV/pH dependence over the pH range studied

Figure 3.5 The occupancy of the quinone binding site of membrane-bound cytochrome bo_3 by ubisemiquinone as a function of E_h, at different pH values.

The concentration of the semiquinone is converted to site occupancy (assuming one semiquinone stabilising site per low-spin haem *b*) and plotted against the ambient redox potential (E_h). Redox titrations were performed as described in chapter 2.8. The concentration of cytochrome bo_3 varied from 5-10μM with the protein content of the RG145 membranes being typically 30mg/ml. The buffer was 200mM bis-tris-propane adjusted to the required pH. The theoretical curves were obtained as described in chapter 2.10 using the following parameters:- (a) pH7.5, E_1=47.5mV, E_2=132.75 mV; (b) pH8.0, E_1=18.75 mV, E_2=107.5 mV; (c) pH8.5, E_1=-10.75 mV, E_2=73.5 mV; (d) pH9.0, E_1=-26.0 mV, E_2=30.0 mV; (e) pH9.5, E_1= -29.0 mV, E_2=-20.0 mV.

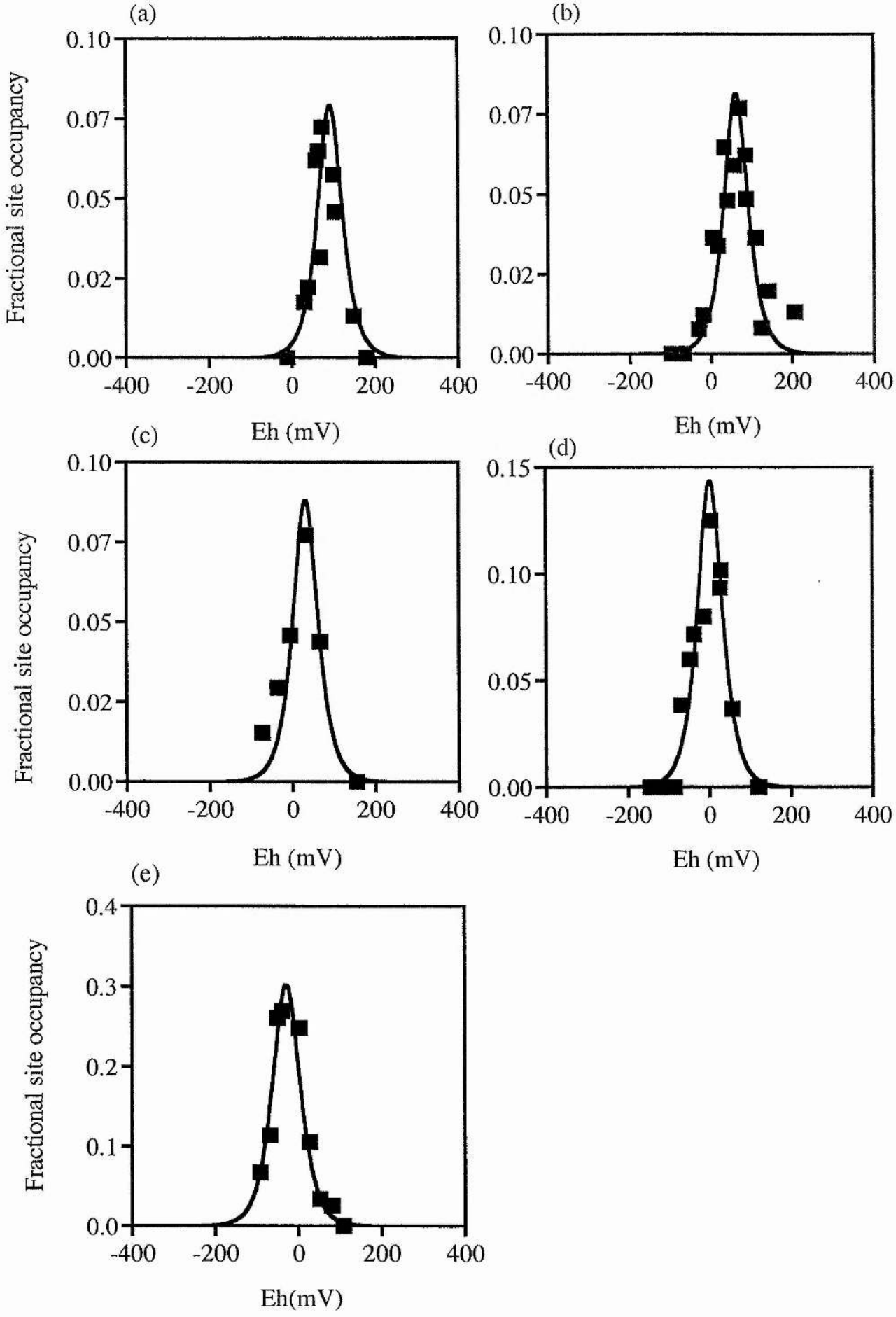
(a)
(b)
(c)
(d)
(e)
Fractional site occupancy
Eh (mV)
Eh(mV)
0.10
0.07
0.05
0.02
0.00
0.15
0.10
0.4
0.3
0.2
0.1
0.0
-400
-200
0
200
400

Figure 3.6 The pH dependence of the maximum site occupancy derived from membrane-bound cytochrome bo_3.

The maximum site occupancy is obtained from the theoretical curve data. The semiquinone concentration is normalised to unity. This assumes that there is one semiquinone stabilising site per low-spin haem *b*.

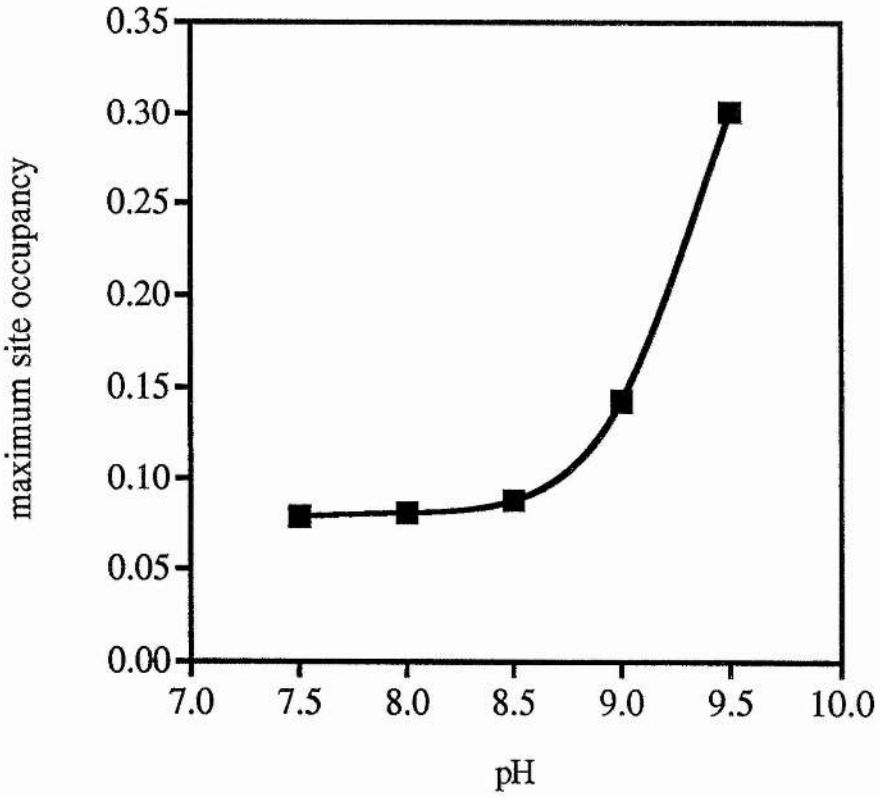
maximum site occupancy
0.35
0.30
0.25
0.20
0.15
0.10
0.05
0.00
7.0
7.5
8.0
8.5
9.0
9.5
10.0
pH

indicates that the predominant two-electron couple is Q/QH_2 (a $2H^+/2e^-$ reaction) instead of the other possibility of $Q/QH^{\cdot -}$. The data-fit suggests that pK_1=8.9 (quinone). The value assigned to pK_2 (quinol) of 11.2 lies outwith the pH range and so this assignment must be viewed as tentative. From pH7.5 to 8.5 all three couples have -60mV/pH dependencies indicating $Q \Leftrightarrow Q^{\cdot} H \Leftrightarrow QH_2$. Above pH8.5, E_1 tends towards pH independence and E_2 tends towards a -120mV/pH dependency indicating $Q \Leftrightarrow Q^{\cdot -} \Leftrightarrow QH_2$ with, the anion form of the semiquinone being the dominant species at high pH. These results are summarised in Table 3.1(a).

A requirement for quinol oxidation is the stabilisation of the semiquinone in order to roughly equalise the potentials of the two one-electron transfers. Extrapolation of the theoretical curves indicate that E_1 and E_2 would be equalised at approximately pH=9.8 when the cytochrome *bo*$_3$ complex is in the membrane. At pH7.5 the semiquinone is still stable in comparison to free ubisemiquinone. The difference in E_1 and E_2 is approximately 90mV with the quinol/semiquinone couple being of higher potential at 132.75mV, pH7.5. If a -60mV/pH dependence is assumed this would give E_2 a value of around +160mV, pH7.0. This would allow efficient electron transfer to occur between Q_{bo} and the low-spin haem *b* the most likely electron acceptor.

When the data from the *in situ* cytochrome *bo*$_3$ complex is compared to that of the similar studies of the purified enzyme there is a clear difference in both the midpoint potentials of the one-electron couples and the maximum amount of semiquinone formed (Ingledew *et al.*, 1995; Sato-Watanabe *et al.*, 1995). The pH

Figure 3.7 The pH dependence of the redox couples E_1, E_2 and E_m for the ubisemiquinone derived from membrane-bound cytochrome bo_3.

The values for the two half potentials E_1(▲) and E_2(▼) were obtained from the theoretical curves for figure 3.5. E_m(■)values are a function of E_1 and E_2. Each is shown as a function of pH. The theoretical curves were simulated using the relationship for E_1 and E_2 described in the text. The values for each parameter were as follows $E_{1'}$=40.75mV, $E_{2'}$=-76.5mV, pK_1=8.9 and pK_2=11.2.

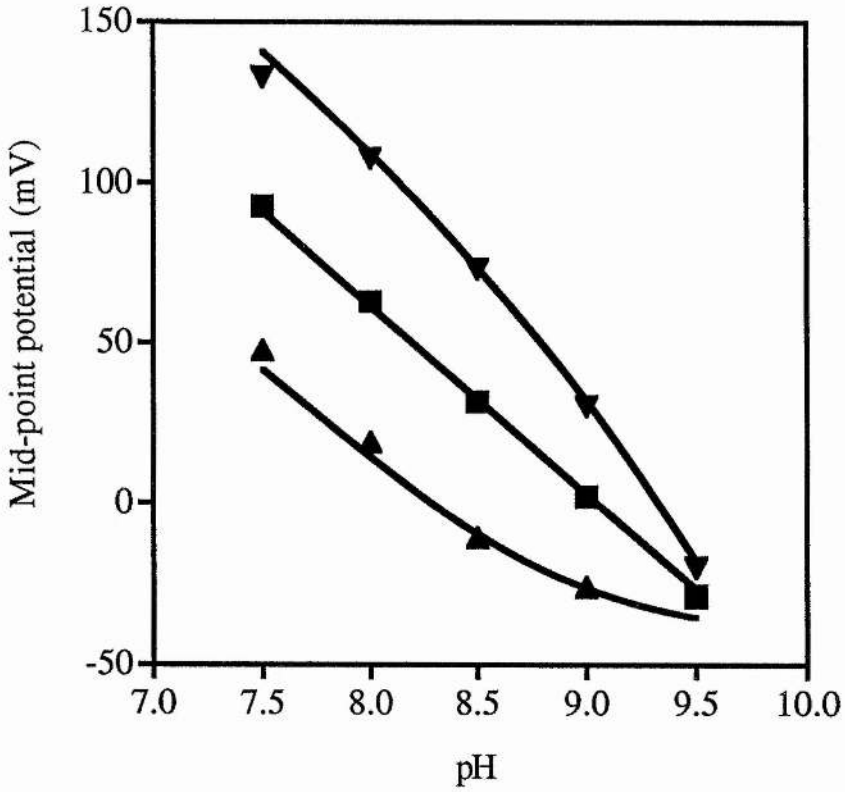
150
100
50
0
-50
Mid-point potential (mV)
7.0
7.5
8.0
8.5
9.0
9.5
10.0
pH

dependency of the E_m of the two-electron couple remains at -60mV/pH but there was also an apparent shift in E_m for the membrane-bound cytochrome *bo*$_3$ ubisemiquinone radical of approximately -40mV. In view of these discrepancies it was decided to repeat the experiments of the previous studies on the purified enzyme.

3.2.2.2 Octylglucoside/triton X-100 extracted cytochrome *bo*$_3$ with decylubiquinone (Q-2) and ubiquinone-1.

The previous experiments of Ingledew *et al.*, 1995 and Sato-Watanabe *et al.*, 1995 were repeated in light of the results from the potentiometric analysis of the membrane-bound cytochrome *bo*$_3$ complex. A his-tagged form of the enzyme was extracted with octylglucoside/triton X-100 and purified as described in chapter 2.4. An excess of a ubiquinone-2 analogue, decylubiquinone (1mM) was added and the redox titrations conducted as described previously. Figure 3.8 shows the results of these titrations at various pH's. The values for E_1 and E_2 differed from those of the previous studies and from the membrane-bound complex but the E_m values agreed well with those of the *in situ* enzyme. The $E_{m,7}$ was +105.75 similar to that of the free ubiquinone/ubiquinol of approximately 100mV. For comparison a redox titration in using 1mM ubiquinone-1 was conducted at pH 9.0. As expected a similar result to that using excess decylubiquinone was obtained and is shown in figure 3.9.

The maximum amount of semiquinone formed (figure 3.10) was about double that found with the membrane-bound enzyme with

Figure 3.8 The occupancy of the quinone binding site of octyl-glucoside/triton X-100 extracted cytochrome bo_3 by decyl-ubisemiquinone as a function of E_h, at different pH values.

The concentration of the semiquinone is converted to site occupancy (assuming one semiquinone stabilising site per low-spin haem *b*) and plotted against the ambient redox potential (E_h). Redox titrations were performed as described in chapter 2.8. The concentration of cytochrome bo_3 varied from 5-10μM. Excess ubiquinone-2 analogue decylubiquinone was added to a final concentration of 1mM. The buffer was 200mM bis-tris-propane adjusted to the required pH. The theoretical curves were obtained as described in chapter 2.10 using the following parameters:- (a) pH7.0, E_1=43.0mV, E_2=168.5mV; (b) pH7.8, E_1=32.5mV, E_2=97.0 mV; (c) pH8.4, E_1=31.5mV, E_2=27.5 mV; (d) pH9.0, E_1=25.5mV, E_2=-35.0 mV.

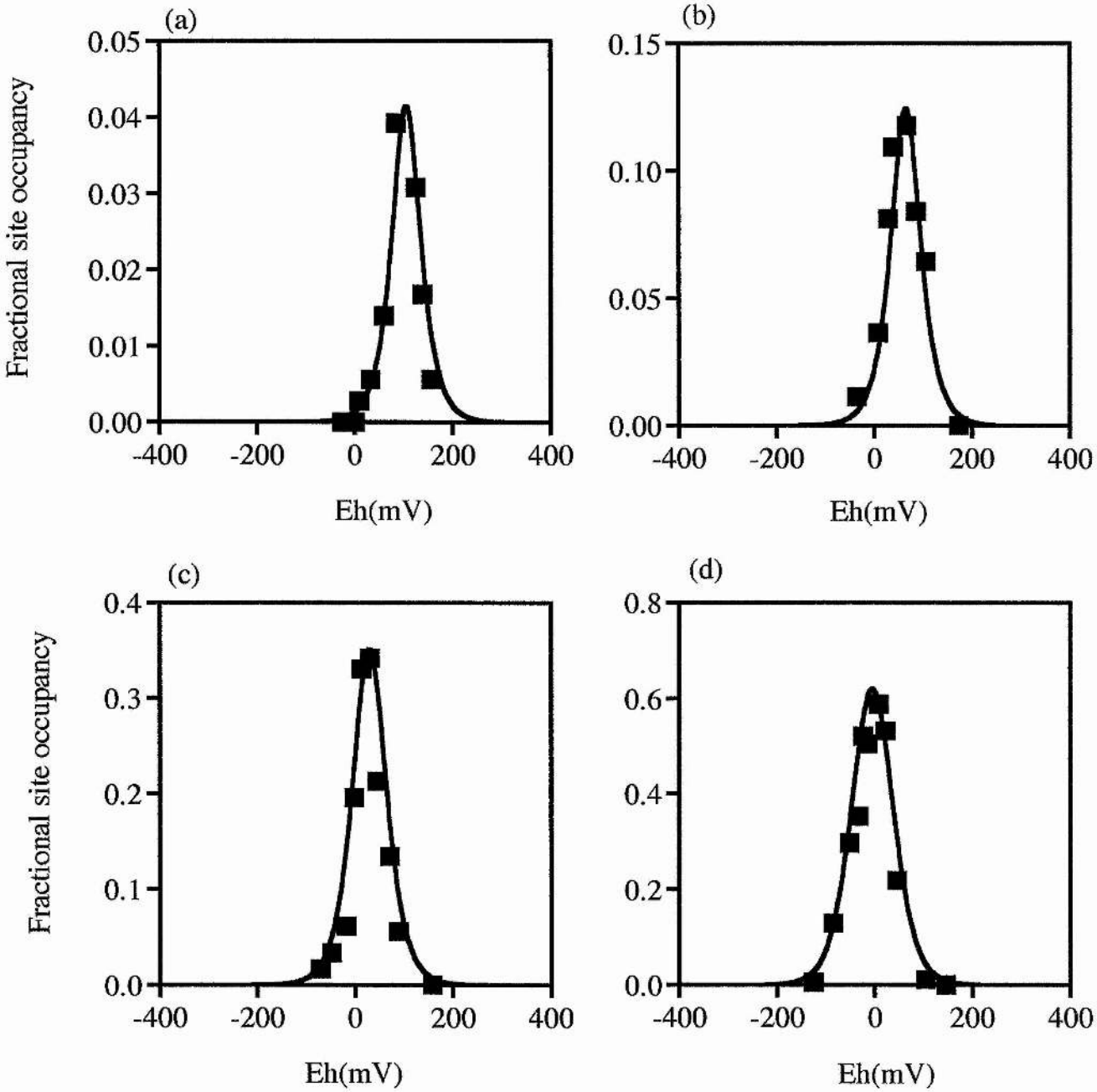
(a)
(b)
(c)
(d)
Fractional site occupancy
Fractional site occupancy
0.05
0.04
0.03
0.02
0.01
0.00
0.15
0.10
0.05
0.00
0.4
0.3
0.2
0.1
0.0
0.8
0.6
0.4
0.2
0.0
-400
-200
0
200
400
Eh(mV)

Figure 3.9 The occupancy of the quinone binding site of octyl-glucoside/triton X-100 extracted cytochrome bo_3 by ubisemiquinone as a function of E_h, at pH9.0.

Redox titrations were performed as described in chapter 2.8. The concentration of cytochrome bo_3 was 5μM. Excess ubiquinone-1 was added to a final concentration of 1mM. The buffer was 200mM bis-tris-propane adjusted to pH9.0. The theoretical curve was obtained as described in chapter 2.10 using the following parameters:- pH9.0, E_1=25.5mV, E_2=-35.0 mV.

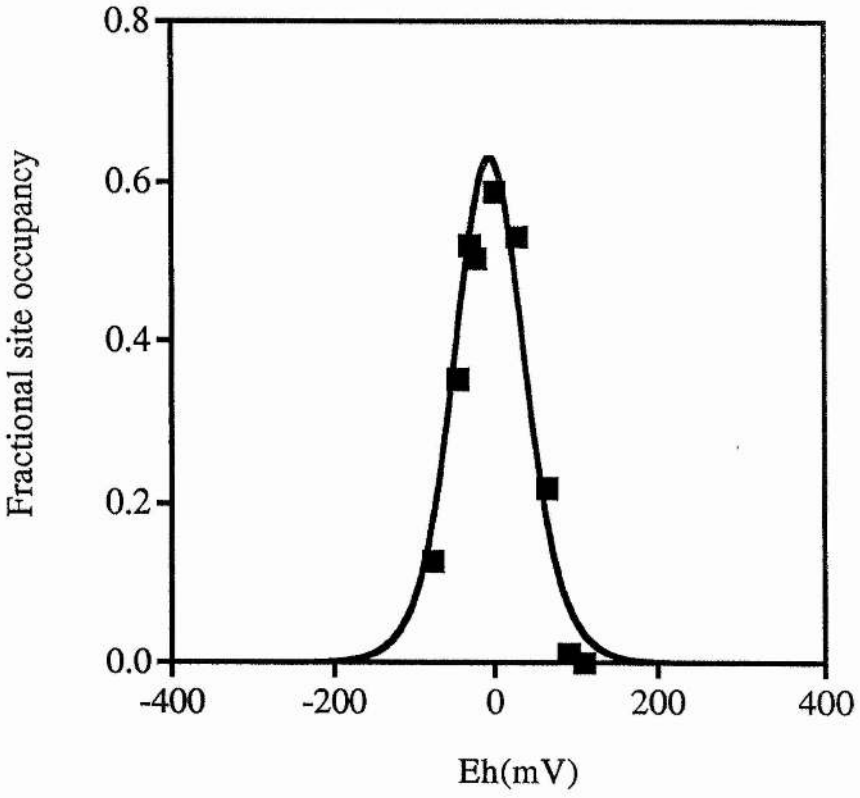
0.8
0.6
0.4
0.2
0.0
Fractional site occupancy
-400
-200
0
200
400
Eh(mV)

Figure 3.10 The pH dependence of the maximum site occupancy by semiquinone derived from octylglucoside/triton X-100 extracted cytochrome bo_3

The maximum semiquinone concentration is obtained from the theoretical curve data. The semiquinone concentration is normalised to unity. This assumes that there is one semiquinone stabilising site per low-spin haem *b*.

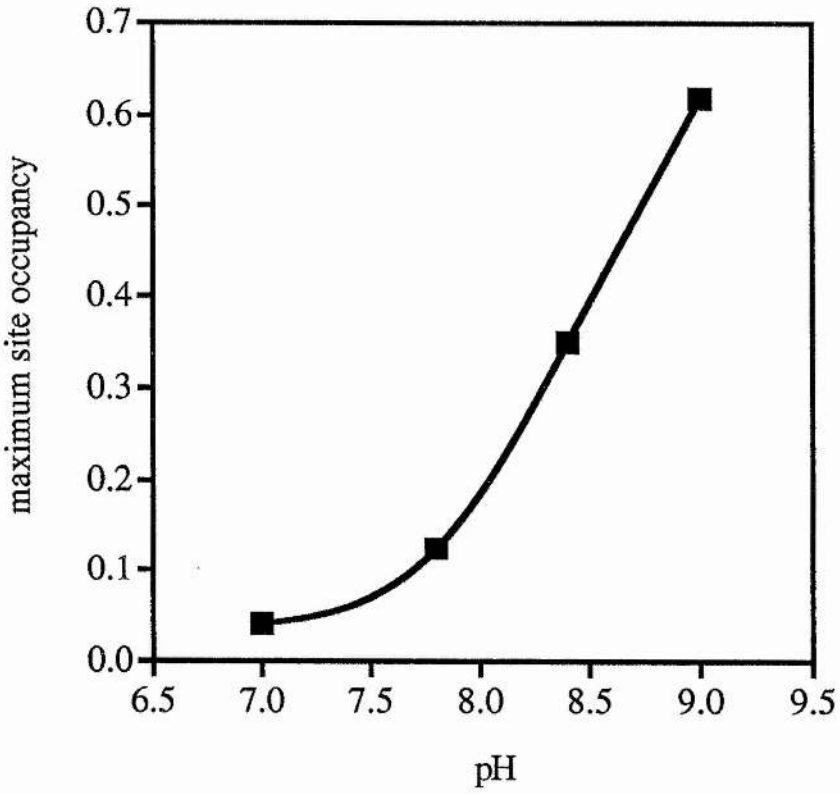
maximum site occupancy
0.7
0.6
0.5
0.4
0.3
0.2
0.1
0.0
6.5
7.0
7.5
8.0
8.5
9.0
9.5
pH

the endogenous quinone but similar to that found by Ingledew *et al.*, 1995. The values of E_1 and E_2 are dependant on the semiquinone concentration therefore a 20% reduction in semiquinone concentration will cause a 10mV change in the separation of E_1 and E_2 and vice versa. Thus the decrease in separation of E_1 and E_2 in the purified complex is enough to account for the increased semiquinone concentration observed and most probably results from a slight alteration of quinone binding in this preparation. This has implications for the values of the pK_1, pK_2, $E_{1'}$ and $E_{2'}$ which are 7.2, 10.15, +22mV, -3mV respectively (figure 3.11). However, these pK assignments must be viewed as tentative as they lie near to or outwith the limits of the data. These results are summarised in Table 3.1(b).

The shift in E_m when compared to the values found by Ingledew *et al.*, 1995 is within experimental error with the discrepancy most likely due to the different enzyme preparations.

3.2.2.3 Octylglucoside/triton X-100 extracted cytochrome bo_3 with menadione

The cytochrome bo_3 complex can oxidise *p*-napthoquinones as efficiently as *p*-benzoquinones and does not appear to discriminate between the two (Kita *et al.*, 1984a). Under the growth conditions where this oxidase is maximally expressed levels of menaquinones are low as this is the quinone utilised in anaerobic conditions. Figure 3.4 showed that binding of menaquinone analogue vitamin K_1 is slightly different from ubiquinone indicated by the difference in the ESR spectra of the semiquinone species. Figure 3.12 displays the redox behaviour of the menasemiquinone species at pH9.0. The

Figure 3.11 The pH dependence of the redox couples E_1, E_2 and E_m for the decylubisemiquinone detected in octyl-glucoside /triton X-100 extracted cytochrome bo_3.

The values for the two half potentials E_1(▲) and E_2(▼) were obtained from the theoretical curves for figure 3.8. E_m(■)values are a function of E_1 and E_2. Each is shown as a function of pH. The theoretical curves were simulated using the relationship for E_1 and E_2 described in the text. The values for each parameter were as follows $E_{1'}$=22.0mV, $E_{2'}$=-3.0mV, pK_1=7.2 and pK_2=10.15.

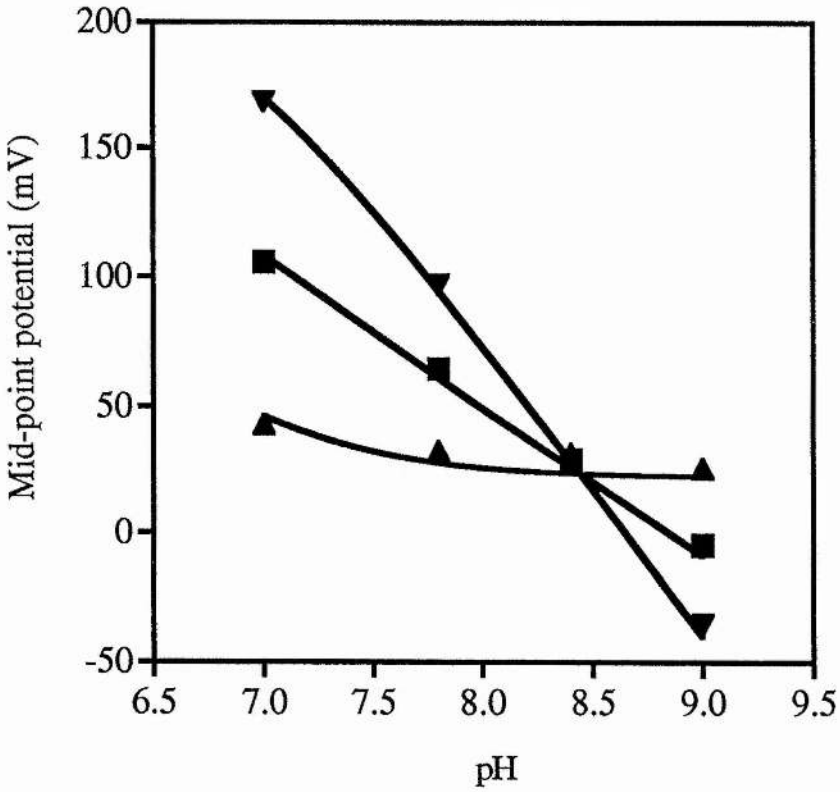
200
150
100
50
0
-50
Mid-point potential (mV)
6.5
7.0
7.5
8.0
8.5
9.0
9.5
pH

Figure 3.12 The occupancy of the quinone binding site of octyl-glucoside/triton X-100 extracted cytochrome *bo*$_3$ by menasemiquinone as a function of E_h, at pH9.0.

Redox titrations were performed as described in chapter 2.8. The concentration of cytochrome *bo*$_3$ was 5μM. Excess vitamin K_1 (a menaquinone-2 analogue) was added to a final concentration of 1mM. The buffer was 200mM bis-tris-propane adjusted to pH9.0. The theoretical curve was obtained as described in chapter 2.10 using the following parameters:- pH9.0, E_1=-94.5mV, E_2=-155.0 mV.

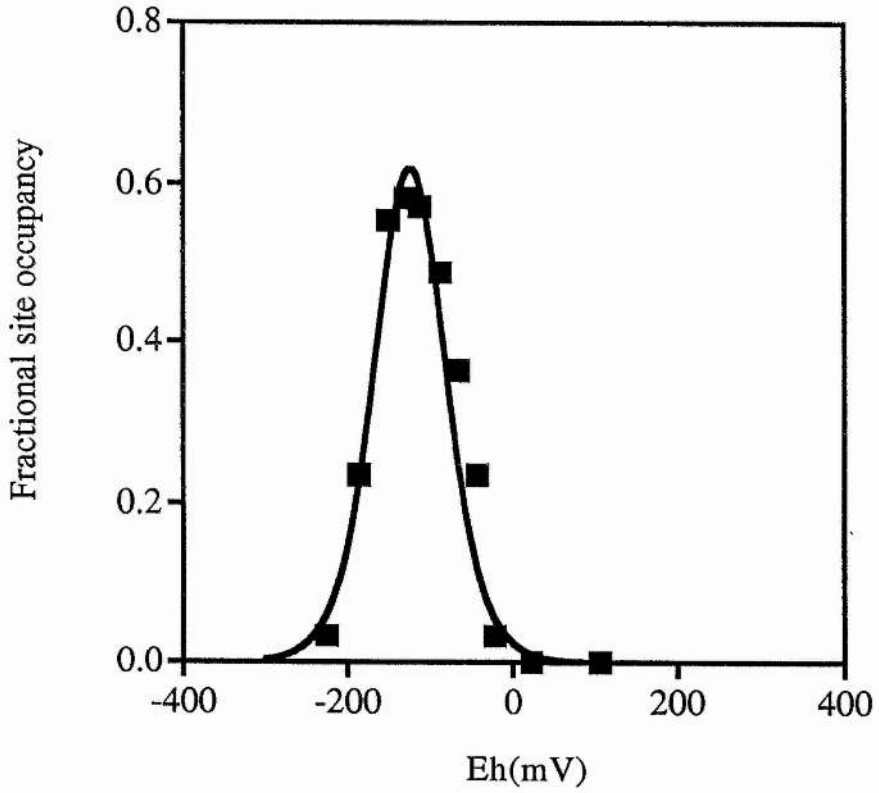
0.8
0.6
0.4
0.2
0.0
Fractional site occupancy
-400
-200
0
200
400
Eh(mV)

E_{m9} of the quinone/quinol couple is much lower than the corresponding value for ubiquinone at -125mV, this is simply a reflection of the E_m of the free system (E_{m9} ~ -120mV) and would still allow electron transfer to proceed to the low-spin haem *b*. These results are summarised in Table 3.1(b).

3.2.2.4 Sucrose monolaurate extracted cytochrome *bo*$_3$

Extracting the cytochrome *bo*$_3$ complex from the membrane with dodecylmaltoside or sucrose monolaurate results in a near stoichiometric amount of ubiquinone-8 co-purifying with the complex (Sato-Watanabe *et al.*, 1994b; Puustinen *et al.*, 1996). This was proposed to be bound to a novel high affinity quinone binding site (Q_H) separate from the site of quinol oxidation. A preparation of the cytochrome *bo*$_3$ complex extracted with sucrose monolaurate with 0.6 quinone/complex (a gift from Prof. R.B. Gennis, University of Illinois) was titrated as before in the absence of any quinone or any 'quinone-like' redox mediators. The resulting ESR spectrum (not shown) was similar to that shown in figure 3.2(a). The enzyme was present at 5μM in the titration mixture giving a quinone concentration of approximately 3μM. The occupancy of the quinone binding site by semiquinone at pH9.0 was approximately 70% less than expected in comparison at 0.095. (figure 3.13(a)). Therefore the quinone which co-purifies with the complex is most probably bound non-specifically to the enzyme with only a small amount present at the actual quinone binding site. When excess decylubiquinone is added at 1mM a similar maximum concentration to that described in chapter 3.2.3.2 is achieved, figure 3.13(b). The $E_{m,9}$'s of both the bound quinone and that of cytochrome *bo*$_3$ with

Figure 3.13 The occupancy of the quinone binding site of sucrose monolaurate extracted cytochrome *bo*$_3$ by (decyl)ubisemiquinone as a function of E_h, at pH9.0.

Redox titrations were performed as described in chapter 2.8. The concentration of cytochrome *bo*$_3$ was 5μM. The buffer was 200mM bis-tris-propane adjusted to pH9.0. The enzyme preparation had 0.6 quinone/complex. with (a) no exogenous quinone added. (b) with 1mM decylubiquinone. The theoretical curves were obtained as described in chapter 2.10 using the following parameters:- (a) E_1=-42.0mV, E_2=38.0mV (b) E_1=28.0mV, E_2=-29.0mV

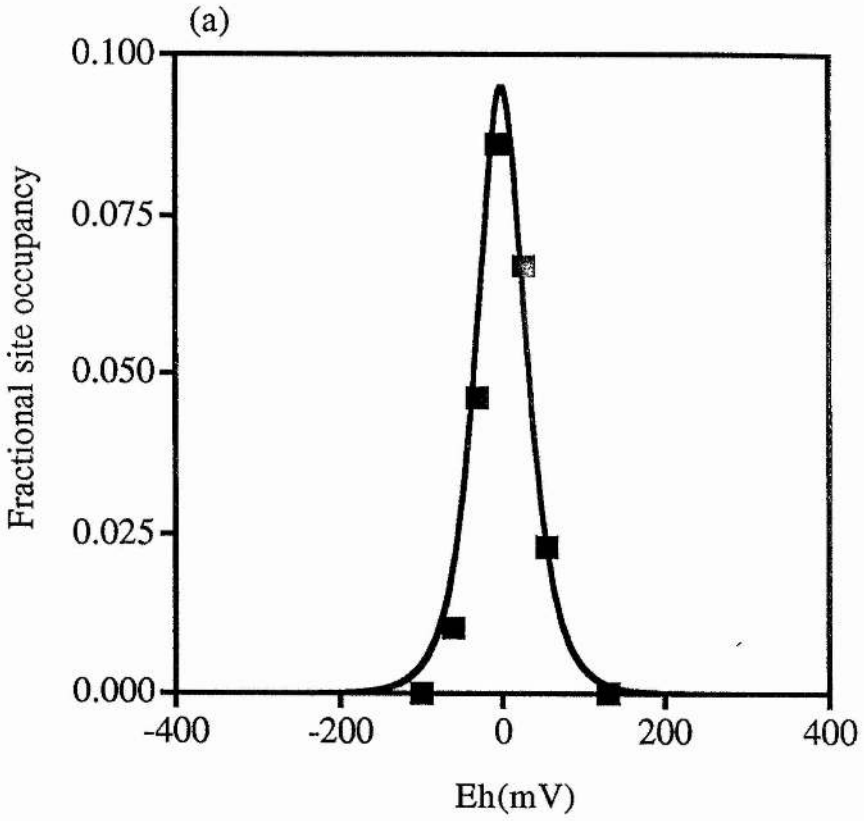
(a)
0.100
0.075
0.050
0.025
0.000
Fractional site occupancy
-400
-200
0
200
400
Eh(mV)

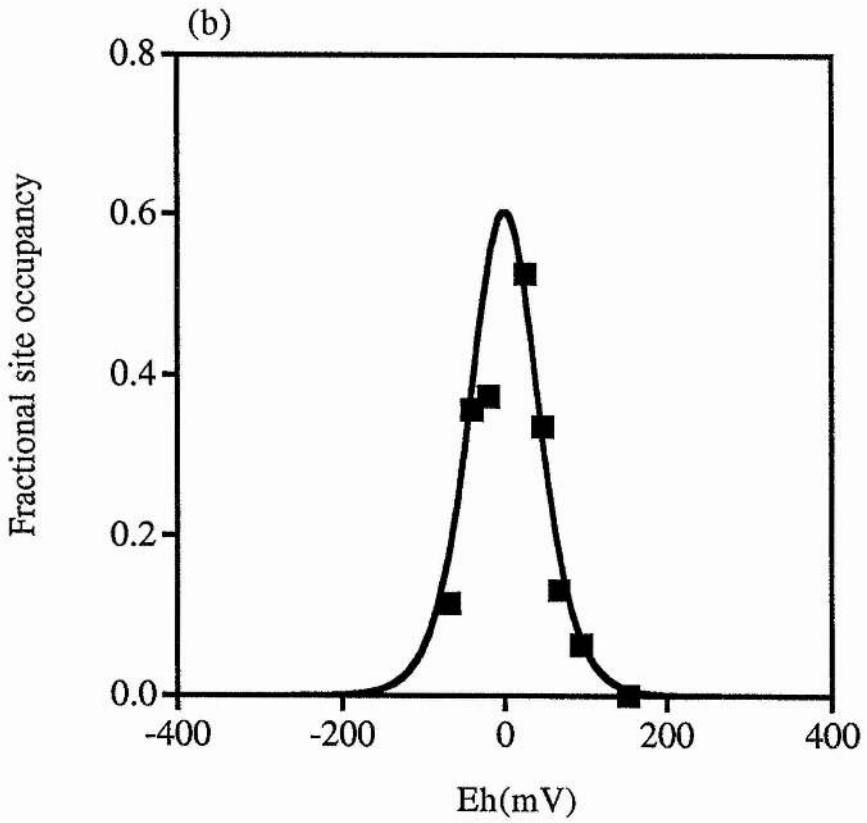
(b)
0.8
0.6
0.4
0.2
0.0
Fractional site occupancy
-400
-200
0
200
400
Eh(mV)

excess decylubiquinone are comparable, -2mV and -0.5mV respectively. It would therefore seem likely that the ESR semiquinone signal is derived from the tightly bound quinone which co-purifies with the complex. These results are summarised in Table 3.1(c).

3.2.3 The effect of Q-site inhibitors on semiquinone stabilisation.

In one set of redox titrations the inhibitor 2-heptyl-4-hydroxyquinoline-N-oxide (HOQNO) was added to 50μM. HOQNO is a well characterised competitive inhibitor of Q-sites and is known to inhibit quinol oxidation by the cytochrome bo_3 complex (Krab & Wikström, 1980; Kita *et al.*, 1984a; Lam, 1984). This caused a marked quenching of the ESR signal and did not affect the shape of the theoretical curve of the redox titration. HOQNO would appear to be a reasonably good inhibitor of Q_{bo} given the high concentration of quinone competing for this site.

An competive inhibitor with a high specificity for cytochrome bo_3 was described by Meunier *et al.*, 1995. Tridecyl-stigmatellin (TDS) is a very effective inhibitor of quinol oxidation by cytochrome bo_3 but has virtually no effect on quinol oxidation by cytochrome *bd*. When a stoichiometric amount of TDS was present in a redox titration mixture containing the preparation of cytochrome bo_3 with 0.6quinone/complex no semiquinone ESR signal was observed.

Table 3.1 Summary of E_1, E_2, E_m and maximum site occupancy values for cytochrome bo_3 semiquinone

(a) Membrane-bound cytochrome bo_3

pH	E_1(mV)	E_2(mV)	E_m(mV)	maximum site occupancy
7.5	47.5	132.75	90.12	0.07
8.0	18.75	107.5	63.12	0.08
8.5	-10.75	73.5	31.38	0.08
9.0	-26.0	30.0	2.0	0.14
9.5	-29.0	-20.0	-24.5	0.29

(b) Octylglucoside/triton X-100 extracted cytochrome bo_3

pH	E_1(mV)	E_2(mV)	E_m(mV)	maximum site occupancy
7.0[a]	43.0	168.5	105.75	0.04
7.8[a]	32.5	97.0	64.75	0.13
8.4[a]	31.5	27.5	29.5	0.35
9.0[a]	25.5	-35.0	-4.75	0.61
9.0[b]	25.5	-35.0	-4.75	0.61
9.0[c]	-94.5	-155.0	-124.75	0.61

[a] 1mM decylubiquinone; [b] 1mM ubiquinone-1; [c] 1mM menaquinone

(c) Sucrose monolaurate extracted cytochrome bo_3

pH	E_1(mV)	E_2(mV)	E_m(mV)	maximum site occupancy
9.0[d]	-42.0	38.0	-2.0	0.09
9.0[e]	28.0	-29.0	-0.5	0.60

[d] no added quinone; [e] 1mM decylubiquinone

3.2.4 Quinone binding to *cyo*A fragment

The C-terminal periplasmic domain of subunit II of the cytochrome bo_3 complex, known as the *cyo*A fragment has been crystallised at 2.5Å resolution (Van der Oost *et al.*, 1992; Wilmanns*et al.*, 1995). Subunit II has been implicated through photo-affinity labelling studies as being or forming part of the quinone binding site (Welter *et al.*, 1994). The fragment is cleaved at thr111 however the first 14 amino acid residues are disordered in the crystal. No quinone molecules were found to be associated with the fragment. However, given that the quinone binding site is likely to be in the vicinity of this domain, if the site remained intact it could still stabilise the semiquinone state under the conditions of a redox titration where the redox mediators would provide a route for the entry and exit of electrons.

The *cyo*A fragment was isolated and purified as described in chapter 2.7. Redox titrations at pH7.0 and pH9.0 were conducted in the presence of excess (1mM) decylubiquinone where the concentration of the *cyo*A fragment was 5μM. The resulting samples were shown to have no detectable ESR semiquinone signals. From this, it would seem unlikely that the *cyo*A fragment itself forms the quinone binding site but rather another part of the complex, most likely subunit I, given the large interface between the two, interacts with *cyo*A to make up Q_{bo}. Many quinone binding sites have participant residues present on different polypeptide chains as appears likely with Q_{bo} (Allen *et al.*, 1987; Deisenhoffer & Michel, 1989; Westenberg *et al.*, 1990).

3.2.5 Sequence alignment of subunit II from haem-copper quinol oxidases and cytochrome *c* oxidases

As outlined in chapter 1.10 the cytochrome bo_3 complex is a member of the haem-copper respiratory oxidase superfamily and within this the members share significant sequence and structural similarities (Garcia-Horsman *et al.*, 1994; Calhoun *et al.*, 1994). The haem-copper respiratory oxidases can be separated into two sub-groups according to their reductant, quinol or cytochrome *c* (Welter *et al.*, 1994; Iwata *et al.*, 1995). The major structural differences between the sub-groups is in subunit II, the proposed location of the quinone and cytochrome *c* binding sites. This is reflected in the low sequence identity between subunit II of cytochrome bo_3 and the cytochrome *c* oxidases of *P.denitrificans* and bovine heart of 10%. In addition the Cu_A site is absent in cytochrome bo_3. By aligning the sequences of subunit II of both quinol and cytochrome *c* oxidases from various sources any residues highly conserved in one sub-group but absent in the other may identify the location of the reductant binding site. Residues highly conserved in both sub-groups may be implicated in electron transfer pathways.

A similar study lead to the mutagenesis of around 30 amino acid residues of *cyo*A (10% of the total) with only one, W136A, having a major effect on quinone binding (Ma, 1995). The low success rate is most likely due to the relatively small number of residues required for quinone binding, perhaps only two or three but may also be attributed to a misalignment of the sequences. Figure 3.14 displays a sequence realignment of subunit II from four haem-copper quinol oxidases and three cytochrome *c* oxidases. This

Figure 3.14 Sequence alignment of subunit II from four haem-copper type quinol oxidases and three cytochrome *c* oxidases.

The subunit II sequences from four quinol oxidases (*Escherichia coli*, *Paracoccus denitrificans*, *Acetobacter aceti*, *Bacillus subtilis*) were aligned with three cytochrome *c* oxidases (Human, Rat and *Neurosporra crassa*). All sequences used in this alignment were extracted from the Swiss-Prot database. Alignments were carried out using the PILEUP program of the GCG package and the profile alignment option of the CLUSTALV program to introduce more divergent sequences followed by manual adjustment where necessary. α1 and α2 indicate the positions of the membrane spanning regions of the subunit. βI to βX indicate the β-sheets of the subunit based on the crystal structure of the *E. coli cyo*A fragment (Wilmanns *et al.*, 1995). · indicates the residues in *E. coli cyo*A already mutated (Ma, 1995). Δ indicates the positions of *E. coli cyoA* lys118 and trp136.

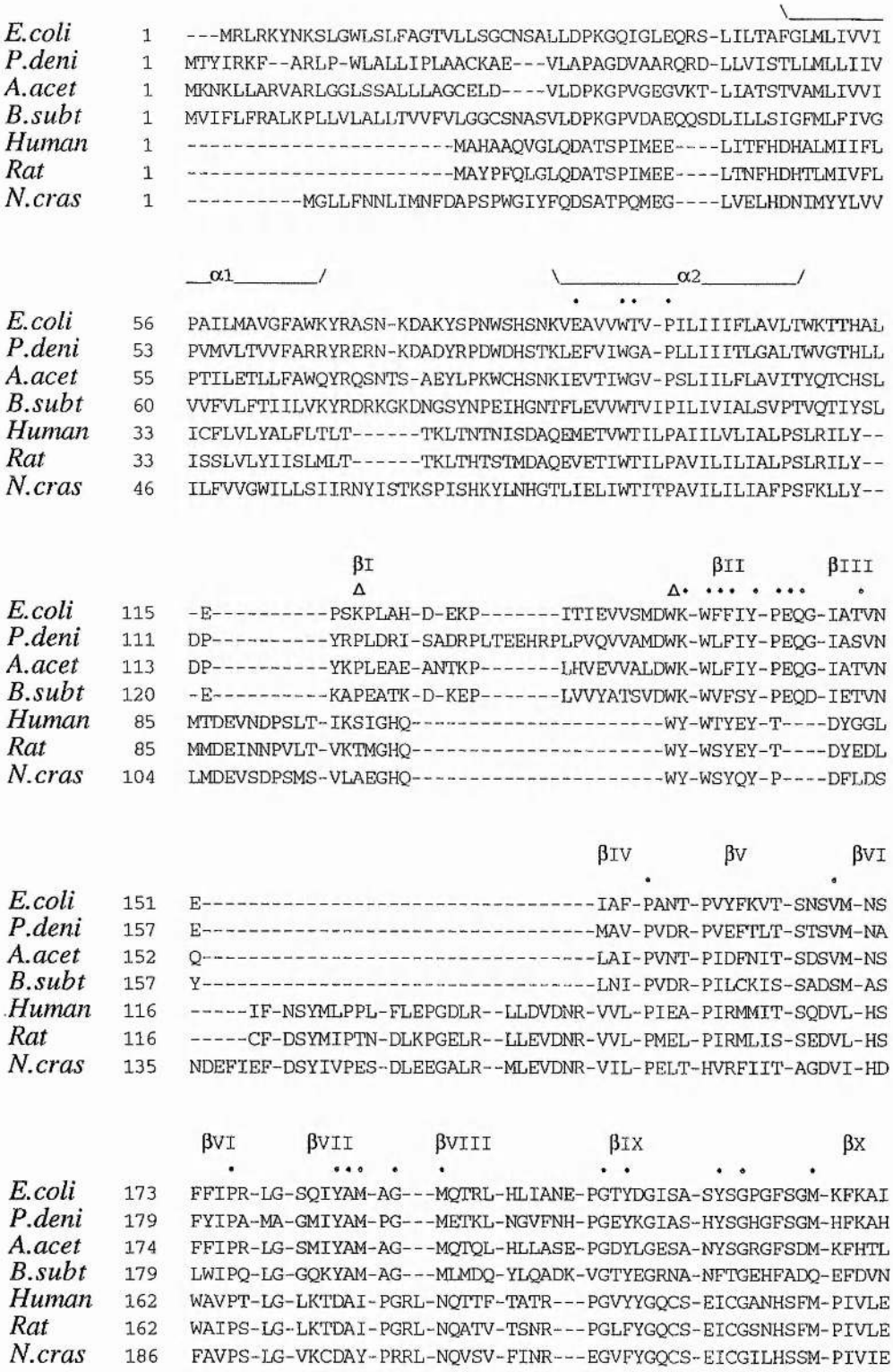
E.coli 1 ---MRLRKYNKSLGWLSLFAGTVLLSGCNSALLDPKGQIGLEQRS-LILTAFGLMLIVVI
P.deni 1 MTYIRKF--ARLP-WLALLIPLAACKAE---VLAPAGDVAARQRD-LLVISTLLMLLIIV
A.acet 1 MKNKLLARVARLGGLSSALLLAGCELD----VLDPKGPVGEGVKT-LIATSTVAMLIVVI
B.subt 1 MVIFLFRALKPLLVLALLTVVFVLGGCSNASVLDPKGPVDAEQQSDLILLSIGFMLFIVG
Human 1 ----------MAHAAQVGLQDATSPIMEE----LITFHDHALMIIFL
Rat 1 ----------MAYPFQLGLQDATSPIMEE----LTNFHDHTLMIVFL
N.cras 1 ----------MGLLFNNLIMNFDAPSPWGIYFQDSATPQMEG----LVELHDNIMYYLVV
α1 α2
E.coli 56 PAILMAVGFAWKYRASN-KDAKYSPNWSHSNKVEAVVWTV-PILIIIFLAVLTWKTTHAL
P.deni 53 PVMVLTVVFARRYRERN-KDADYRPDWDHSTKLEFVIWGA-PLLIIITLGALTWVGTHLL
A.acet 55 PTILETLLFAWQYRQSNTS-AEYLPKWCHSNKIEVTIWGV-PSLIILFLAVITYQTCHSL
B.subt 60 VVFVLFTIILVKYRDRKGKDNGSYNPEIHGNTFLEVVWTVIPILIVIALSVPTVQTIYSL
Human 33 ICFLVLYALFLTLT------TKLTNTNISDAQEMETVWTILPAIILVLIALPSLRILY--
Rat 33 ISSLVLYIISLMLT------TKLTHTSTMDAQEVETIWTILPAVILILIALPSLRILY--
N.cras 46 ILFVVGWILLSIIRNYISTKSPISHKYLNHGTLIELIWTITPAVILILIAFPSFKLLY--
βI βII βIII
E.coli 115 -E----------PSKPLAH-D-EKP-------ITIEVVSMDWK-WFFIY-PEQG-IATVN
P.deni 111 DP----------YRPLDRI-SADRPLTEEHRPLPVQVVAMDWK-WLFIY-PEQG-IASVN
A.acet 113 DP----------YKPLEAE-ANTKP-------LHVEVVALDWK-WLFIY-PEQG-IATVN
B.subt 120 -E----------KAPEATK-D-KEP-------LVVYATSVDWK-WVFSY-PEQD-IETVN
Human 85 MTDEVNDPSLT-IKSIGHQ----------WY-WTYEY-T----DYGGL
Rat 85 MMDEINNPVLT-VKTMGHQ----------WY-WSYEY-T----DYEDL
N.cras 104 LMDEVSDPSMS-VLAEGHQ----------WY-WSYQY-P----DFLDS
βIV βV βVI
E.coli 151 E----------IAF-PANT-PVYFKVT-SNSVM-NS
P.deni 157 E----------MAV-PVDR-PVEFTLT-STSVM-NA
A.acet 152 Q----------LAI-PVNT-PIDFNIT-SDSVM-NS
B.subt 157 Y----------LNI-PVDR-PILCKIS-SADSM-AS
Human 116 -----IF-NSYMLPPL-FLEPGDLR--LLDVDNR-VVL-PIEA-PIRMMIT-SQDVL-HS
Rat 116 -----CF-DSYMIPTN-DLKPGELR--LLEVDNR-VVL-PMEL-PIRMLIS-SEDVL-HS
N.cras 135 NDEFIEF-DSYIVPES-DLEEGALR--MLEVDNR-VIL-PELT-HVRFIIT-AGDVI-HD
βVI βVII βVIII βIX βX
E.coli 173 FFIPR-LG-SQIYAM-AG---MQTRL-HLIANE-PGTYDGISA-SYSGPGFSGM-KFKAI
P.deni 179 FYIPA-MA-GMIYAM-PG---METKL-NGVFNH-PGEYKGIAS-HYSGHGFSGM-HFKAH
A.acet 174 FFIPR-LG-SMIYAM-AG---MQTQL-HLLASE-PGDYLGESA-NYSGRGFSDM-KFHTL
B.subt 179 LWIPQ-LG-GQKYAM-AG---MLMDQ-YLQADK-VGTYEGRNA-NFTGEHFADQ-EFDVN
Human 162 WAVPT-LG-LKTDAI-PGRL-NQTTF-TATR---PGVYYGQCS-EICGANHSFM-PIVLE
Rat 162 WAIPS-LG-LKTDAI-PGRL-NQATV-TSNR---PGLFYGQCS-EICGSNHSFM-PIVLE
N.cras 186 FAVPS-LG-VKCDAY-PRRL-NQVSV-FINR---EGVFYGQCS-EICGILHSSM-PIVIE

```
E.coli   223  A-TP---DRAAFDQWVAKAK-QS-PNTMSDMAAFEKLAAPSEYNQVEYFSNVKPDLFAIN
P.deni   229  A-T----DEAGFDAWIEKAR-ASGGTLDRPRYLE--LEAPSE-N-VPPMSFAEVDPHLFQ
A.acet   224  A-VSG--DE--FNAWVEKVK-SS-SEQLDS-QTYPKLAAPSE-NPVEYFAHVEPGMFNVA
B.subt   229  A-VTEK-DFNSWVKKTQNEA-PKLTK--EKYDELMLPENVDELTFSSTHLKYVDHDAEYA
Human    212  L-I----PLKIFEMGPVFTL-----------------------------------------
Rat      212  M-V----PLKYFENWSASMI-----------------------------------------
N.cras   236  S-V----SLEKFLTWLEE-Q-----------------------------------------

E.coli   277  KFMAHGKSMDM-TQPEGEH--SAHEGMEGMDMSHAESAH---------------------
P.deni   279  RIVNMRIVNMCVEPGKICMAEMMALDAQGGTGLAGTMNMTRLTYDKDQRRGTRAPVLGWE
A.acet   275  KYNN-GMVMDKSTGKMIQVQQSAMSDMN-MKE----------------------------
B.subt   284  MEARKRLG-YQAVSPHCKTDPFENVKKNEFKKSDDTEE----------------------
Human    227  ----------------------------------------------------------
Rat      227  ----------------------------------------------------------
N.cras   250  ----------------------------------------------------------

E.coli   313  ----------------------------------------------------------
P.deni   339  PFQVASFCTPEDSALMFGKSPELARAPVDMTPMRGHALTPPKGPFTPSQDNAVTLLDPAADRARNF
A.acet   305  ----------------------------------------------------------
B.subt   321  ----------------------------------------------------------
Human    227  ----------------------------------------------------------
Rat      227  ----------------------------------------------------------
N.cras   250  ----------------------------------------------------------
```

aligment is based partly on the secondary structure determinations from the crystal structure of the *cyo*A fragment and identified a region around β-strands I and II of the quinol oxidases which was absent from the cytochrome *c* oxidases. This contained several positively charged residues which if present at or near the site may help to stabilise the semiquinone intermediate of these K118(lys118) and K125(lys125) were identified as targets for site directed mutagenesis.

3.2.6 Studies of *cyo*A mutants K118L and W136A

Of the residues identified in the above sequence alignment only lys118 was mutated in this study and was changed to a leucine. The mutant enzyme was capable of supporting aerobic growth and produced a cell growth rate and reduced minus oxidised difference spectrum indistinguishable from that of the wild-type bacterium. The effect of this mutation on quinol oxidation was minimal and gave a ubiquinol oxidase activity similar to that of the wild type enzyme. In addition the semiquinone species produced was identical to that of wild-type cytochrome bo_3 and is shown in figure 3.15(a). It would appear unlikely that lys118 plays any significant functional role in ubiquinol oxidation.

W136 (Trp136) is highly conseved in both quinol and cytochrome *c* oxidases and is located close to the engineered Cu_A site in the purple *cyo*A fragment and native Cu_A site in the cytochrome *c* oxidase crystal strucure (Wilmanns et al., 1995, Tsukihara *et al.*, 1996). The W136A mutation is known to increase the K_m for quinol oxidation five-fold and is therefore likely to be at or near the quinone binding site or form part of the electron

Figure 3.15 ESR spectra of the ubi-semiquinone radical formed by the mutant cytochrome bo_3 complexes K118L and W136A in *E. coli* strain GO105 membranes.

The zero cross over point is approximately g=2.004, the line width of the radical is 0.945mT. (a) Signal derived from cytochrome bo_3 mutant K118L present in GO105 membranes washed with 200mM bis-tris-propane pH9.0 then overnight anaerobic incubation at 4°C. (b) As (a) but cytochrome bo_3 complex mutant W136A The membranes contained approximately 35mg protein ml^{-1}. EPR conditions were as in figure 3.1.

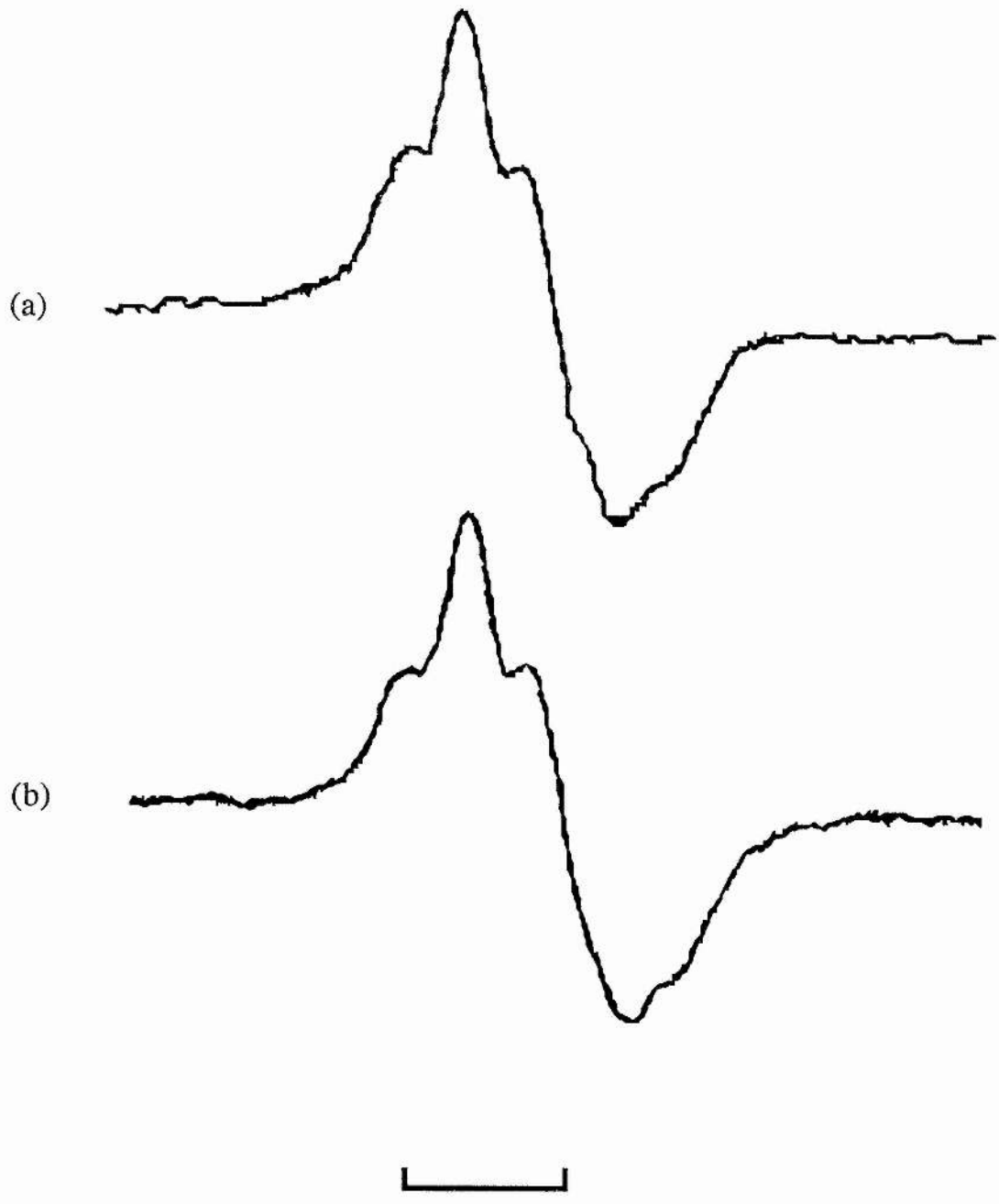
(a)
(b)
1mT

transfer pathway from the site to the low-spin haem *b* (Ma, 1995; R.B. Gennis, personal communication). Aromatic residues are known to be involved in electron transfer in similar systems and conduct electrons through their delocalised π orbital system (Moser et al., 1992). The Q_A and Q_B sites of the bacterial reaction centres each have aromatic residues very close to the site, in particular the ring of tryptophan M252 in *Rb. sphaeroides* (M250 in *Rsp. viridis*) is arranged parallel to the quinone ring allowing fast and efficient electron transfer to occur; mutagenesis of this residue to a valine markedly reduces photosynthetic growth (Deisenhofer & Michel, 1989; Feher *et al.*, 1989). Mutagenesis of tyr147 of the cytochrome bc_1 complex from *Rb. capsulatus* by alanine was found to impair electron transfer from the ubiquinol oxidation site Q_o but had no effect on the occupancy of the site (Saribas *et al.*, 1995).

W136A was studied by redox potentiometry and the semiquinone produced monitored using ESR. Figure 3.15 (b) shows the ESR spectrum of this semiquinone and is similar to the wild-type spectrum. This suggests that the mutation does not disturb the electronic structure of the bound semiquinone as this would have had an effect on the hyperfine couplings. If the mutation exerted a small effect this, could be detected using matrix ENDOR spectropscopy.

Figure 3.16 shows the redox behaviour of the ubisemiquinone intermediate associated with the membrane-bound cytochrome bo_3 mutant W136A. The radical clearly displays unusual redox properties when compared to that of the wild-type membrane-bound complex (dotted line). In the direction of quinol oxidation

Figure 3.16 The occupancy of the quinone binding site of membrane-bound W136A mutant cytochrome bo_3 by ubisemiquinone as a function of E_h at pH9.0.

The concentration of the radical signal is normalised to unity (assuming one semiquinone stabilising site per low-spin haem *b*) and plotted against the ambient redox potential (E_h). The redox titration was performed as described in chapter 2.8. The concentration of cytochrome bo_3 varied from 7.5μM with the protein content of the GO105 membranes being 35mg/ml. The buffer was 200mM bis-tris-propane pH9.0.

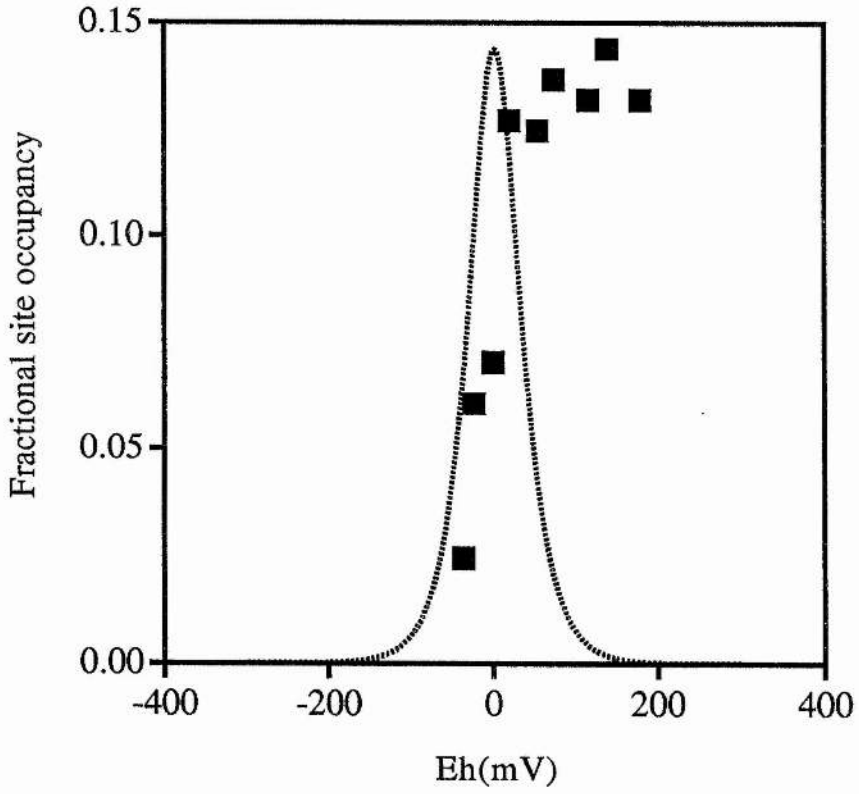
0.15
0.10
0.05
0.00
Fractional site occupancy
-400
-200
0
200
400
Eh(mV)

the increase in semiquinone concentration occurs as normal with increased redox potential up to the maximum semiquinone concentration at the E_m of the quinol/quinone couple. After this the semiquinone concentration remains maximal and shows no indication of oxidising further to the quinone state. The replacement of the tryptophan residue with an alanine in no way impairs the occupancy of the site as this was similar to the wild-type enzyme, rather the mutation seems to effect electron transfer from the site. The formation of the semiquinone suggests the first electron can be transferred but the removal of the second electron appears more difficult which may indicate that a branched electron transfer pathway to the low-spin haem exist.

Very recently, two quinone binding peptides from subunit II have been identified using a photoreactive azido-ubiquinone derivative followed by proteolysis and MALDI-mass spectroscopy (R.B. Gennis, personal communication). The peptides correspond to residues 167-178 and 254-270 and are located close to W136 in the crystal structure of *cyo*A as demonstrated in figure 3.17 (Wilmanns *et al.*, 1995) The related residues of both bovine heart cytochrome *c* oxidase and *P.denitrificans* subunit II are in close association with subunit I (Iwata et al., 1995; Tsukihara *et al.*, 1996). A projection crystal structure of cytochrome bo_3 at 6Å resolution also indicates that these subunits and specific residues are in close association (Gohlke *et al.*, 1997). The quinone binding site is probably located on subunit II near the surface of the protein in the vicinity of W136 in a hydrophobic cleft formed by subunits I and II.

Figure 3.17 The position of W136 relative to the quinone binding peptides of *cyo*A.

(a) The position of W136 is indicated in the crystal structure of the *cyo*A fragment and displayed in spacefill-mode. The quinone binding peptides 1 & 2 corresponding to residues 167-178 and 254-270 of subunit I and are displayed within the protein backbone in red and blue respectively. (b) as (a) but rotated 90° clockwise in the x-direction

(a)

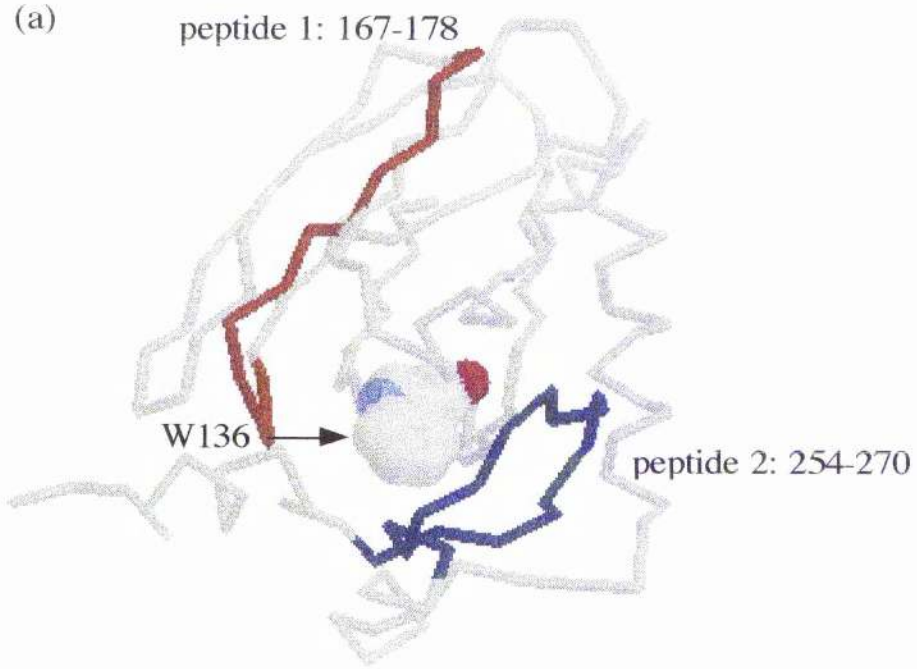

(b)

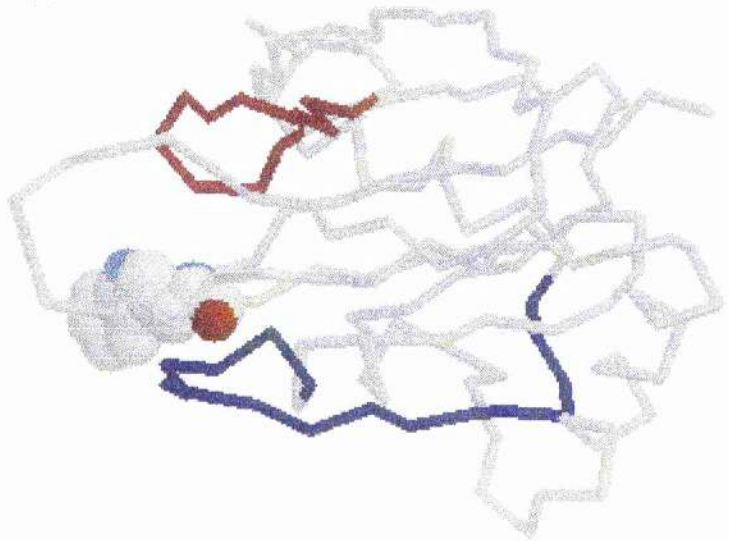

3.3 Conclusion

This chapter sought to expand on the previous studies of semiquinone stabilisation by the cytochrome bo_3 complex (Ingledew *et al.*, 1995; Sato-Watanabe *et al.*, 1995). A new method of poising the semiquinone samples was developed, achieving much higher concentrations of the semiquinone species providing ESR spectra with better resolved hyperfine splittings of 0.4mT. ^{15}N-labelling of the complex and deuterium exchange of the solvent ruled these nuclei out as being the major cause of the hyperfine interactions. The presence of exchangeable protons at the site were detected by the change in the ESR spectrum of the deuterium exchanged purified enzyme. No change was observed in the membrane-bound sample indicating that in the *in situ* enzyme the site is not readily accessible to the aqueous medium. The generation of concentrated semiquinone samples (>40μM) will make it possible to probe the electronic structure of the site by ESEEM and ENDOR spectroscopies, techniques used in other systems (Salerno *et al.*, 1990; Rigby *et al.*, 1996; Astashkin *et al.*, 1995; Deligiannakis *et al.*, 1995). These techniques are explored in the forthcoming chapters.

The semiquinone associated with the membrane-bound complex was characterised. The ESR spectrum showed no differences when compared to spectra of shorter chained quinones indicating that the length of the quinone tail (hence, the hydrophobicity) has little influence on the binding of the head group. The redox characteristics of the semiquinone were different from the purified enzyme but the redox behaviour over the pH range studied still suggested a $2H^+/2e^-$ reaction with efficient electron transfer to the

low-spin haem *b*. The differences in the values of midpoint potentials of the one electron reactions and the pK's of semiquinone protonation most likely reflect slight differences in quinone binding in the purified enzyme.

Although thought to be more specific for ubiquinone, cytochrome bo_3, was equally capable of stabilising and oxidising menasemiquinone species. Binding of a napthoquinone to the site produced a slightly different ESR spectrum when compared to that of a ubisemiquinone species. This change reflected the differences in structure between napthoquinones and benzoquinones and suggested that the replacement of the methoxy-groups of ubiquinone with an aromatic ring perturbs the electronic structure of the bound semiquinone.

From the data presented here the presence of a second quinone binding site seems unlikely. The potentiometric behaviour of the semiquinone species derived from both the endogenous ubiquinone-8 or exogenous quinone is consistent with a quinone/quinol redox system. A fundamental requirement of quinol oxidation (or quinone reduction) is the equalising of the mid-point potentials of the two one-electron couples, E_1 and E_2, (Rich, 1982). This is achieved in this system at approximately pH8 for the purified enzyme and slightly higher for the membrane-bound system. The quinone co-purifying with the complex can produce a semiquinone species similar to that previously described and this is displaced on the addition of inhibitors of quinol oxidation, tridecyl-stigmatellin is particularly effective at Q_{bo}. Sato-Watanabe *et al.*, 1995b have suggested that the semiquinone associated with the complex is stabilised at a site distinct from the quinol oxidation site. This site

would have a role similar to Q_A of photosystem II and mediate electron transfer form the quinol oxidation site. Quinol oxidation of this type would still have to proceed through a semiquinone intermediate and this state would require stabilisation. One site of quinol oxidation that does not require a stabilised semiquinone is associated with the cytochrome bc_1 complex, due to the two discrete electron acceptors being separated both spatially and thermodynamically with a difference of 400mV (Crofts *et al.*, 1992). Such a system could not operate in cytochrome bo_3 as the electron acceptors known or proposed are likely to be similar both electrically and in space (Salerno *et al.*, 1990; Iwata *et al.*, 1995). The data presented here is consistent with there being only one semiquinone species and that this can be generated from a tightly bound quinone that co-purifies with the complex and is located in the site of quinol oxidation, Q_{bo}.

The *cyo*A fragment alone cannot stabilise the semiquinone intermediate. However, the mutation W136A in the intact enzyme was shown to affect the redox behaviour of the semiquinone although not affecting the occupancy of the site nor the electronic structure of the bound radical. This residue most likely forms part of the electron transfer pathway between the quinol and the low-spin haem, a feature of other similar quinone binding systems. W136 was shown to be in close association with two recently identified quinone binding peptides, both an integral part of the *cyo*A fragment. These peptides and W136 are likely to be near or at the interface with subunit I as indicated by the crystal structures of both the cytochrome c oxidases so far determined (Iwata *et al.*, 1995; Tsukihara *et al.*, 1996).

The quinone binding site of cytochrome bo_3 is therefore likely to be located in a hydrophobic cleft, between subunits I and II with the semiquinone stabilising residues residing on subunit II. The role of subunit I could be supportive, enabling the correct positioning of the quinone head-group in the site perhaps through interactions with first few carbons of the quinone tail.

4.0 SEMIQUINONE STABILISATION BY CYTOCHROME *bd*

4.1 Introduction

The cytochrome *bd* complex is less studied than the other terminal oxidase of *E. coli*, cytochrome bo_3. As discussed in chapter 1.8, cytochrome *bd* has a similar function to cytochrome bo_3, being a quinol oxidase that is expressed at low aeration. As the growth conditions approach anaerobosis menaquinone overtakes ubiquinone as the predominant electron carrier in the *E. coli* membrane. It is thought therefore that menaquinone may be the 'natural' reductant of cytochrome *bd.*

Although several studies have reported aspects of the location of the cytochrome *bd* quinone binding site (Lorence *et al.*, 1988; Ghaim *et al.*, 1995) none have dealt specifically with the thermodynamics of quinol oxidation. It was suspected that as with the cytochrome bo_3 complex a semiquinone intermediate would be formed and that this would require a specific site to stabilise the species. A stable semiquinone was identified by Kaysser, 1993, by 'trapping' the intermediate through reacting the oxidase with nitric oxide which bound to haem *d*. This technique, although of interest to the reaction mechanism of the enzyme yielded little information on the structure and thermodynamic behaviour of the quinone binding site.

In the present study a technique for achieving high concentrations of semiquinone associated with the both membrane-bound and purified cytochrome *bd* complex are employed and the resulting semiquinone observed using ESR. To study the thermodynamics of quinol oxidation the semiquinone was observed in redox titrations and the pH dependencies of the semiquinone

concentration and the two one electron couples determined. Both ubiquinone and menaquinone analogues were used and the resulting semiquinone species characterised. Also the effects of two inhibitors of quinone binding sites, the more general inhibitor HOQNO and the cytochrome *bd* specific aurachin D, on semiquinone formation were observed (Kita *et al.*, 1984b; Meunier *et al.*, 1994).

It should be noted that three mutations in subunit I all located in the 'Q-loop' are known to produce a complex unable to sustain aerobic growth of the bacterium. These had normal optical spectra but had no quinol oxidase activity (R.B. Gennis, personal communication). These mutants specifically ser299cys, ser326cys and thr376cys were available for this study. Unfortunately expression of the mutant oxidase was too low to determine whether any semiquinone species could be stabilised.

4.2 Results & Discussion

4.2.1 ESR spectra of semiquinone species associated with the cytochrome *bd* complex.

As described in chapter 3.2.1, in order for quinol oxidation to proceed in an enzyme complex like this a semiquinone intermediate must be produced and the instability of this free radical species requires a site that can confer thermodynamic and kinetic stability. As mentioned in the preceeding section, a semiquinone species associated with the cytochrome *bd* complex has been identified (Kaysser, 1993). This was produced by 'trapping' the semiquinone state through binding nitric oxide to the *d* haem. The ESR spectrum of this semiquinone species was overlaid with the Fe(II).NO radical although these can easily be distinguished by their differing temperature and power dependencies.

In this study alternative novel methods are employed to produce concentrated samples of the semiquinone for analysis by ESR. Figure 4.1 shows the ESR spectra derived from both the membrane-bound cytochrome *bd* complex and the purified complex reconstituted with excess ubiquinone and menaquinone analogues. The linewidth of the semiquinone is approximately 0.9mT, with the zero cross-over point at g=2.003. The semiquinone derived from FUN4 membranes displays slight hyperfine splittings at 0.3mT (figure 4.1(a)). These interactions are not as dramatic as in the cytochrome bo_3 semiquinone. In the purified cytochrome *bd* reconstituted with decylubiquinone the splittings are not as pronounced although still present. However, the splittings are more distinct when decylubiquinone is replaced by the menaquinone

Figure 4.1 ESR spectra of semiquinone radicals stabilised by the cytochrome *bd* complex.

The zero cross over point is approximately g=2.003, the linewidth of the radical is 0.9mT. (a) Signal derived from cytochrome *bd* present in FUN4 membranes washed with 200mM AMPSO, pH9.0 then overnight anaerobic incubation at 4°C. The membranes contained approximately 35mg protein ml^{-1}. (b) Signal derived purified cytochrome *bd* (~200μM) in 200mM AMPSO, pH9.0, reconstituted with excess (1mM) ubiquinone-2 analogue, decylubiquinone and reduced using sodium dithionite. (c) as (a) but reconstitued with excess menaquinone-2 analogue vitamin K_1. ESR conditions were as follows : Temperature, 100K; modulation frequency, 100kHz; modulation amplitude, 0.1mT, microwave frequency, 9.45GHz; microwave power 0.2mW. Average of 100 scans.

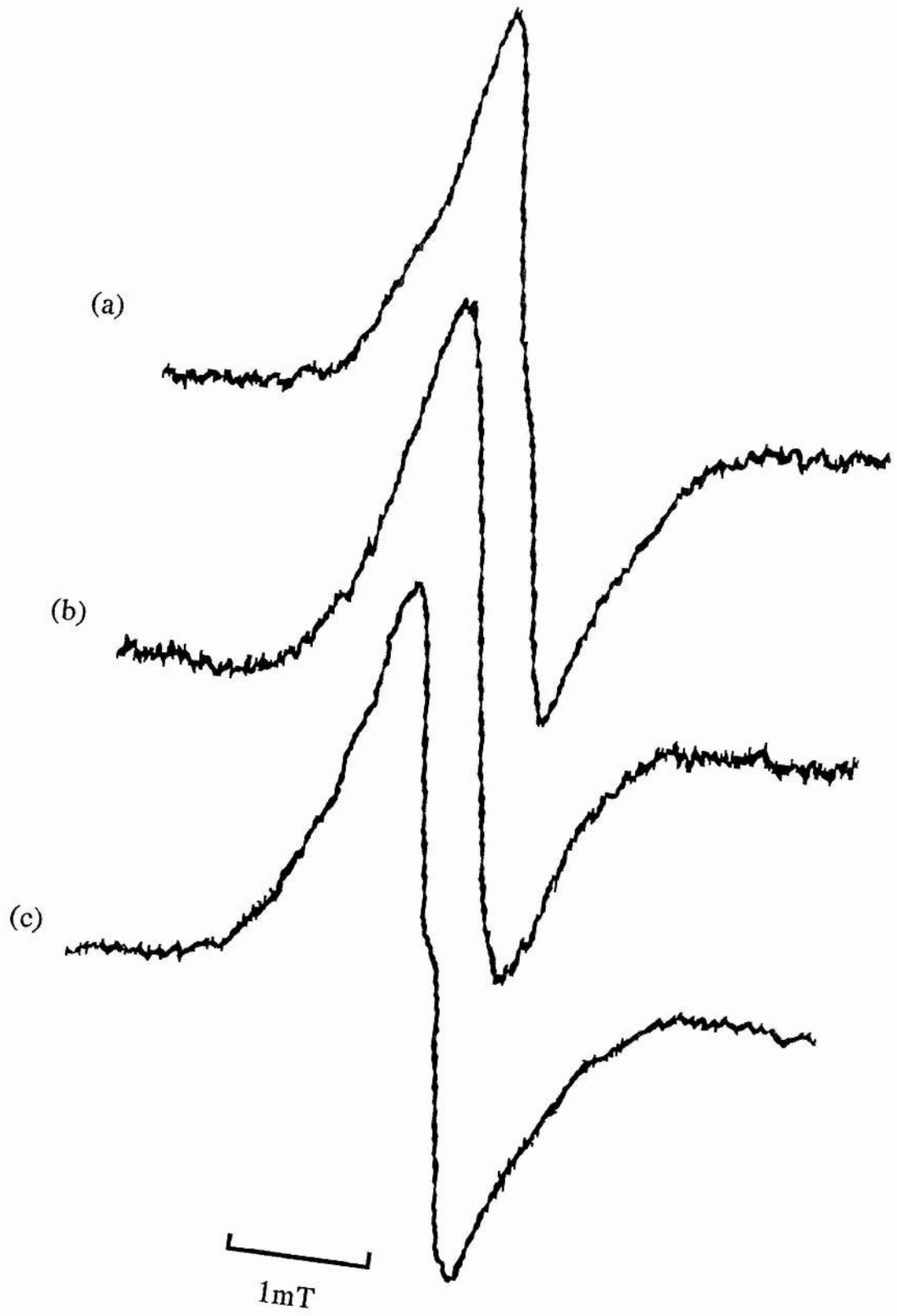
(a)
(b)
(c)
1mT

analogue vitamin K_1. In the membrane, under the conditions of low aeration that the bacteria were grown it is likely that both ubiquinone-8 and menaquinone-8 will make up the quinone pool. Therefore the ESR spectrum in figure 4.1(a) will be consist of both ubisemiquinone and menasemiquinone species. Although cytochrome *bd* can oxidise menaquinol and ubiquinol equally well it appears that the binding of each is slightly different (Kita *et al.*, 1984b). These differences can be accounted for by the replacement of the methoxy groups by the aromatic ring as outlined in chapter 3.2.1. Replacement of these methoxy groups by bulkier ethoxy substituents has an effect on rates of quinol oxidation by the oxidase, similar to the cytochrome bo_3 complex (Sakamoto *et al.*, 1996). The presence of the extra aromatic ring will exert an effect on electronic structure of the semiquinone leading to changes in the hyperfine interactions of each semiquinone.

When the oxidase is exchanged into deuterium oxide as shown in figure 4.2 a subtle difference in the ESR spectrum of the ubisemiquinone can be observed. The hyperfine splittings diminish (figure 4.2(b)); this as with cytochrome bo_3 is due to the lessening of the line broadening effects of protons. The hyperfine splittings in the ubisemiquinone would appear to be mostly due to coupling to exchange protons at the site. With the menasemiquinone these protons would probably contribute a small part to the interactions although it is likely another magnetic interaction is contributing to the ESR spectrum. Further studies by ENDOR spectroscopy would be necessary to define these interactions and a preliminary study on the membrane-bound cytochrome *bd* complex is reported in chapter 5.2.8

Figure 4.2 ESR spectra of the ubisemiquinone radical stabilised by the purified cytochrome *bd* complex, H_2O and D_2O exchanged.

(a) Signal derived purified cytochrome *bd* (~200μM) in 200mM AMPSO, pH9.0, reconstituted with excess (1mM) ubiquinone-2 analogue, decylubiquinone and reduced using sodium dithionite. (b) As (a) but exchanged with buffer in D_20, pD9.0. (c) Difference spectrum (a) minus (b). ESR conditions same as in figure 4.1.

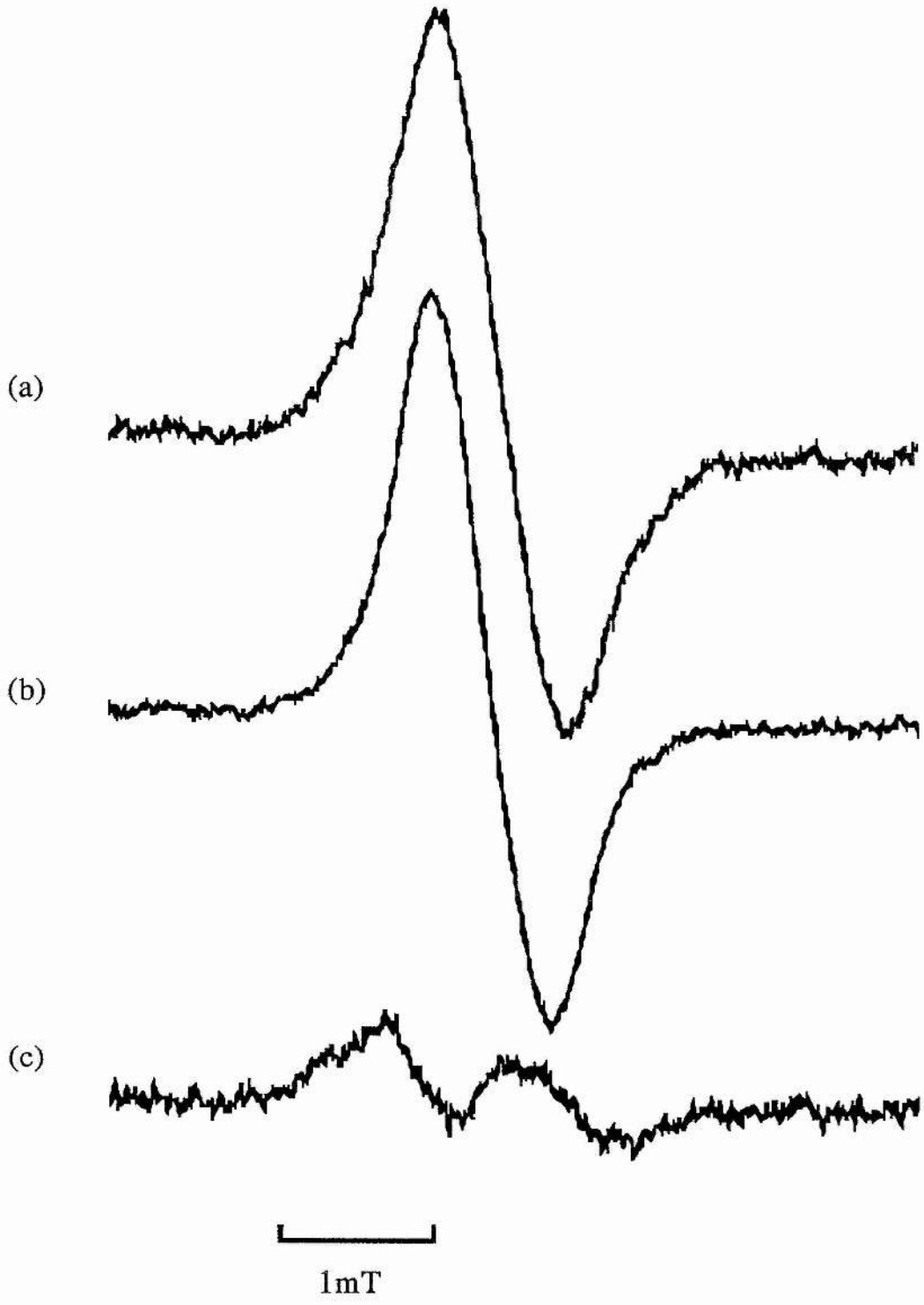
(a)
(b)
(c)
1mT

4.2.2 Thermodynamics of semiquinone stabilisation by cytochrome *bd* with excess decylubiquinone and menaquinone analogues.

The results of the potentiometric titrations of the purified cytochrome *bd* complex are shown in Fig 4.3. The enzyme was reconstituted with excess decylubiquinone (1mM). As expected the semiquinone species exhibits the expected 'bell shape' behaviour of a thermodynamic intermediate. At pH=7.0 the ubisemiquinone is much less stable than at pH=9.0 but significantly stabilised with respect to free semiquinone. The E_{m7} is +102.5mV for decylubiquinone whilst the value for the unbound species is approximately +100mV, which indicates that the site does not discriminate significantly between benzoquinones and benzoquinols. Results obtained from redox titrations at pH=9.0 where decylubiquinone is replaced by an excess of the menaquinone analogues menadione (1mM) and vitamin K_1 (1mM) are shown in figure 4.4. These menaquinone analogues also produce a highly stabilised semiquinone species. The data is fitted as described in chapter 2.10 by (a) menadione :- E_1=-45mV, E_2=-120mV and (b) vitamin K_1 :- E_1=-48.5 and E_2=-118.5mV. This compares with E_1=17.5mV, E_2=-55mV for decylubiquinone. The E_{m9}'s are -82.5mV (menadione), -83.5mV (vitamin K_1) and -19mV (decylubiquinone). The lower potentials for the napthoquinones are consisitent with the values for the unbound species (E_{m9} for free menadione is approx. -120mV and vitamin K_1 approx., -125mV.). The difference between the projected unbound values and the measured values of approximately 35mV suggests that the site binds

Figure 4.3 The occupancy of the quinone binding site of purified cytochrome *bd* by decyl-ubisemiquinone as a function of E_h, at different pH values.

The concentration of the semiquinone is converted to site occupancy assuming one site per low-spin haem b_{558} and plotted against the ambient redox potential (E_h). Redox titrations were performed as described in chapter 2.8 with 1mM decylubiquinone, cytochrome *bd* concentration was 3.5-7.0μM. The following buffers were used at the pH's indicated : (a) pH7.0, 200mM BES; (b) pH8.0, 200mM tricine; (c) pH8.5, 200mM AMPSO; (d)pH9.0, 200mM AMPSO. The theoretical curves were obtained as described in chapter 2.10 using the following parameters:- (a) E_1=22.5mV, E_2=182mV; (b) E_1=15mV, E_2=70mV; (c) E_1=15mV, E_2=10mV; (d) E_1=17.5mV, E_2=-55mV.

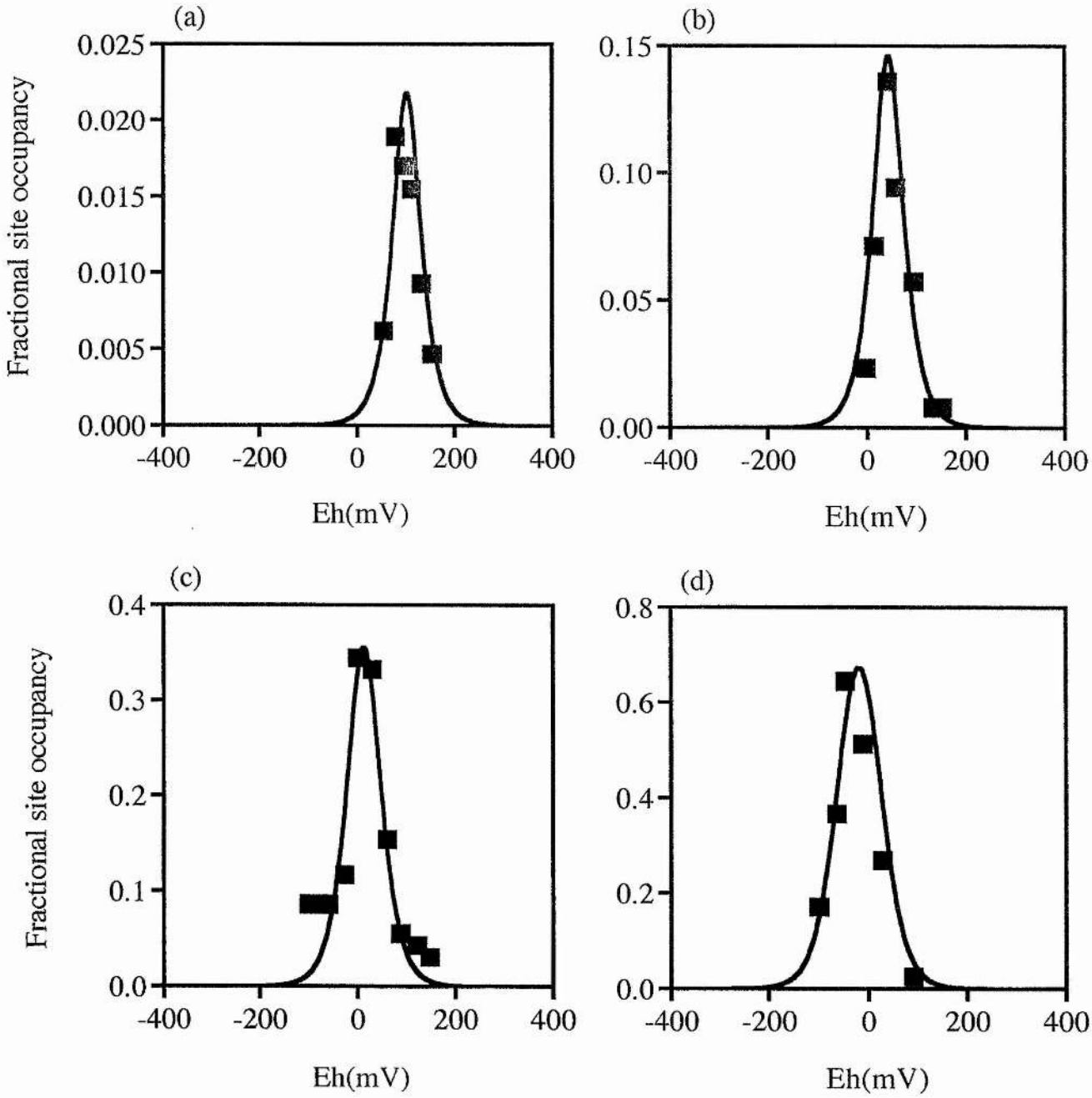
(a)
(b)
(c)
(d)
Fractional site occupancy
Fractional site occupancy
0.025
0.020
0.015
0.010
0.005
0.000
0.15
0.10
0.05
0.00
0.4
0.3
0.2
0.1
0.0
0.8
0.6
0.4
0.2
0.0
-400
-200
0
200
400
Eh(mV)
Eh(mV)
Eh(mV)
Eh(mV)

Figure 4.4 The occupancy of the quinone binding site of cytochrome *bd* by mena-semiquinone as a function of E_h, at pH9.0.

The concentration of the semiquinone is converted to site occupancy assuming one site per low-spin haem b_{558} and plotted against the ambient redox potential (E_h). Redox titrations were performed as described in chapter 2.8 with (a) 1mM menadione and (b) 1mM vitamin K_1. The cytochrome *bd* concentration was 4.0μM and the buffer was 200mM AMPSO. Best fits were obtained as described in the text using the following parameters: (a) E_1=-45mV, E_2=-120mV; (b) E_1=-48.5mV, E_2= -118.5mV.

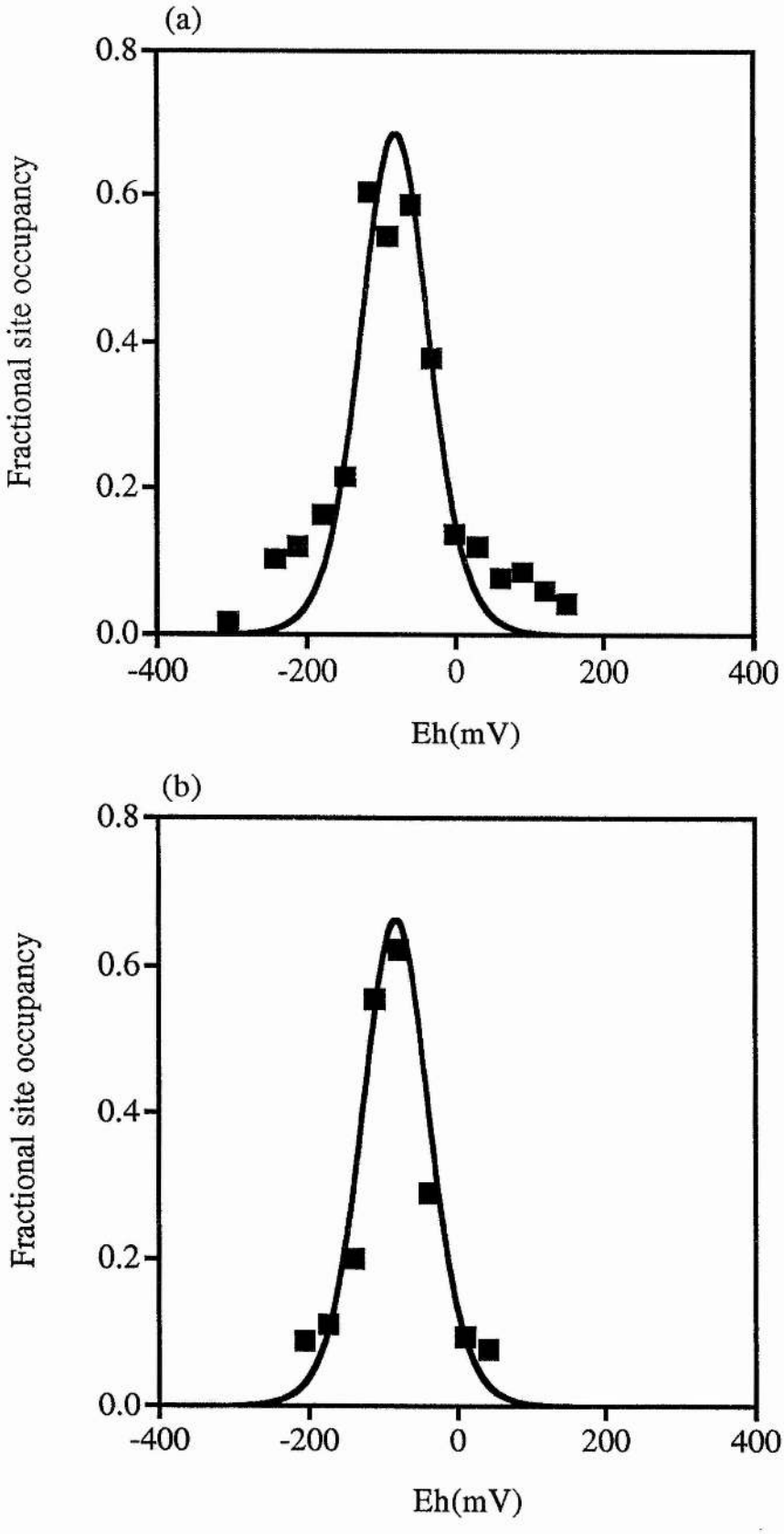
(a)
0.8
0.6
0.4
0.2
0.0
Fractional site occupancy
-400
-200
0
200
400
Eh(mV)
(b)
0.8
0.6
0.4
0.2
0.0
Fractional site occupancy
-400
-200
0
200
400
Eh(mV)

napthoquinols slightly more strongly than napthoquinones (approx. 4 fold).

The pH dependence of the maximum radical concentration formed during the potentiometric titrations of the decylubiquinone is illustrated in figure 4.5. As expected the radical displays greater stability at more alkaline pH with the anionic form of the semiquinone predominating. As the pH is lowered this stability decreases and the two electron couple shifts to a higher potential. This is apparent in figure 4.6 which shows the variation of E_1, E_2 and E_m with pH. The theoretical curves for the data are obtained using the values E_1=15mv, E_2=32.5mV, pK_1=6.8 and pK_2=9.75. For the pH range covered by these titrations E_m has an approximate dependency of -60mV/pH confirming an overall $2H^+/2e^-$ reaction, the pH independence of E_1 and the -120mv dependence of E_2 shows the two electron process (quinone to quinol) is comprised of a $Q \Leftrightarrow Q^{\bullet -} \Leftrightarrow QH_2$ reaction. As the theoretical values, pK_1=6.8 and a pK_2=9.75, both lie outwith the pH range studied, their values are tentative. These results are summarised in Table 4.1.

The cytochrome *bd* complex carries out the four electron reduction of oxygen to water, using electrons derived from quinol groups in the cytoplasmic membrane (Minghetti & Gennis, 1988). Thus the full oxidation of two quinols result from the reduction of an oxygen molecule. The electrons are proposed to pass through haem b_{558}. Both half-couples at pH=7.0, can reduce the low-spin haem b_{558}, the putative electron acceptor, E_{m7}=+250mV (Green *et al.*, 1986; Lorence *et al.*, 1988; Reid & Ingledew, 1979). However,

Figure 4.5 pH dependence of the maximum site occupancy by semiquinone derived from the purified cytochrome *bd* complex.

The maximum semiquinone concentration is obtained from the theoretical curve data. The semiquinone concentration is normalised to unity. This assumes that there is one semiquinone stabilising site per low-spin haem b_{558}

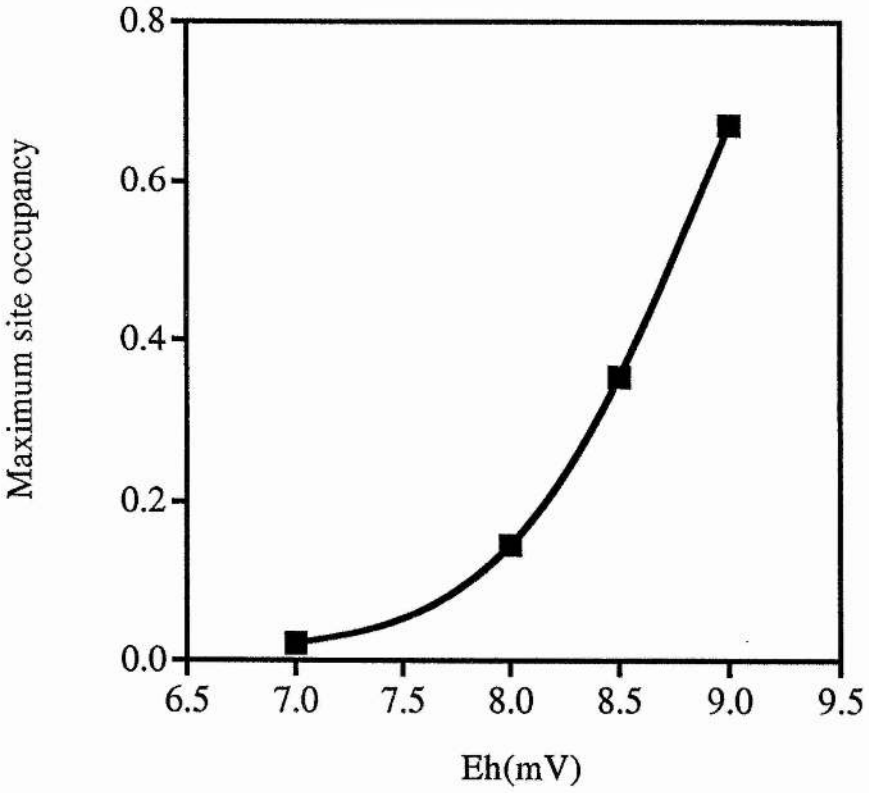
Maximum site occupancy
0.8
0.6
0.4
0.2
0.0
6.5
7.0
7.5
8.0
8.5
9.0
9.5
Eh(mV)

Figure 4.6 The pH dependence of the redox couples E_1, E_2 and E_m for the semiquinone derived from purified cytochrome *bd*.

The values of the two half potentials E_1(▲); E_2(▼); and midpoint potential E_m(■) are obtained from the simulated best fits (figure 4.3) and are shown as a function of pH. The theoretical curves are generated as described in chapter 3.2.2.1 using the values: E_1=15mV, E_2=32.5mV, pK_1=6.80 and pK_2=9.75.

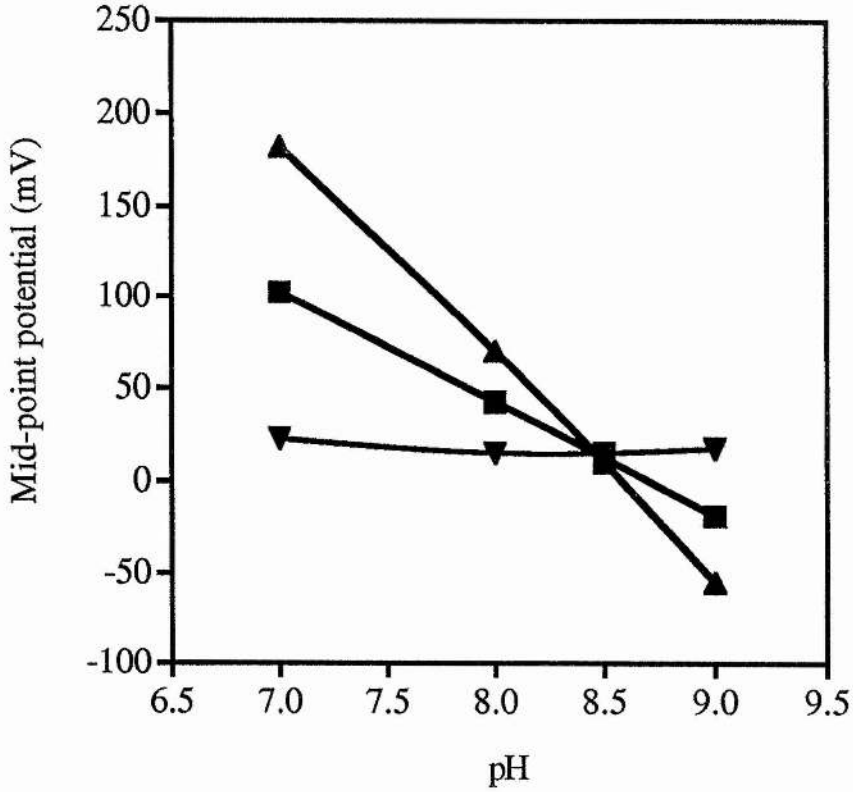
250
200
150
100
50
0
-50
-100
Mid-point potential (mV)
6.5
7.0
7.5
8.0
8.5
9.0
9.5
pH

Table 4.1 Summary of E_1, E_2, E_m and maximum site occupancy values for the cytochrome *bd* semiquinone

pH	E_1(mV)	E_2(mV)	E_m(mV)	maximum site occupancy
7.0[a]	22.5	182.0	102.25	0.02
8.0[a]	15.0	70.0	42.5	0.14
8.5[a]	15.0	10.0	12.5	0.34
9.0[a]	17.5	-55.0	-18.75	0.63
9.0[b]	-45.0	-120.0	-82.5	0.63
9.0[c]	-48.5	-118.5	-83.5	0.63

[a] 1mM decylubiquinone; [b] 1mM menadione; [c] 1mM vitamin K_1

Jünemann & Wrigglesworth, 1995, proposed that electrons from a quinone binding site can go to either haem b_{558} or haem *d* (or b_{595}) in *Azotobacter vinelandii* cytochrome *bd*. The highest potential case, haem *d* has an E_{m7} of approx. 280mV increasing the ΔE_m for the reaction with quinol by approximately 120mV. However, the quinone binding site and the haem b_{595} are thought to be on opposite sides of the membrane (Ingledew *et al.*, 1992), this would have consequences for electron transfer rates. If such a mechanism operated in the *E. coli* enzyme this site could still be regarded as an oxidation site and the requirement for stabilisation would remain. The menaquinone analogue values being lower are also compatible with electron transfer through haem b_{558}.

4.2.3 The displacement of semiquinones by inhibitors

The effect of the inhibitor HOQNO was studied by including it in a redox titration. HOQNO is a known competitive inhibitor of electron transfer and known to act at quinone binding sites (Krab & Wikström, 1980; Kita *et al.*, 1984b; Lam, 1984). Its presence at 1mM caused a quenching of the semiquinone signal. The requirement for such a high concentration of inhibitor reflects its low effectiveness at this site and the high concentration of exogenous quinone competing with it (1mM). A more effective competitive inhibitor of cytochrome *bd* is aurachin D (Kunze *et al.*; 1987; Meunier *et al.*; 1984) its presence at 50μM causes a similar attenuation of the semiquinone signal, again the high concentration required was a reflection of the level of quinone competing for the site.

4.3 Conclusion

The cytochrome *bd* complex, in common with the other *E. coli* terminal oxidase cytochrome bo_3 is an effective stabiliser of the semiquinone intermediate of quinol oxidation. This semiquinone is readily displaced by treatment with the inhibitors HOQNO and aurachin D. The site is interesting as it would appear to bind napthoquinone and benzoquinone species differently. This is indicted in the change in the ESR spectrum when a ubiquinone analogue is replaced by a menaquinone analogue due to increased hyperfine interactions in the latter. The semiquinone radical associated with the membrane-bound complex would appear to be hetrogeneous with both ubiquinone and menaquinone species contributing to the overall ESR spectrum. This would be expected as the bacteria were grown in conditions of low aeration and harvested in late log phase, conditions where menaquinone formation are high. Slight differences in the ESR spectra of menaquinones and ubiquinones were also evident with the cytochrome bo_3 complex. Although this, as with cytochrome *bd*, could be due to a simple rearrangement of the electronic structure of the bound semiquinone arising from differences in the structure of two types of quinone, it is also possible that the protein is binding each slightly differently. This would be of little consequence with cytochrome bo_3 as under the conditions where it is maximally expressed levels of menaquinone would be low. With cytochrome *bd* where the bacterial membrane will contain a mixture of quinones any differences in quinone binding will have implications for bacterial respiration.

The protein environment is known to have a big influence on the midpoint potential of a bound semiquinone, in an extreme case, the A_1 site of photosytstem I can distort the E_{m7} of the phylloquinone (or vitamin K_1) by around -700mV to -800mV (E_{m7} of free phylloquinone ~ -100mV) (Heathcote *et al*, 1996). The results of the redox titrations shown in figures 4.3 and 4.4 would suggest that cytochrome *bd* does not distort significantly the E_m of ubiquinones but does do it to menaquinones by around 35mV. Thus it would appear that the protein environment of Q_{bd} can increase the midpoint potential of a menaquinone to achieve a greater efficiency in electron transfer to the low-spin haem b_{558}, E_{m7}=+250mV (Reid & Ingledew, 1979). Electron transfer from ubiquinol will not require this distortion as the $E_{m's}$ of the ubisemiquinone and haem b_{558} are more comparable. Futher studies of the semiquinone by ENDOR and ESEEM spectroscopies would yield more information on the electronic structure of the radical and the protein-quinone interactions leading to semiquinone stabilisation.

The presence of exchangeable protons at the site were indicated by deuterium exchange. As with cytochrome bo_3 the replacement of protons with deuterons reduces line broadening effects in the ESR spectrum.

The overall redox chemistry occuring at the site is indicative of a $2H^+/2e^-$ reaction over the pH range studied. The anionic form of the semiquinone predominates at higher pH's, as expected. Analysing the ESR spectra and the redox titration results it can be concluded that the data can be readily fitted by assuming only a single quinone binding site and there is no indication spectrally or thermodynamically of multiple semiquinone species where there is

one quinone type present. With the oxidation of menaquinol or ubiquinol both half-couples are capable of reducing haem b_{558}. Studies on the cytochrome *bd* from *A.vinelandii* have suggested a branched electron transfer pathway for the two electrons one going to haem b_{558} and the other to haem *d* (via haem b_{595}) (Jünemann & Wrigglesworth; 1995). If *E. coli* transfered electrons in this way semiquinone stabilisation would still be required.

5.0 ENDOR STUDIES OF CYTOCHROMES bo_3 & bd SEMIQUINONES

5.1 Introduction

Enhancing our understanding of the interactions involved in the binding and subsequent stabilisation of semiquinone intermediates is a crucial part in gaining an insight into the overall process of quinol oxidation.

Chapters 3.0 and 4.0 sought to utilise ESR spectroscopy to probe the thermodynamics and obtain structural information relating to quinone binding to the cytochrome bo_3 and cytochrome *bd* complexes. ESR spectroscopy can communicate much about the overall process of quinol oxidation and to a lesser extent indicate the interactions stabilising the semiquinone intermediate. Making definitive assignments to these interactions in terms of the surrounding protein environment and their subsequent effect on the properties of the semiquinone is outwith the practical capabilities of ESR. In order for such assignments to be made the related technique of Electron Nuclear Double Resonance Spectroscopy (ENDOR)[a] can be used. ENDOR spectroscopy has been used to characterise several bound semiquinones including those associated with the bacterial reaction centres of *Rhodobacter sphaeroides* and *Rhodopseudomonas viridis*, Q_A and Q_B (Allen *et al*, 1987a, b; Burghaus *et al*, 1993; Deisenhofer *et al*, 1985), the Q_c site

---

[a] Electron Nuclear Double Resonance Spectroscopy (ENDOR) is an extension of electron spin resonance. ENDOR detects radiofrequency induced NMR transitions by the change in the ESR signal (Dorio & Freed, 1979; Kurreck *et al.*, 1988). Its principal use, therefore, is to measure the hyperfine splittings which are often unresolved by ESR. ENDOR combines the sensitivity of ESR with the resolution of NMR. ENDOR spectra are recorded in a modified ESR cavity around which NMR radiofrequency coils are wound.

semiquinone of quinol cytochrome *c* reductase complex (Salerno *et al*, 1990) and also the $A_1^{\bullet -}$ semiquinone of Photosystem 1 (Rigby *et al*, 1996). In each case the electronic structure, in particular the spin density distribution of the bound semiquinone radical, has been determined by analysis of the hyperfine coupling constants (hfc) which were poorly resolved by ESR techniques.

The ENDOR studies on $A_1^{\bullet -}$ are of interest as they demonstrate in a striking way how the immediate protein environment can exert large changes in the properties of the bound semiquinone. In the cyanobacteria *Anabaena variabilis* the $A_1^{\bullet -}$ is a phylloquinone radical (vitamin K_1 or menaquinone-2), a napthoquinone, which accepts electrons from a chlorophyll *a* molecule termed A_0 and then transfers them to several iron-sulphur centres (Heathcote *et al*, 1996). The E_m's of both the donor and acceptor are very electronegative and in order for electron transfer to proceed through A_1 the E_m for this phylloquinone must be correspondingly electronegative with an E_m of ca. -800mV. Free phylloquinone has a $E_{m,7}$ of -100mV and to achieve a reduction in E_m of this magnitude the protein must interfere with and distort the electronic structure of the bound quinone to this end. ENDOR studies on this system have shown that the unpaired electron spin density distribution is altered relative to the free phylloquinone radical with hyperfine couplings to the methyl group of the phylloquinone ring and to two protons hydrogen bonded to the quinone oxygens (Rigby *et al*, 1996). Which hyperfine interaction is responsible for the large negative shift in E_m is not clear.

Given the complexity of the semiquinone radical associated with the cytochrome *bo*$_3$ complex, in particular the presence of the

partially resolved hyperfine splittings in the ESR spectrum described in chapter 3.0 and by Ingledew *et al*, 1995, still unassigned, ENDOR would seem a useful technique by which to study the fine electronic structure of this semiquinone radical and the protein-quinone interactions. The aim of this work would be to assign the nature of the hyperfine couplings and to suggest their role in enzyme function. It would also reinforce the conclusions made in chapter 3.0 that only one semiquinone radical is associated with the complex and that this is at the site of quinol oxidation. The binding of phylloquinone, ubiquinone, duroquinone and plastoquinone are also investigated as the differences in the structures of these benzo- and napthoquinones will be reflected in the electronic structure of the corresponding semiquinones and detectable by ENDOR.

The semiquinone radical associated with the cytochrome *bd* complex is also to be studied by ENDOR. As described previously, in chapter 4.0, the cytochrome *bd* complex can oxidise either benzoquinones or napthoquinones through the corresponding semiquinone intermediate but knowing that the expression of the complex is favoured by micro-aerobic conditions, menaquinone-8, is more likely to be the preferred reductant (Ingledew & Poole, 1984). This is not reflected in the binding of each semiquinone form to the complex. There is however an indication of partially resolved hyperfine splittings in the menasemiquinone ESR spectrum that are absent from the corresponding ubisemiquinone spectrum as well as a shift in the E_m for menasemiquinones that is not observed when ubiquinone is used as the reductant. Again, as with cytochrome *bo*$_3$, the differences in structure of benzoquinones and

napthoquinones will be reflected by differences in the electronic structures of each semiquinone form which can be investigated using ENDOR.

5.2 Results & Discussion

5.2.1 ESR spectroscopy of semiquinone radicals.

Figure 5.1 shows the ESR spectra of the protonated and deuterated ubisemiquinone radicals associated with the cytochrome *bo*$_3$ complex recorded in the ENDOR cavity. These are essentially the same as that described by Ingledew *et al.*, 1995 and in figure 3.1 and demonstrate that H-bond hyperfine couplings (hfc) contribute to the ESR spectrum and without them the larger hfc is better resolved. For comparison, the ESR spectrum of a decyl-ubisemiquinone anion radical in isopropanol is included (figure 5.1(c)). This is produced by reduction of the quinone with sodium borohydride in alkaline solvent and clearly shows a smooth isotropic lineshape. The differences in the ESR spectra of the ubisemiquinone radical associated with the cytochrome *bo*$_3$ complex and those of the *in vitro* radical must be due to the influence of the protein environment.

5.2.2 ENDOR spectroscopy of the ubisemiquinone radical associated with the cytochrome *bo*$_3$ complex.

ENDOR spectroscopy reveals the electronic structures of radicals as expressed in the unpaired electron spin density of the singly occupied molecular orbital (SOMO) (Rigby *et al.*, 1996). The ENDOR spectrum of the cytochrome *bo*$_3$ ubisemiquinone radical is shown in figure 5.2(a). This is achieved by recording the ENDOR spectra at the ESR zero cross-over point. This region of the ENDOR spectrum shows features that arise from the hyperfine coupling of the radical to protons. A proton gives an ENDOR

Figure 5.1 ESR spectra of ubisemiquinones *in vitro* and associated with the cytochrome *bo*$_3$ complex.

ESR spectra of (a) ubisemiquinone radical associated with the purified cytochrome bo_3 complex in 100mM H_2O bis-tris-propane, pH8.5; (b) as (a) in 100mM D_2O bis-tris-propane, pH8.5; (c) decyl-ubisemiquinone radical in isopropanol. All spectra were recorded in the ENDOR cavity. Conditions: microwave power 30mW; modulation amplitude 1.2mT; modulation frequency 12.5KHz; temperature 60K. (a) and (b) are the sums of two scans.

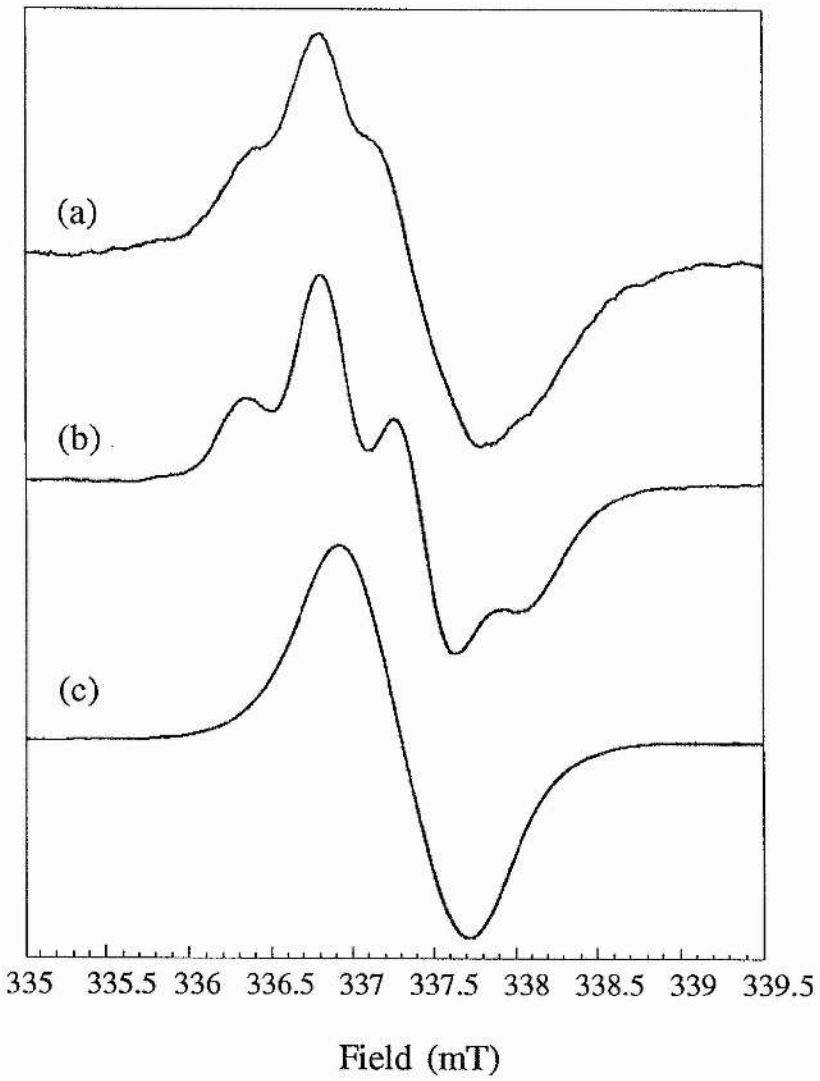
(a)
(b)
(c)
335
335.5
336
336.5
337
337.5
338
338.5
339
339.5
Field (mT)

spectrum that consists of two features at the free proton NMR frequency υ_{NMR} that is split from this frequency by $\pm A/2$, where a is the hyperfine coupling.

$$\upsilon_{ENDOR}=\upsilon_{NMR} \pm A/2.$$

ENDOR spectra of frozen solutions (or powder spectra) taken at this position in the ESR spectrum typically show all orientations of the molecules in the external field and cause a spread in the proton ENDOR frequencies with a build-up at the principal values ($A_{||}$ and $A_{\perp}$) (O'Malley & Babcock, 1986).

ENDOR spectra of semiquinones in frozen solutions show large features due to hyperfine couplings to the methyl groups that are attached (β) to the delocalised π orbital system of the quinone ring (O'Malley & Babcock, 1984) which is the location of the unpaired electron as the singly occupied molecular orbital (SOMO). Intense features also arise from hyperfine couplings to protons hydrogen bonded to the quinone oxygens (O'Malley & Babcock, 1986). Both the hfc's of the β-methyl group and the hydrogen bonded protons have axial lineshapes under these ENDOR conditions, each has an intense $A_{\perp}$ component which possesses a zero cross-over point and a smaller $A_{||}$ component at the turning point of the principal value of the hyperfine tensor (O'Malley & Babcock, 1984, 1986). Other features which may be observed include hfc's to methylene protons β to the SOMO that appear under some circumstances as with ENDOR studies of tyrosine radicals and A_1 of photosystem I (Rigby *et al.*, 1994a; Rigby *et al.*, 1996). In figure 5.2(a) the most intense features are 4 and 6. Both have lineshapes characteristic of an $A_{\perp}$ and $A_{||}$ components with the

Figure 5.2 ENDOR spectra of the ubisemi-quinone radical associated with the purified cytochrome bo_3 complex

Spectra taken at centre of the ESR spectrum in (a) 100mM H_2O bis-tris-propane, pH8.5; (b) 100mM D_2O bis-tris-propane, pH8.5; (c) difference spectrum of (a) minus (b). Conditions: microwave power 3.0mW; r.f. power 100W; r.f. modulation depth 140KHz; time constant 655ms; scan time 84s; average of 120 scans; temperature 60K.

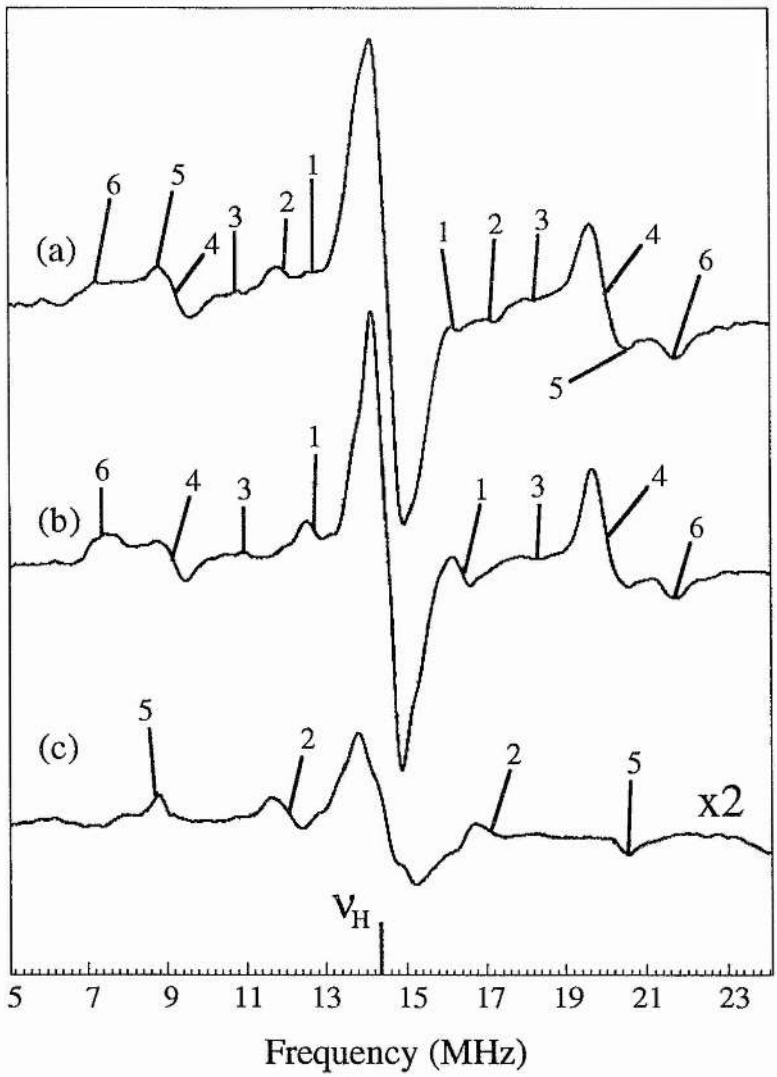
(a)
(b)
(c)
x2
ν_H
5 7 9 11 13 15 17 19 21 23
Frequency (MHz)

same hyperfine coupling. The difference between the two components ($A_{\|}$ - $A_{\perp}$) is 3.6MHz which is in agreement with values of methyl groups β to a semiquinone (O'Malley & Babcock, 1984). Thus features 4 and 6 can be assigned to the 2-methyl group of the cytochrome *bo*$_3$ semiquinone which is the only methyl group β to the ring of ubiquinone. Figure 5.3 shows the structures and numbering system of the quinones used in this study.

The remaining intense features of figure 5.2(a) 1, 2 and 3 are likely to arise from hyperfine couplings to protein or solvent protons hydrogen bonded to the carbonyl oxygens of the semiquinone and also to the methylene protons β to the quinone ring on the farnesyl chain attached to position 3. The later protons which are covalently attached to the quinone can easily be distinguished from those hydrogen bonded to the quinone by exchanging the solvent with deuterium oxide. The ENDOR spectrum of the deuterium exchanged cytochrome *bo*$_3$ ubisemiquinone sample is shown in figure 5.2(b) with the difference spectrum (a)-(b) shown in figure 5.2(c). As with the ESR spectrum deuterium exchange leads to a change in lineshape with increased resolution of the proton hyperfine features of the ENDOR spectrum. Any features present in figure 5.2(a) due to exchangeable protons will not be present in figure 5.2(b) as they will have been exchanged for deuterons. The difference spectrum (figure 5.2(c)) therefore shows only those features due to exchangeable protons which are most likely to be hydrogen bonded to the semiquinone oxygens. Feature 2 is therefore exchangeable and has a lineshape of a $A_{\perp}$ component of an axial hfc. Figure 5.2(c) also reveals a new feature, 5, which was hidden in (a) and (b) by the large methyl hfc

Figure 5.3 Structures and numbering systems of quinones

The structures of the quinones and the numbering system used in this study were as follows:(a) phylloquinone (vitamin K_1, menaquinone-2); (b) decylubiquinone; (c) decylplastoquinone; (d) duro-quinone (tetramethylbenzo-quinone)

(a)

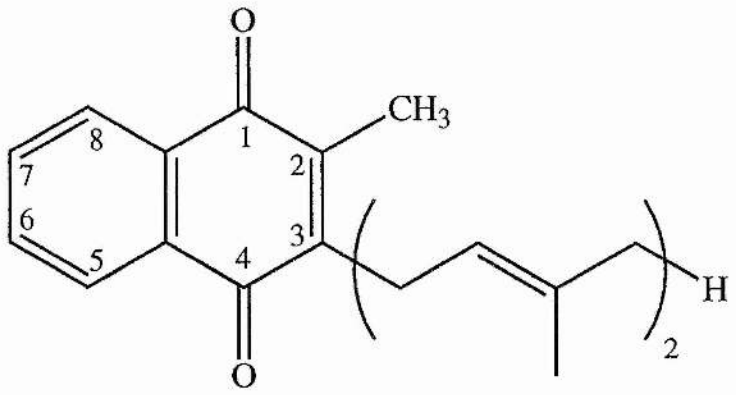
O
CH3
8
1
2
7
3
6
4
5
H
2
O

(b)

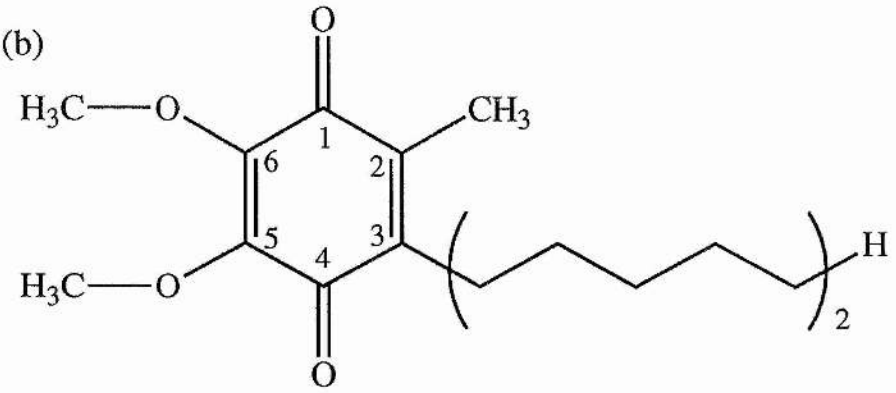
O
H3C—O
CH3
1
6
2
5
3
4
H3C—O
H
2
O

(c)

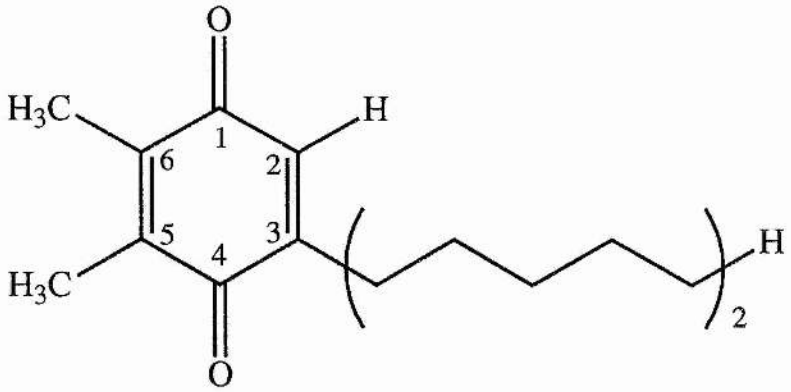
O
H3C
H
1
6
2
5
3
4
H3C
H
2
O

(d)

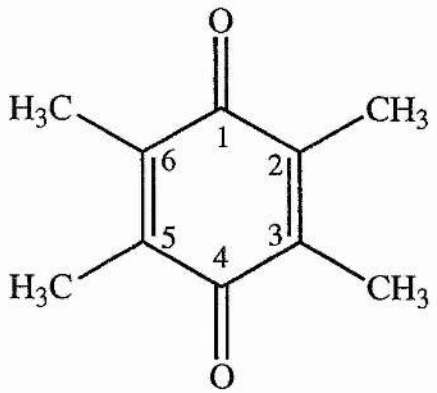
O
H3C
CH3
1
6
2
5
3
4
H3C
CH3
O

Table 5.1 Hyperfine coupling constants and resonance assignments for the cytochrome bo_3 semiquinone and the decylubisemiquinone anion radical in alkaline isopropanol.

Feature	Hyperfine coupling (MHz)		Assignment
	cytochrome bo_3	isopropanol	
1	3.8	----	β-CH_2 $A_\perp$
2	-5.1	-1.7	H-bond $A_\perp$
		-2.4	H-bond $A_\perp$
3	7.5	----	β-CH_2 $A_\parallel$
4	10.8	4.8	Methyl $A_\perp$
5	11.7	4.9	H-bond $A_\parallel$
		6.1	H-bond $A_\parallel$
6	14.4	7.9	Methyl $A_\parallel$

and has the expected lineshape of the $A_{||}$ component. It is not possible to ascertain using ENDOR whether these exchangeable proton features are due to one or more hydrogen nuclei bonded to one or both carbonyl oxygens of the quinone.

The remaining features, 1 and 3 which are not exchanged with deuterium must be due to the protons covalently attached to C1' of the farensyl chain. These protons hfc's appear to be identical and cannot be distinguished by this technique. The hfc's values of all of these features (1 to 6) are summarised in table 5.1.

5.2.3 Orientation selected ENDOR of the ubisemiquinone radical associated with cytochrome bo_3.

ESR spectra of frozen solutions or powders is the superposition of spectra arising from electron spins with completely random orientations to the direction of the magnetic field. If the g tensor is anisotropic, i.e. varies with the direction of the applied magnetic field, the edges of the ESR spectrum at field values of g_z or g_x (g_y is effectively equivalent to g_x) arise from electron spins for which the g tensor is oriented along the z or x axes. The g_x and g_y components are defined as being at right angles to each other in the plane of the quinone ring and g_z is perpendicular to the quinone ring plane (O'Malley & Babcock, 1986). The g_z component is significantly different from the values of g_x and g_y; radicals with the electron spin for which the g tensor has a z-axis orientation contribute most to the high field side of the ESR spectrum. By recording the ENDOR spectrum at a higher field value (here 8mT up-field of the zero cross-over point) the effects of the g_x and g_y components are minimised and only those hyperfine interactions

Figure 5.4 Orientation selected ENDOR spectra of the ubisemiquinone radical associated with the purified cytochrome bo_3 complex

Spectra taken 8mT upfield of the centre of the ESR spectrum in (a) 100mM H_2O bis-tris-propane, pH8.5 and (b) 100mM D_2O bis-tris-propane, pH8.5; Conditions: microwave power 3.0mW; r.f. power 100W; r.f. modulation depth 199KHz; time constant 655ms; scan time 84s; average of 160 scans; temperature 60K.

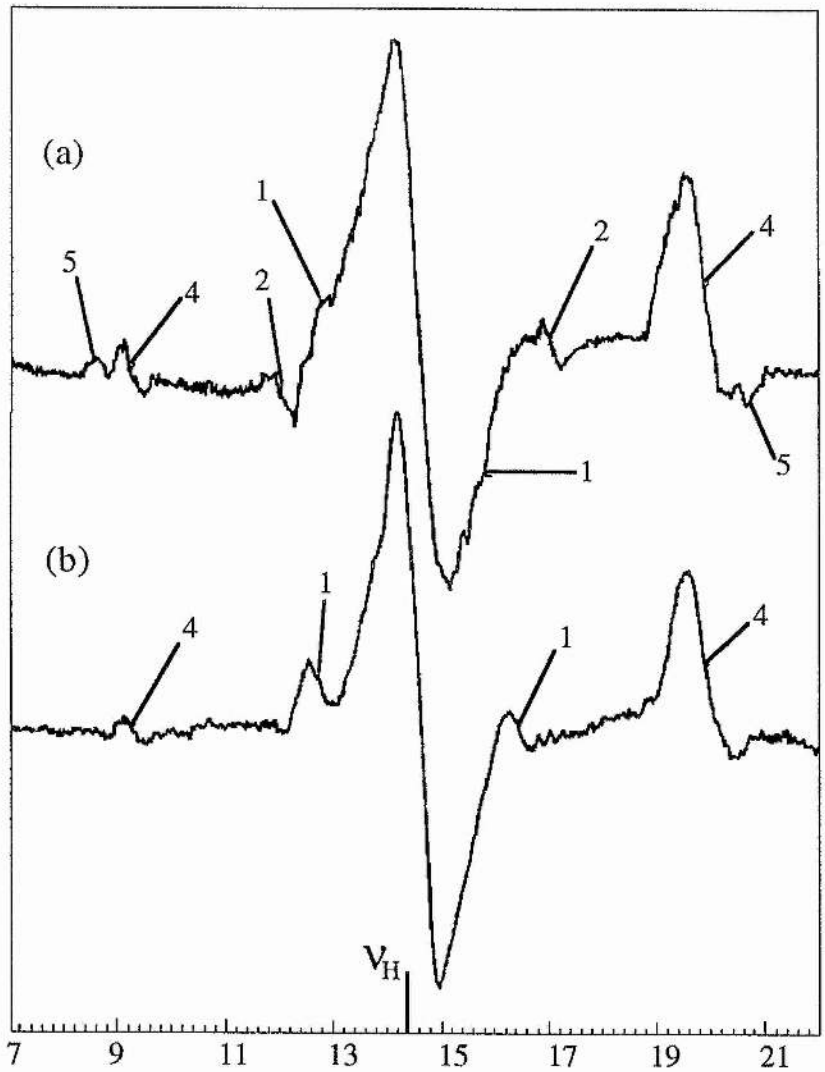
(a)
1
2
4
5
4
2
1
5
(b)
4
1
1
4
ν_H
7
9
11
13
15
17
19
21
Frequency (MHz)

lying oriented along the z-axis will contribute to the ENDOR spectrum. The g_z component is chosen as it has been shown by high-field ESR that the g tensors of semiquinone anion radicals are almost axial and that g_x and g_y contribute to each other (Burghaus *et al.*, 1993).

In this study the assignments made to the ENDOR spectrum of the cytochrome *bo*$_3$ semiquinone in the preceeding section are clarified using orientation selected ENDOR allowing for the determination of the orientation of the hyperfine couplings relative to the ring plane (Rist & Hyde, 1968; O'Malley & Babcock, 1984). Quinone ring substituents that are covalently attached (i.e. β to the ring), such as methyl and methylene groups, under these conditions would be expected to show only their $A_\perp$ features. However, hydrogen bonds would be expected to show both $A_\perp$ and $A_\parallel$ features unless they lie in the plane of the ring in which case only the $A_\perp$ feature would be evident. Figure 5.4(a) shows the ENDOR spectrum of the cytochrome *bo*$_3$ ubisemiquinone anion taken at the g_z edge of the ESR spectrum. These spectra have a lower signal to noise ratio due to them not being recorded at the maximum of the ESR spectrum. Features 1, 2, 4, and 5 are present in this spectrum but in the deuterium exchanged sample (figure 5.4(b)) where only feature 1 and 4 are evident. This confirms the previous assignment that feature 1 and 4 are due to the $A_\perp$ component of the 3-CH_2 and 2-methyl groups respectively. Features 2 and 5 are due to the $A_\perp$ and $A_\parallel$ of the hydrogen bond hyperfine coupling and the fact that both are present suggests that the hydrogen bonds lie not in the plane of the quinone ring but at an angle to it between 0° and 90° but it cannot be precisely determined from these spectra this would

require the exact values of the three g-tensor components. The absence of the hydrogen bond features in the deuterium exchanged sample confirms the assignments of features 2 and 5.

5.2.4 Matrix ENDOR of the ubisemiquinone radical associated with cytochrome bo_3.

Figure 5.5 shows the ENDOR spectrum from the matrix region of the cytochrome bo_3 ubisemiquinone radical. This region, between 12.5 and 16MHz in this experiment, is centred on the free proton frequency and shows small hyperfine couplings of exchangeable protons from the protein and perhaps water molecules which are in the vicinity (around 5-6Å) and weakly coupled to the SOMO (Salerno *et al.*, 1990). Protons from the C5 and C6 methoxy groups may also contribute to the features in this region. The matrix ENDOR of the deuterium exchanged sample shows fewer features and this confirms the presence of exchangeable protons from the protein or solvent.

The matrix region is particularly sensitive to subtle changes in the surrounding protein environment and would prove a useful technique with which to monitor the effects of site directed mutagenesis at or near the quinone binding site

5.2.5 ENDOR spectroscopy of '*in vitro*' decylubisemiquinone anions

Figure 5.1(c) demonstrated the smooth isotropic lineshape of the '*in vitro*' decyl-ubisemiquinone anion radical. The absence of any hyperfine structure in the ESR spectrum means that any differences between this radical and that associated with cytochrome

Figure 5.5 Matrix ENDOR of the ubi-semiquinone radical associated with the purified cytochrome bo_3 complex.

(a) In 100mM H_2O bis-tris-propane, pH8.5; (b) 100mM D_2O bis-tris-propane, pD8.5. Conditions: microwave power 3.0mW; r.f. power 100W; r.f. modulation depth 35KHz; time constant 655ms; scan time 84s; average of 80 scans; temperature 60K.

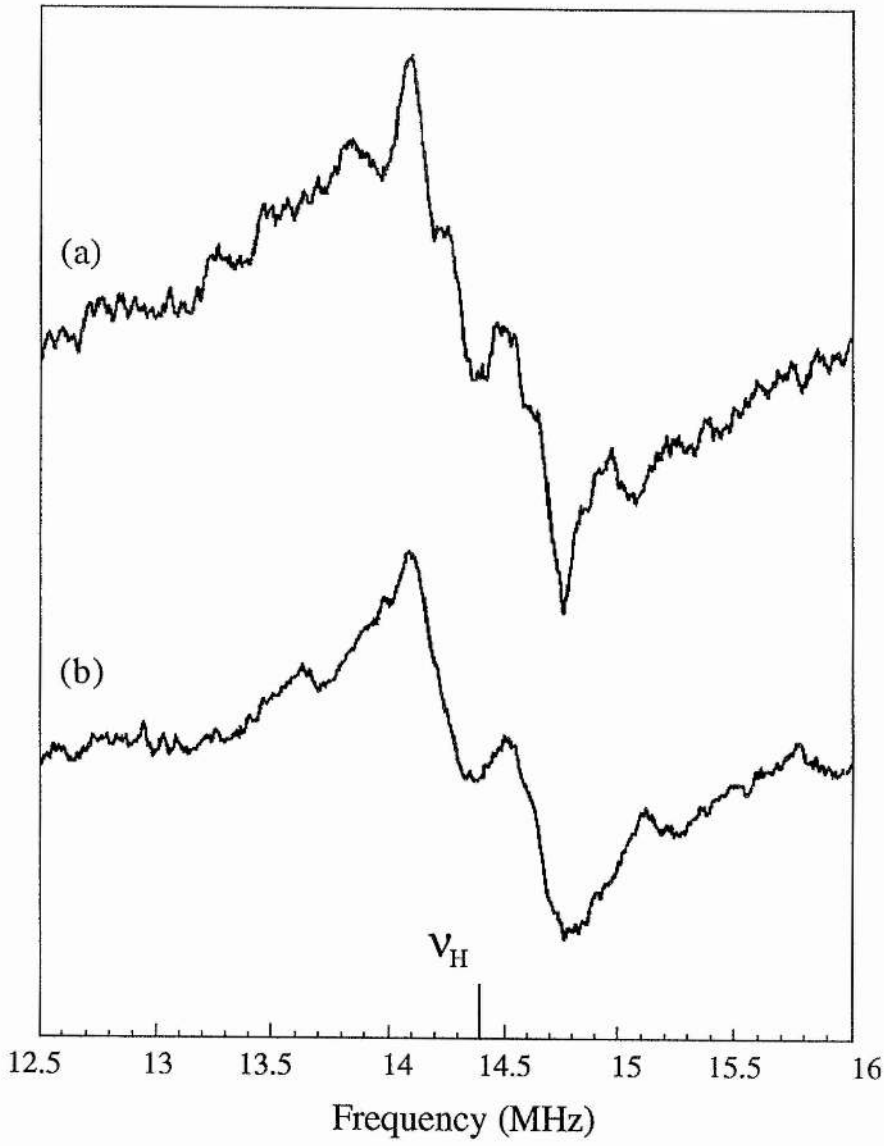
(a)
(b)
ν_H
12.5
13
13.5
14
14.5
15
15.5
16
Frequency (MHz)

bo_3 can be attributed to interactions with the protein environment of the quinone binding site. The ENDOR spectra of the decyl-ubisemiquinone radical can thus provide a model by which to interpret the ENDOR spectra described previously.

Figure 5.6(a) and (b) show the ENDOR spectra of the '*in vitro*' decyl-ubisemiquinone anion radical in protonated and deuterated isopropanol (deuterated at the hydroxyl group only). These spectra are recorded under the same conditions as those for the cytochrome bo_3 associated semiquinone for comparison but it should be noted that this is not necessarily the ideal conditions for the '*in vitro*' system. Features 1 and 3 due to the β-CH2 groups are not visible in these spectra, this is most likely due to them being hidden under the large central matrix feature. Deuteration of the solvent (figure 5.6(b)) reveals the hyperfine couplings due to the covalently attached methyl groups (features 4 and 6) with the values of each being in agreement with those of a study on plasto-semiquinones (MacMillan *et al.*, 1995). Both hyperfine coupling components for the methyl group are considerably less than those from the cytochrome bo_3 ubisemiquinone as demonstrated in Table 5.1. The remaining features 2 and 5 revealed by the difference spectrum of (a)-(b), figure 5.6(c) show those features arising from hydrogen bonded protons. These suggest two similar but not identical hyperfine couplings and both appear in the orientation selected spectrum, figure 5.6(d), so these hydrogen bonds are not in the plane of the quinone ring.

Figure 5.6 ENDOR spectra of the decyl-ubisemiquinone anion radical in isopropanol.

(a) in protonated isopropanol; (b) in isopropan(*ol-d*) (i.e. deuterated at the hydroxyl group only); (c) difference spectrum (a) minus (b); (d) orientation selection spectrum taken at 8mT upfield of the ESR spectrum. Conditions: microwave power 3.0mW; r.f. power 100W; r.f. modulation depth 50KHz; time constant 655ms; scan time 84s; average of 40 scans for (a) and (b) 100 scans for (d); temperature 60K.

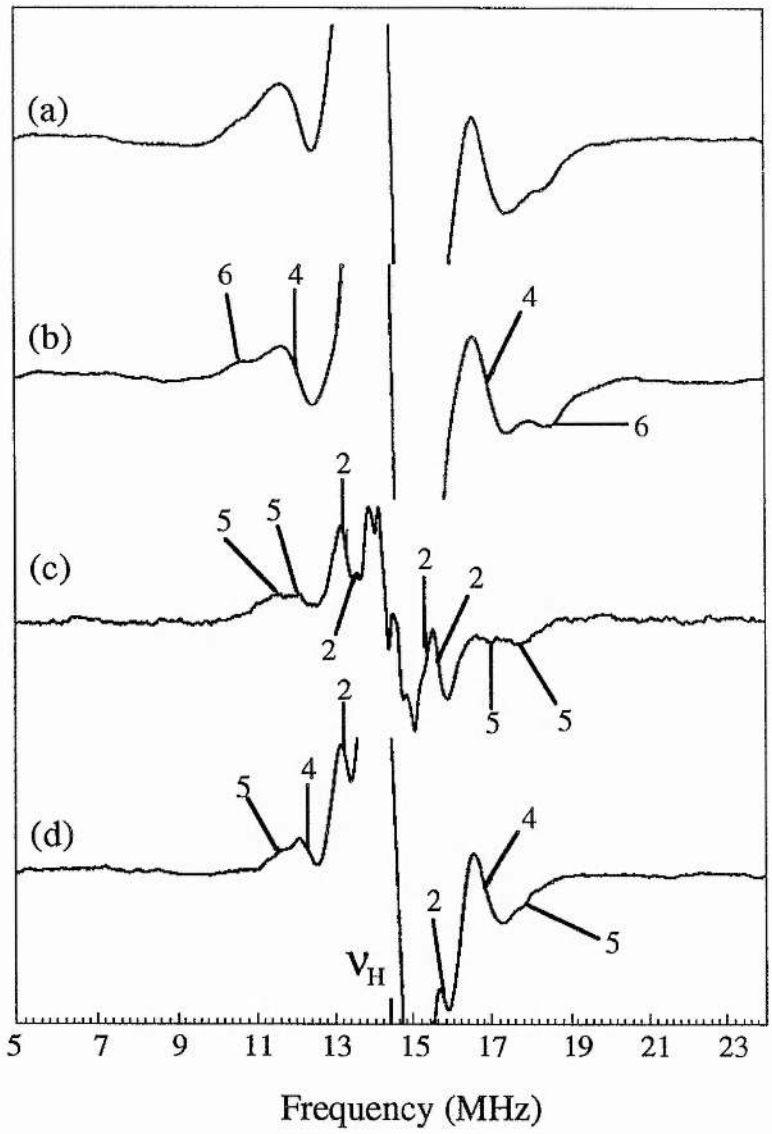
(a)
(b)
(c)
(d)
6
4
4
6
2
5
5
2
2
2
5
5
2
5
4
4
5
2
2
4
5
ν_H
5
7
9
11
13
15
17
19
21
23
Frequency (MHz)

5.2.6 ENDOR spectroscopy of the ubisemiquinone radical associated with the membrane-bound cytochrome bo_3 complex.

ENDOR spectra of the ubisemiquinone radical associated with the membrane-bound cytochrome bo_3 complex were recorded in addition to the purified complex. The ESR spectrum of the ubiquinol-8 semiquinone (figure 3.1) is identical to that of the purified cytochrome bo_3 associated decyl-ubisemiquinone indicating that the length of the quinone tail was of little significance to the binding of the head group. Exchanging the membranes into deuterium oxide had little effect on the ESR spectrum a result of the inaccessibility of the site to the solvent. The normal ENDOR spectra and orientation selected spectra of the membrane-bound complex semiquinone were very similar to those of the purified cytochrome bo_3 associated decyl-ubisemiquinone and are shown in figure 5.7 (a) and (b). The hyperfine couplings are summarised in table 5.2. The matrix ENDOR (figure 5.7(c)) showed slight differences when compared to the spectrum of figure 5.5(a), these can be accounted for by changes in the ENDOR conditions but may also be due to small perturbations in the protein environment of the quinone binding site. These presumably will be the result of removing the complex from the membrane. Overall, the ENDOR spectra of the semiquinone associated with the purified and membrane-bound cytochrome bo_3 are almost identical.

Figure 5.7 ENDOR spectra of the ubi-semiquinone-8 radical associated with the membrane-bound cytochrome bo_3 complex.

(a) ENDOR spectra of the ubisemiquinone radical associated with the membrane-bound bo_3 complex taken at centre of the ESR spectrum in 100mM H_2O bis-tris-propane, pH8.5.

(b) Orientation selected ENDOR spectra taken 8mT upfield of the centre of the ESR spectrum. Conditions: microwave power 3.0mW; r.f. power 100W; r.f. modulation depth 199KHz; time constant 655ms; scan time 84s; average of 160 scans; temperature 60K.

(c) Matrix ENDOR spectrum. Conditions: microwave power 3.0mW; r.f. power 100W; r.f. modulation depth 35KHz; time constant 655ms; scan time 84s; average of 80 scans; temperature 60K.

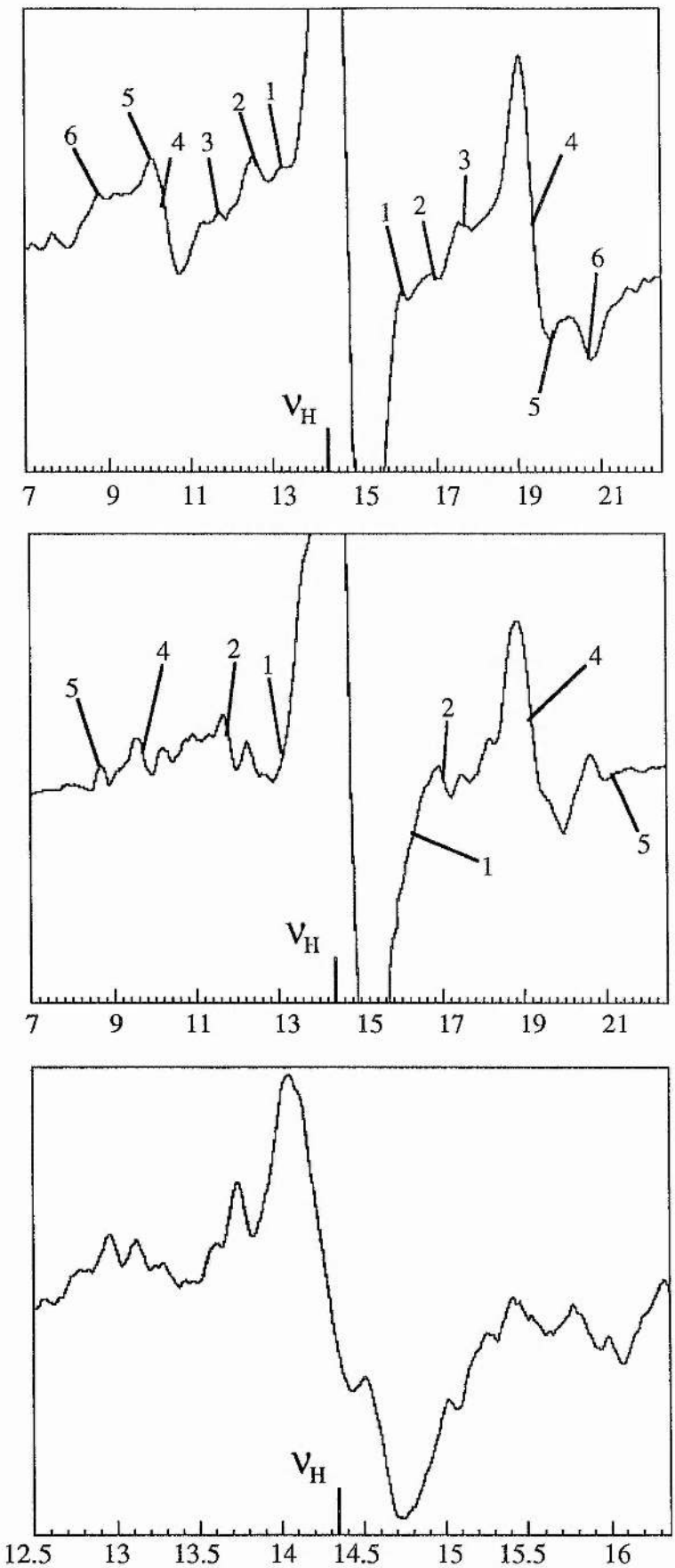
6
5
4
3
2
1
ν_H
7
9
11
13
15
17
19
21
1
2
3
4
5
6
ν_H
12.5
13
13.5
14
14.5
15
15.5
16
Frequency (MHz)

Table 5.2 Hyperfine coupling constants and resonance assignments for the membrane-bound cytochrome bo_3 semiquinone.

Feature	Hyperfine coupling (MHz)	Assignment
1	3.6	β-CH_2 $A_\perp$
2	-5.1	H-bond $A_\perp$
3	7.2	β-CH_2 $A_\parallel$
4	10.8	Methyl $A_\perp$
5	11.7	H-bond $A_\parallel$
6	14.4	Methyl $A_\parallel$

5.2.7 ESR and ENDOR of *p*-benzosemiquinones and *p*-naptho-semiquinones associated with the cytochrome bo_3 complex

In addition to oxidising ubiquinol the cytochrome bo_3 complex can also oxidise other substituted *p*-benzoquinones and *p*-napthoquinones (Kita *et al.*, 1984a). These reactions also proceed through a stable semiquinone intermediate which should have a different electronic structure reflecting the differences in the molecular structure of the quinone. These changes can be detected by ESR, which show subtle differences when compared to the 'normal' ubisemiquinone radical as in figure 5.8. The structures and numbering system for the quinones used are displayed in figure 5.3. The ESR spectra shown give little information on the electronic structure of the radical except that the large hyperfine coupling due to the methyl group is still evident. All three quinones used have methyl group(s) covalently attached to the quinone ring.

The ENDOR spectra, shown in figure 5.9, give more information on the electronic structure of each radical. The hyperfine coupling constants for each feature (1 to 6) are summarised in table 5.3, no deuterium exchanged samples were prepared therefore values for feature 5 are estimated. The hfc values are very similar to those of the ubisemiquinone radical (see table 5.1) which suggests that the differences observed in the ENDOR spectra on binding the semiquinones to the cytochrome bo_3 complex are essentially independent of the covalent structure of the quinone and must therefore be a function of the site.

Figure 5.8 ESR spectra of replacement semiquinones associated with the cytochrome bo_3 complex.

ESR spectra of (a) phyllosemiquinone radical associated with the purified cytochrome bo_3 complex in 100mM bis-tris-propane, pH8.5; (b) as (a) with substitution by decyl-plastoquinone (c) as (a) with substitution by duroquinone. All spectra were recorded in the ENDOR cavity. Conditions as in figure 5.1.

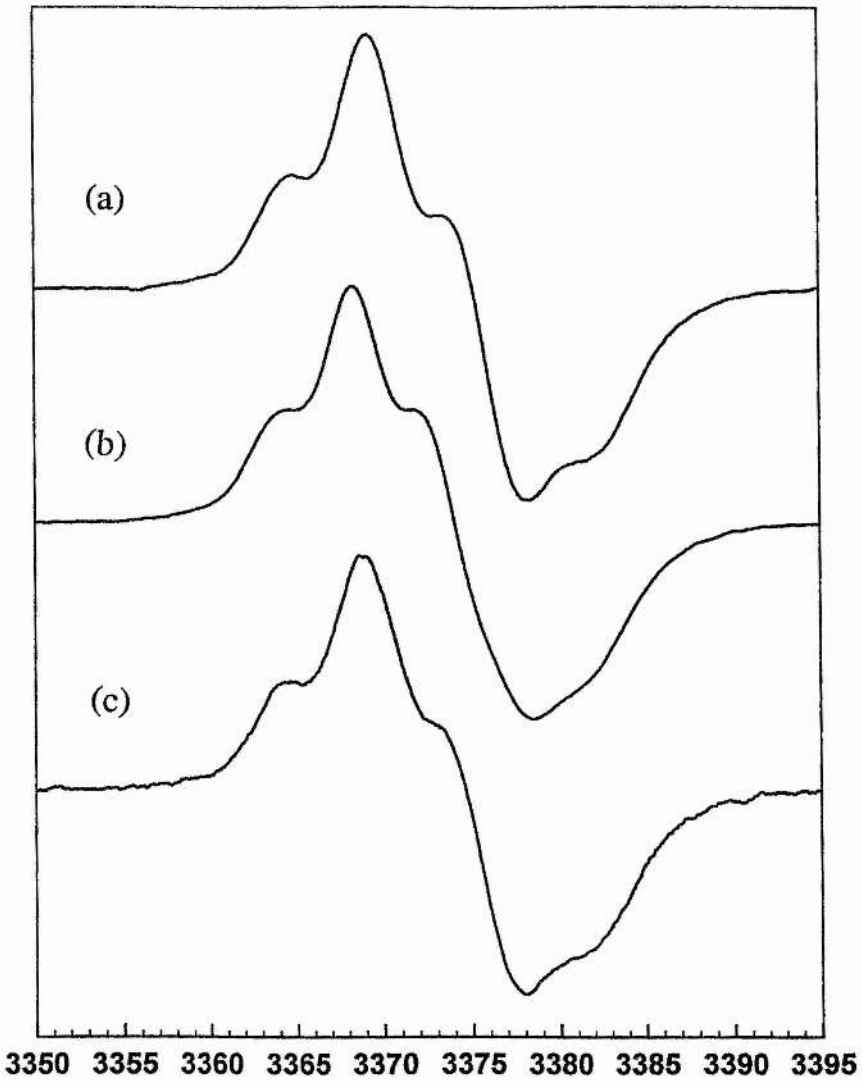
(a)
(b)
(c)
3350 3355 3360 3365 3370 3375 3380 3385 3390 3395
Field (mT)

Figure 5.9 ENDOR spectra of the replaced semiquinone radicals associated with the purified cytochrome bo_3 complex

Spectra taken at centre of the ESR spectrum in 100mM bis-tris-propane, pH8.5; (a) phyllo-semiquinone radical (b) decyl-plastosemiquinone radical (c) durosemi-quinone radical . Conditions as in figure 5.2.

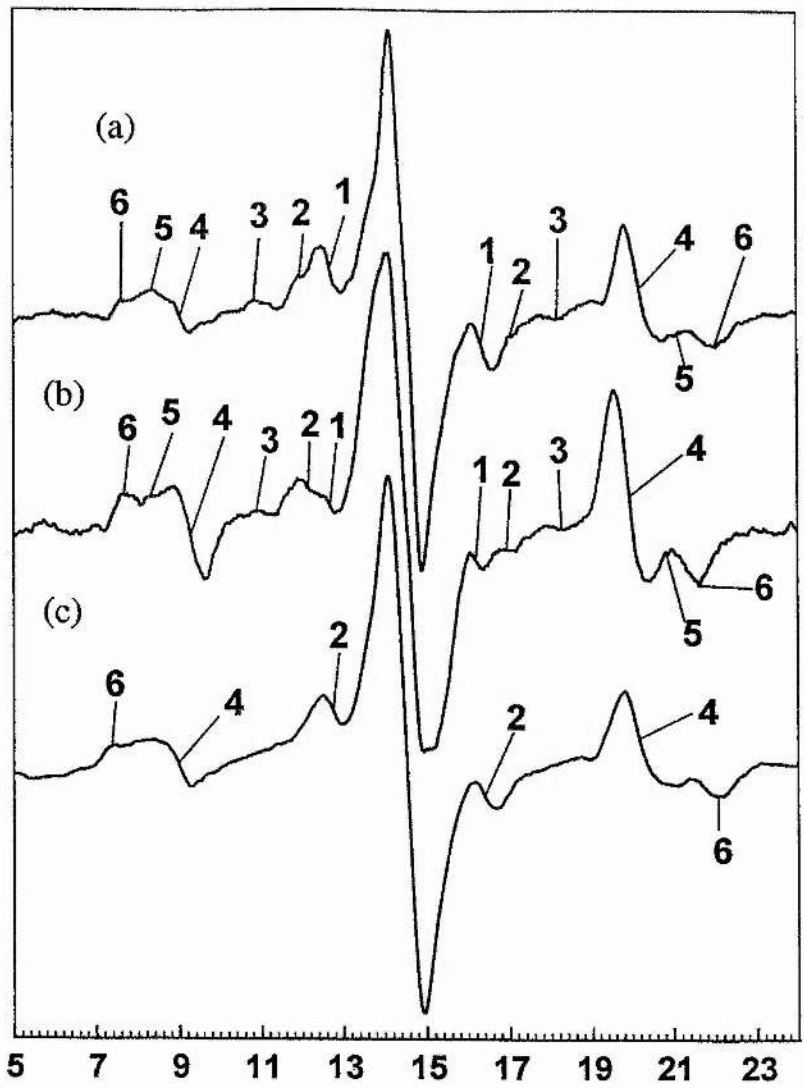

Frequency (MHz)

Table 5.3 Hyperfine coupling constants and resonance assignments for replacement quinones cytochrome bo_3 semiquinone.

Feature	Hyperfine coupling (MHz)			Assignment
	PhQ	PQ	DQ	
1	3.6	3.6	----	β-CH_2 $A_\perp$
2	-5.1	-4.6	3.7	H-bond $A_\perp$
3	7.3	7.3	----	β-CH_2 $A_\parallel$
4	11.2	10.8	11.2	Methyl $A_\perp$
5*	12.7	12.4	----	H-bond $A_\parallel$
6	14.4	13.9	14.6	Methyl $A_\parallel$

*Estimated: no deuterium exchange data available for construction of difference spectra.

The ENDOR spectrum of the phyllosemiquinone radical bound to cytochrome *bo*$_3$, figure 5.9(a), gives H-bond hfc's of similar value to those of the same semiquinone bound in the A_1 site of Photosystem I (Rigby *et al.*, 1996). The methyl group hfc's in cytochrome *bo*$_3$ in a similar comparison are much larger suggesting an even greater distortion of the SOMO of this semiquinone. The major difference between the two sites is that the E_m of the A_1 semiquinone is 700mV more negative than Q_{bo}. Thus the mid-point potential of a bound semiquinone appears to be independent of the electron structure of that quinone. This is apparent in figure 5.9(b) which shows the ENDOR spectrum of the decyl-plastosemiquinone radical in Q_{bo}. This quinone is an analogue of the native quinone of the Q_A site of Photosystem II and has an E_m similar to that of the quinone in Q_{bo} but the decyl-plastosemiquinone in the latter site has a much larger methyl group hfc (Rigby *et al.*, 1995).

Placing duroquinone in the binding site of cytochrome *bo*$_3$ is of interest as it has only methyl groups covalently attached to the site and the ENDOR spectrum should give no β-CH_2 hfc's. Figure 5.9(c) shows no β-CH_2 features and only shows one methyl group hfc. Thus, all four methyl groups in the bound durosemiquinone radical are equivalent, suggesting a high degree of symmetry in the binding site.

5.2.8 Estimations of the spin density distribution of ubisemiquinone radicals associated with cytochrome *bo*$_3$.

By far the most striking feature of the ENDOR spectra from the cytochrome *bo*$_3$ ubisemiquinone is the large 2-methyl group hyperfine-coupling. Some radicals have been reported which show

an increase in the methyl hfc, accounted for by the increase in unpaired electron spin density at the ring carbon to which the methyl group is covalently attached (Rigby *et al.*, 1996). O'Malley & Babcock, 1986 observed that in a *p*-benzosemiquinone radical most of the unpaired electron spin is located at the carbonyl groups with 0.138 and 0.188 at each oxygen and carbon respectively. The remaining spin is distributed amongst the other four carbons, in the case of benzosemiquinone, 0.087 at each. The unpaired electron spin density at each ring carbon is related to the proton hfc by the McConnell relations (McConnell, 1956).

$$A_{iso}=81\rho$$

for methyl groups and

$$A_{iso} = 162\rho\cos^2\theta$$

for β-CH_2 groups. A_{iso} is the isotropic hyperfine coupling constant [i.e., $^1/_3$ $(A_{\parallel} + 2A_{\perp})$], ρ is the unpaired electron spin density at the attached ring carbon and θ is the angle between the C-H bond and the quinone ring normal for fixed β-CH_2 protons. These formulae can be used to determine the unpaired electron spin density at the C2, the ring carbon for the methyl group and indirectly the spin density for C3 the ring carbon for the methylene group both with the cytochrome bo_3 semiquinone and the '*in vitro*' semiquinone.

When compared to the '*in vitro*' semiquinone the cytochrome bo_3 semiquinone methyl group hfc increases from 0.07 to 0.15 an rise of 107%. This appears a large increase but means that the protein is inducing only an 8% redistribution of the total unpaired electron spin density. It is not possible to directly quantify the spin

density of the C3, the ring carbon adjacent to the β-CH_2 group of the farensyl chain, as the hfc's for these groups have not been determined '*in vitro*' however it can be estimated by assuming that as only one hfc is observed for the β-CH_2 protons, these protons must be equivalent and symmetrically orientated around the normal of the quinone ring plane at an angle, θ, of 60°. When quantified using the McConnell relation shown above a spin density of 0.12 at C2 is calculated. This again suggests that the protein causes under 10% redistribution of the total unpaired electron spin density. Thus a simple redistribution of the electron spin density is not sufficient to account for the increase in methyl and β-CH_2 hfc's as the hydrogen bonded proton hfc also increase. This would require the removal of spin away from the carbonyl group and onto the ring as well as onto the carbonyl oxygen at the same time. For the cytochrome *bo*$_3$ radical the spin density would have to be greater than 0.5 on each carbonyl group (i.e. more than one electron) to achieve the increase in the hydrogen bond proton hfc simply by placing more spin on the oxygen.

The size of the hfc's of protons hydrogen bonded to the carbonyl oxygens are described by a classical dipole-dipole interaction and are dependent on both the unpaired electron spin density at the oxygen atom, ρ_O, and the O---H bond distance (r) according to the equation (Rigby *et al.*, 1996):

$$A_{\perp}, A_{\parallel} \propto \rho_O(1/r^3)$$

By postulating a decrease in the hydrogen bond distance the increased hfc's relative to the '*in vitro*' decyl-ubisemiquinone can be accounted for. The protein environment of the quinone binding site

will easily be able to affect the hydrogen bonding. Hydrogen bonding to quinones is thought to increase the polarisation of the carbonyl bond leading to increased spin density at the carbonyl carbon (Stone, 1963; Burghaus *et al.*, 1993) which then delocalises into the quinone ring causing a 'knock on' effect of increased spin density on the ring carbons (Samoilova *et al.*, 1994; 1995). The decrease in the hydrogen bond distance need not be dramatic to account for the doubling of the cytochrome bo_3 semiquinone hydrogen bond hfc as suggested in table 5.1 as this would require only a 20% reduction in the O---H distance due to the $1/r^3$ dependence. However, without a direct quantitation of the π spin density at each oxygen for both the cytochrome bo_3 semiquinone and the decyl-ubisemiquinone it is not possible to assign the decreased O---H distance as the primary cause of the increased hydrogen bond hfc as an increased spin density at the oxygen may also contributes in a minor way.

5.2.9 ENDOR spectroscopy of the semiquinone radicals associated with the membrane-bound cytochrome *bd* complex.

Figure 5.10 shows the ENDOR spectrum of semiquinones associated with the membrane-bound cytochrome *bd* complex. As with cytochrome bo_3 the most intense features are due to hyperfine coupling of the SOMO to the 2-methyl group. The growth conditions for the cells from which the membranes are derived are likely to result in the quinones present in the membranes being a mixture of menaquinone (phylloquinone) and ubiquinone. Therefore as cytochrome *bd* can oxidise both quinones equally well

Figure 5.10 ENDOR spectra of the semiquinone radicals associated with the membrane-bound cytochrome *bd* complex

Spectra taken at centre of the ESR spectrum in 100mM H_2O AMPSO, pH9.0. Conditions: microwave power 3.0mW; r.f. power 100W; r.f. modulation depth 35KHz; time constant 655ms; scan time 84s; average of 120 scans; temperature 60K.

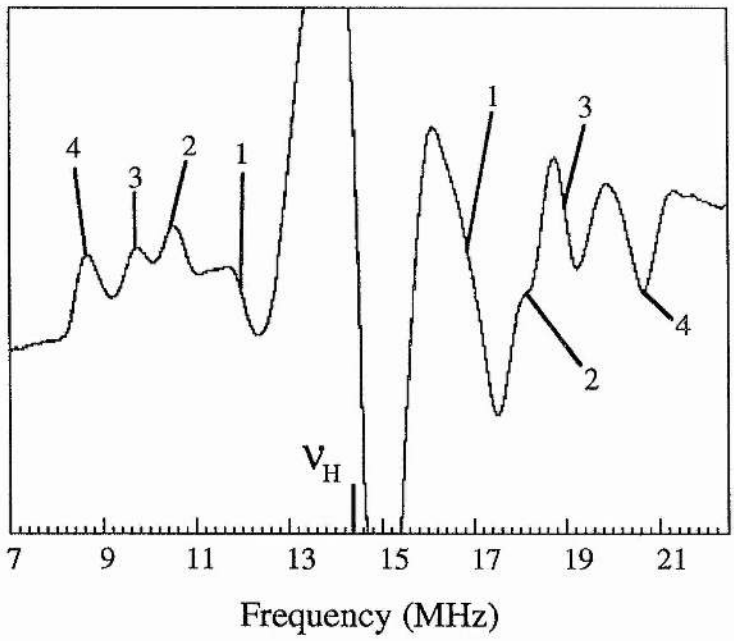
4
3
2
1
1
3
2
4
ν_H
7
9
11
13
15
17
19
21
Frequency (MHz)

Table 5.4 Hyperfine coupling constants and resonance assignments for the cytochrome *b d* semiquinones

Feature	Hyperfine coupling (MHz)	Assignment
1	4.7	UQ Methyl $A_{\perp}$
2	7.8	UQ Methyl $A_{\parallel}$
3	8.7	PhQ Methyl $A_{\perp}$
4	11.6	PhQ Methyl $A_{\parallel}$

it is likely that both mena- and ubisemiquinone species will be present and these will be evident in the ENDOR spectrum. Figure 4.1 showed the ESR spectra of the semiquinones associated with membrane-bound and purified cytochrome *bd*. In each case it appeared that all displayed some hyperfine interactions, these were greater with phyllosemiquinone species and only slightly apparent with ubisemiquinones. The membrane-bound complex with the endogenous quinones appeared somewhere in between the two suggesting that this spectrum was a result of both semiquinone species.

The ENDOR spectra shown in figure 5.10 were recorded under conditions of high signal to noise / low resolution necessitated by the lower concentration of the semiquinone species, together with to the possibility of overlap from the multiple species results in the presence of fewer observed and assignable features as with the cytochrome *bo*$_3$ semiquinone. Table 5.4 summarises the assignments made to the most intense features and suggests that ubiquinone binds without a significant distortion of its electronic structure as the values are within the range reported for the '*in vitro*' samples (O'Malley & Babcock, 1984) whereas phylloquinone is distorted in a similar way to the phylloquinone A_1 of photosystem I (Rigby *et al.*, 1996).

5.3 Conclusion

The ESR spectrum of the ubisemiquinone radical associated with the cytochrome bo_3 complex described by Ingledew *et al.*, 1995 and in chapter 3.0 is unusual due to the presence of the large unresolved hyperfine splittings of 0.4mT. Chapter 3.0 sought to identify the source of these interactions by exchanging the complex into deuterated solvent and labelling with ^{15}N. Neither method provided any further information on the cause of the hyperfine splitting. Deuterium exchange did perturb the ESR spectrum and indicated the presence of exchangeable protons at the site but it also caused an increased resolution of the hyperfine splitting due to the removal of the line broadening effects of protons.

ENDOR spectroscopy has proved useful in other systems to characterise the interactions of several bound semiquinones with proteins including those of the bacterial reaction centres from *Rb. sphaeroides* and *Rsp. viridis* (Deisenhofer *et al.*, 1985; Allen *et al.*, 1987a, b). ENDOR gives information on the spin density distribution around the quinone ring by analysis of the hyperfine coupling constants. Any differences between the hfc's of the '*in vitro*' semiquinone and the protein bound semiquinone must be due to the influence of the protein environment.

The ENDOR spectrum of the ubisemiquinone radical associated with cytochrome bo_3 revealed well resolved easily assigned hfc's and this is consistent with there being only one homogeneous semiquinone species present.

When *p*-benzoquinones or *p*-napthoquinones are bound in the site the values for the hfc's do not differ greatly. The binding of quinones to this site and the interactions involved depend little on the covalent structure of the quinone. In each case the most intense feature in the ENDOR spectra is that attributed to the methyl group covalently attached to the quinone ring and it is this hyperfine coupling more than any other that results in the hyperfine structure observed in the ESR spectra. Larger H-bond and β-CH_2 hfc's also a feature of this site when compared to the '*in vitro*' semiquinone. With the '*in vitro*' p-benzoquinone radical (O'Malley & Babcock, 1986) most of the spin resides on the carbonyl groups, spin must therefore be moved from there and onto the quinone ring to produce the increased hfc's for the other ring substituents. To account for an increase of this size through a simple redistribution of spin would require a spin density on the ring >1 (i.e. more than one electron). However, a shorter hydrogen bonding distance from the protein to the carbonyl oxygens, manifested as larger H-bond hfc's, would increase the polarisation of the carbonyl carbon (Stone, 1963; Burghaus *et al.*, 1993). This would force more spin density onto the ring and cause the increased hfc's of the methyl and β-CH_2 groups (Samoilova *et al.*, 1994; 1995).

The observation of only one β-CH_2 suggests that both the protons must be equivalent and therefore at an angle of 60° about the plane of the quinone ring. The hydrogen bonds to the carbonyl oxygen show both $A_\perp$ and $A_\parallel$ features under orientation selected ENDOR which indicates that they do not lie in the plane of the quinone ring or perpendicular to it because if this were the case only one feature would be evident. These bonds therefore lie at an

angle of between 0 and 90° although the precise value cannot be determined using this data. These findings are summarised in figure 5.11.

The lower semiquinone concentration of the cytochrome *bd* sample made it impossible to detect or assign all the hfc's of this radical. The presence of both ubisemiquinone and mena-semiquinone in the sample was indicated by there being two distinct methyl group hfc's in the ENDOR spectrum. The protein would appear to be distorting the SOMO of menasemiquinone to a greater extent than that of ubisemiquinone. This is consistent with the ESR spectra of the species which show the menasemiquinone having more hyperfine structure than ubisemiquinone.

Figure 5.11 The quinone binding site of the cytochrome bo_3 complex based on ENDOR data

The figure shows ubiquinone in the site. X indicates the protein, R the quinone tail. The hydrogen bonds angles are between 0 and 90° above or below the plane of the quinone ring.

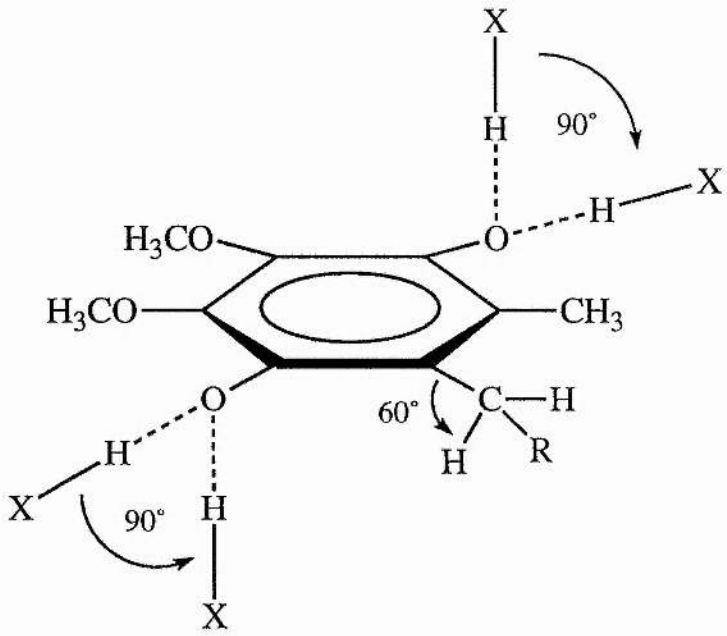
X
H
90°
X
H
O
H3CO
H3CO
CH3
O
60°
C
H
H
R
H
X
90°
H
X

6.0 ESEEM STUDIES OF CYTOCHROME bo_3 SEMIQUINONE

6.1 Introduction

The application of ENDOR spectroscopy, described in the previous chapter, to study the stabilised semiquinone associated with the cytochrome bo_3 complex, yielded much information on the hyperfine interactions involved. Strong hfc's due to the protons attached to the quinone and those from the protein that form hydrogen bonds to the carbonyl oxygens of the quinone were characterised. The detection of weaker hyperfine interactions of the semiquinone with surrounding nuclei, in particular, those of the protein is more suited to electron spin echo envelope modulation spectroscopy or ESEEM[b].

ESEEM has been useful technique in the study of other semiquinones in particular those of the photosynthetic reaction centres, both in bacteria and chloroplasts (Deligiannakis *et al.*, 1995; Bosch *et al.*, 1995). In each case the interaction of the semiquinone with surrounding amino acid nitrogen nuclei was detected.

Nuclei with a nuclear spin, I, $>1/2$, (for ^{14}N, I=1) may have an aspherical distribution of positive charge which gives rise to a nuclear electric quadrapole moment. This moment interacts with the electric field gradient, V, at the nucleus which leads to the

[b] Electron spin echo envelope modulation spectroscopy (ESEEM) is a pulsed ESR technique used to charcterise weak hyperfine coupling interactions of electron spins and nuclear spins. The technique involves subjecting a spin system to a series of radiation pulses and observing the modulated spin echos. For example, if a spin system is subjected to two pulses, separated by a time interval, τ, then a signal, the echo, is observed at a time τ after the second pulse (Dikanov & Tsvetkov, 1992).

establishment of nuclear sub-level splittings even in zero magnetic field. These transitions can be described by three nuclear quadrapole resonance (NQR) frequencies, ν, in a zero magnetic field,

$$\nu_+ = K(3+\eta)$$

$$\nu_- = K(3-\eta)$$

$$\nu_0 = 2K\eta$$

in which K is a quadrapole coupling constant and η is an asymmetry parameter of the electric field gradient. These two parameters provide much information on the molecular environment in which the interacting nitrogen nucleus is located. In a protein there are several possible 'environments' where a nitrogen nucleus may be found. For example, in the peptide backbone, in the histidine imidazole side chain where two nitrogen nuclei ($N^{\delta(1)}$ and $N^{\delta(2)}$) are located and also the indole nitrogen of tryptophan. Each nitrogen nucleus has different NQR parameters which can be used to identify the source of the one contributing to the ESEEM spectrum.

ESEEM studies on the photosynthetic reaction centres revealed that one of the carbonyl oxygens of the primary quinone, Q_A, of *Rb. Sphaeroides*, is hydrogen bonded to the $N^{\delta(1)}$ of a histidine residue. The crystal structure of this reaction centre revealed only one candidate, his M219 (Bosch *et al.*, 1995). A similar study of spinach chloroplast reaction centres revealed two types of nitrogen NQR, one identified as being due the $N^{\delta(1)}$ of a histidine residue probably his D2-215 (equivalent to his M219 of *Rb. Sphaeroides*)

and the other proposed to be due to the peptide backbone nitrogen of ala D2-261 (Astashkin et al., 1995; Deligiannakis et al., 1995).

Nitrogen nuclei hydrogen bonded to a semiquinone are therefore a feature of some quinone binding sites. ESEEM spectroscopy is used here to determine whether any similar interactions operate at the quinone binding site of the cytochrome bo_3. complex. Although ESEEM spectroscopy cannot alone identify specific amino acid residues involved in these interactions, it may be possible to indicate what type of residue is involved in semiquinone stabilisation at Q_{bo}.

6.2 Results & Discussion

Figure 3.2(a) displayed the ESR spectrum of the ubisemiquinone radical associated with the cytochrome bo_3 complex. In figure 6.1 the echo-detected field-swept spectrum of this sample is displayed. This was obtained using a the spin echo pulse sequence, $\pi/2$-τ-π-τ-acquire with and is displayed as a function of the magnetic field. The width of the spectrum between the maximum slope widths is approximately 0.9mT being consistent with the corresponding value in the ESR spectrum.

Figure 6.2 displays the stimulated echo ESEEM decay of the cytochrome bo_3 ubisemiquinone radical using the spin echo pulse sequence, ($\pi/2$-τ-$\pi/2$-T-$\pi/2$-acquire) at time interval, τ=112nS. This was recorded at a static magnetic field of 345.9mT which corresponds to a maximum intensity of the echo-detected field-swept spectrum. Stimulated echo decays are performed in preference to the primary echo decay as they increase the resolution of the spectra obtained. Here the echo decay is determined by the spin-lattice relaxation and is modulated by the fundemental nuclear transition frequencies (Mims, 1972a,b).

The signal to noise ratio of the spectrum is greatly improved by Fourier transformation of the stimulated echo ESEEM. In order to avoid missing certain modulation frequencies due to suppresion effects the echo was recorded and Fourier transformed at different τ values between the first and second microwave pulses (Mims, 1972a,b). These spectra are displayed in figure 6.3. Three narrow line frequency components are resolved with peaks at 0.96MHz, 2.20MHz and 3.16MHz. These correspond to the three nuclear

Figure 6.1 Field swept spectrum of ubisemiquinone radical associated with the purified cytochrome bo_3 complex.

Spectrum obtained using the spin echo pulse sequence, ($\pi/2$-τ-π-τ-acquire) with the following spectral parameters: number of sweeps, 4; shots per loop, 8; shot repetition time, 51.20ms; spectral resolution, 250 data points; sweep width; 10.00mT; microwave frequency, 9.713GHz, temperature, 60K.

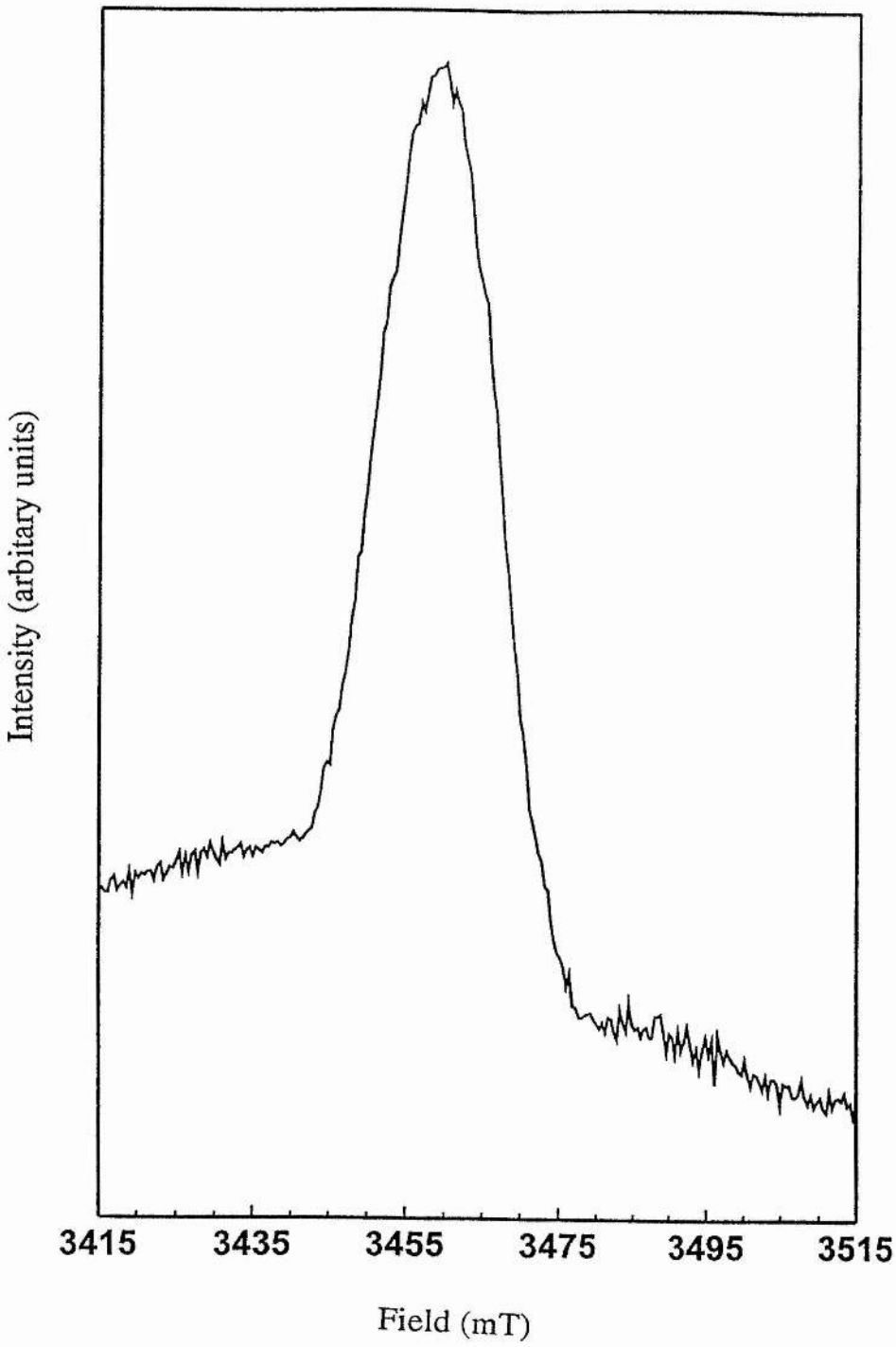
Intensity (arbitary units)
3415
3435
3455
3475
3495
3515
Field (mT)

Figure 6.2 Stimulated echo ESEEM time decay of the ubisemiquinone radical associated with the purified cytochrome bo_3 complex.

Spectrum obtained using the spin echo pulse sequence, ($\pi/2$-τ-$\pi/2$-T-$\pi/2$-acquire) at time interval, τ=112nS, with the following spectral parameters: number of sweeps, 8; shots per loop, 4; shot repetition time, 30.72ms; pulse resolution, 1024 data points; centre field, 3459G (the centre of radical spectrum to allow contributions from all orientations); microwave frequency, 9.714GHz, temperature 3.8K.

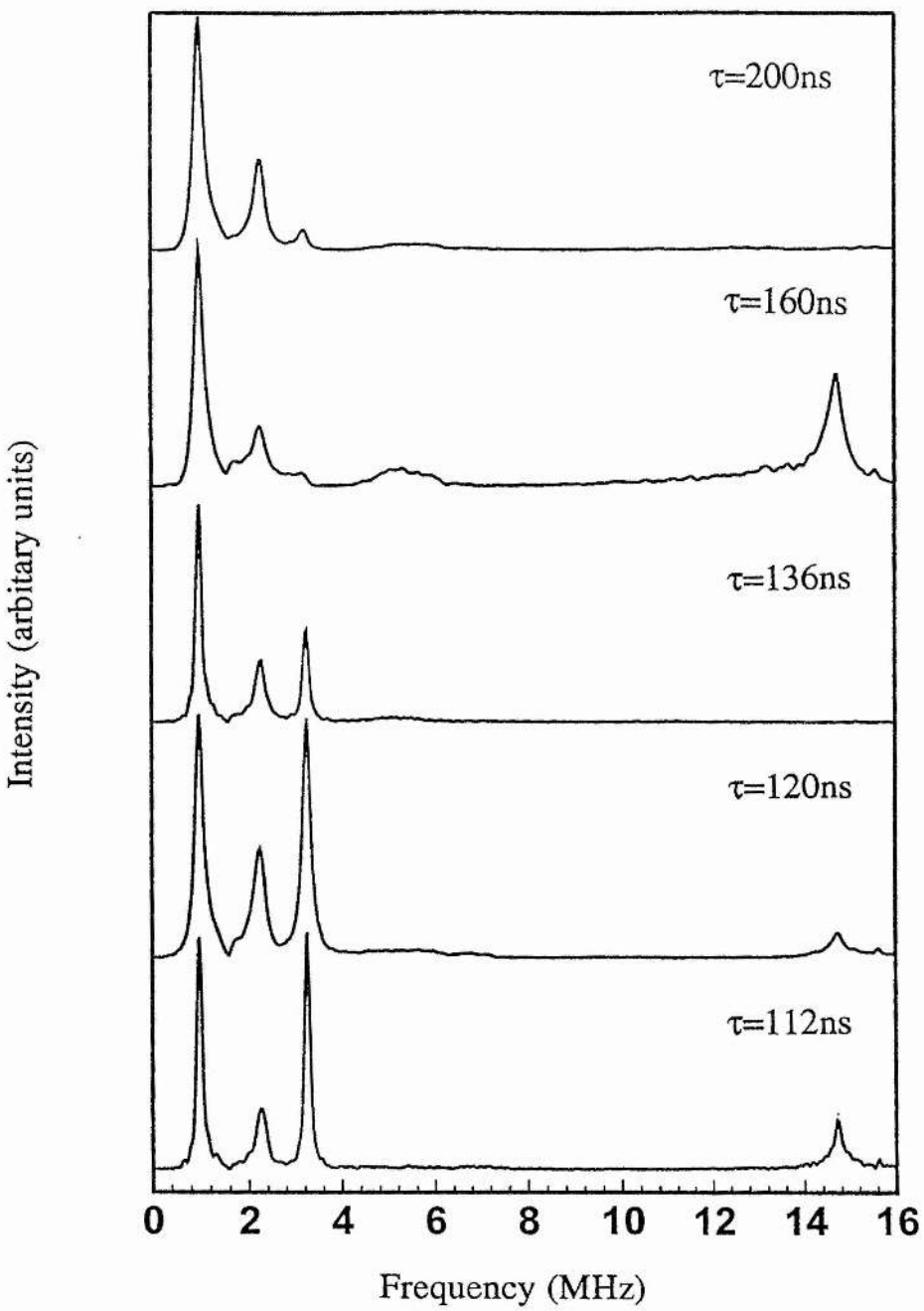
τ=200ns
τ=160ns
τ=136ns
τ=120ns
τ=112ns
Intensity (arbitary units)
0
2
4
6
8
10
12
14
16
Frequency (MHz)

quadrapole resonance frequencies which are ν_0, ν_- and ν_+ respectively. Another line is observed at approximately 15MHz which is attributed to proton hyperfine interactions.

The sum of the above NQR frequencies, $\nu_0 + \nu_-$ equals that of ν_+ and this indicates that these peaks arise from ^{14}N nuclear modulation (Dikanov *et al.*, 1982). These are almost pure quadrapolar lines with no anisotropic broadening and arise from the condition of exact cancellation. Here, the nuclear-Zeeman and electron-nuclear hyperfine interactions effectively cancel each other out leaving only the splittings due to the ^{14}N nuclear quadrapole interaction (Flanagan & Singel, 1987).

The equations in section 6.1 to are solved using the above NQR frequnecies to determine the values of the quadrapole coupling constant and the asymmetry parameter of the electric field gradient which gave K=0.88MHz and η=0.54. These results are summarised in Table 6.1 and can be used to determine the origin of the interacting nitrogen nucleus.

Table 6.1 also shows the K and η values for several reference systems by comparing these with the values obtained from the cytochrome bo_3 semiquinone it appears that the nitrogen nucleus is stiuated in the peptide backbone. The slightly lower than expected values can be attributed to slight perturation in the electronic structure of the nitrogen probably due to it being hydrogen bonded to the quinone.

Only one set of nitrogen NQR frequencies were detected in the ESEEM spectrum. This could arise from two equivalent nitrogen

Figure 6.3 Fourier transformation spectra of the time domain data at various τ values.

The time domain data was apodized with an exponential line function, LB=0.25; zero filling was 12K prior to Fourier transformation. The spectra are presented in the power mode.

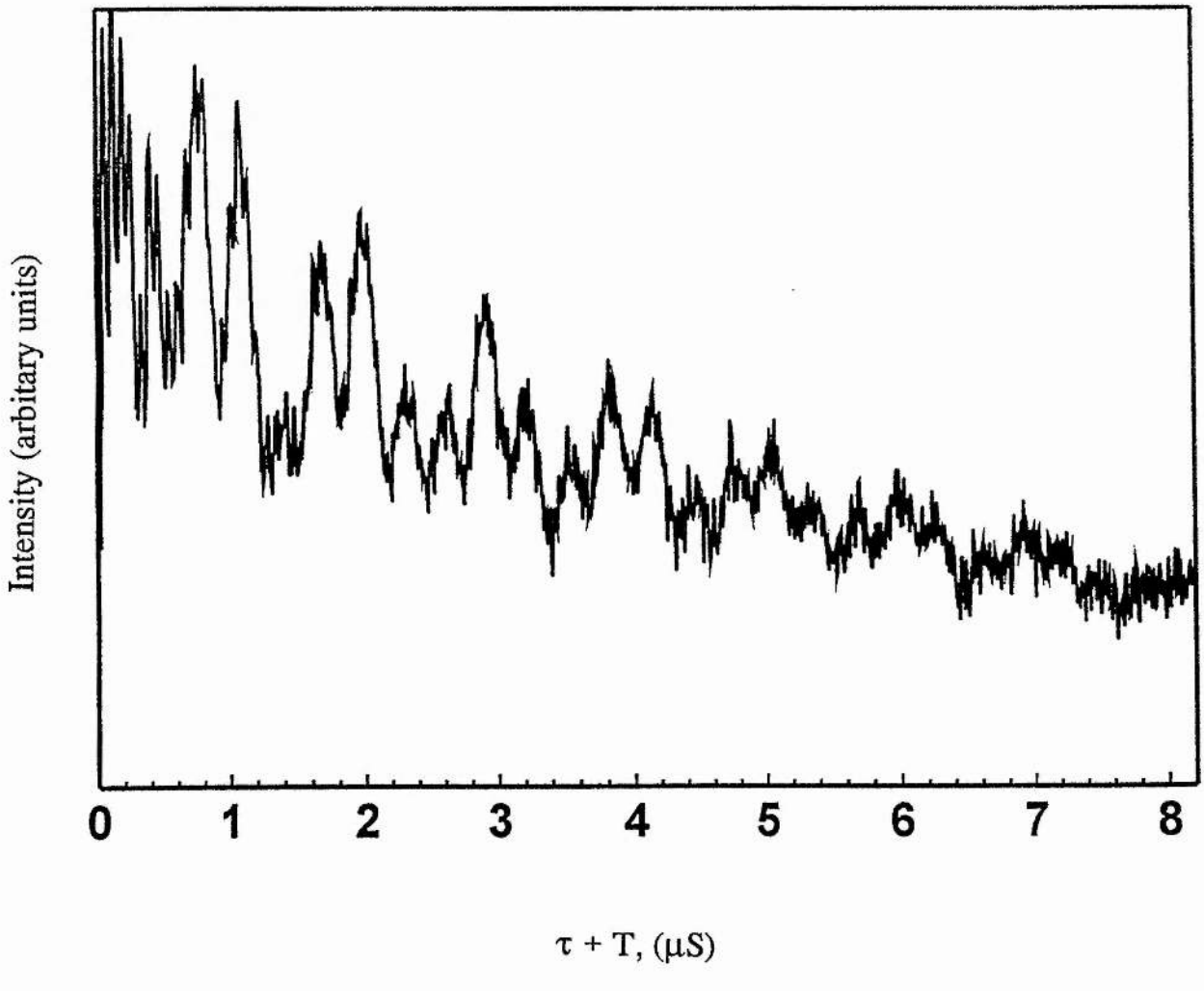
Intensity (arbitary units)
0
1
2
3
4
5
6
7
8
τ + T, (μS)

Table 6.1 ^{14}N-ESEEM data for the ubisemi-quinone species associated with the cytochrome bo_3 complex

cytochrome bo_3 semiquinone			reference systems*		
ν (MHz)	K(MHz)	η	K(MHz)	η	reference
0.96			0.81	0.45	^{14}N-ESEEM
2.20	0.88	0.54			peptide N
3.16			0.80-0.84	0.45-0.51	di/tripeptide
			0.81-0.83	0.13-0.21	imino N his
			0.31-0.34	0.91-0.97	amino N his
			0.79	0.18	indole trp

* Deligiannakis *et al.*, 1995 and references therein.

nuclei hydrogen bonded in an identical way to the carbonyl oxygens of the quinone. A more likely explanation is that one carbonyl oxygen is hydrogen bonded to a peptide nitrogen and the other is hydrogen bonded to another type of amino acid residue probably a serine or threonine which have potential H-bonding -OH groups.

6.3 Conclusion

ESEEM spectroscopy has in previous studies been a useful technique in determining the nature of interactions between quinones and proteins that lead to semiquinone stabilisation (Bosch *et al.*, 1995; Astashkin *et al.*, 1995; Deligiannakis *et al.*, 1995). In each case the quinone carbonyl oxygens were found to be hydrogen bonded to nitrogen nuclei of the protein. This in turn would stabilise the semiquinone intermediate and assist the sequential transfer of electrons. The ESEEM studies of the semiquinone at the Q_A site of the photosynthetic reaction centres were complemented by the availability of the crystal structures. Thus the origin of the nitrogen nuclei could be assigned by comparison of the nuclear quadrapolar resonance frequencies to reference systems and then identifying the particular amino acid residues by referring to the crystal structure.

The ENDOR studies of the cytochrome bo_3 semiquinone revealed the presence of hydrogen bonding to the protein through the carbonyl oxygens. These bonds were not in the plane of the quinone ring but at an angle between 0 and 90° to it. They were unusual as they were shorter than expected which lead to the large methyl, β-CH_2 and proton hyperfine couplings. ESEEM spectroscopy was used to study the cytochrome bo_3 semiquinone and to determine whether a nitrogen atom may be hydrogen bonded to the quinone in a similar way to those found in the bacterial reaction centres.

The ESEEM spectra revealed three low frequency lines indicative of an nuclear quadrapolar resonance originating from

nitrogen nucleus hydrogen bonded to the semiquinone. Comparison of the NQR parameters with reference systems suggest that the interacting nitrogen atom is part of the polypeptide backbone but to which amino acid residue it belongs cannot be determined by ESEEM alone. It is likely that only one nitrogen nucleus is interacting with the quinone and producing the peaks observed in the ESEEM spectra. The other carbonyl carbon must be hydrogen-bonded to another atom probably the oxygen of the side chain of a serine or threonine residue. These results are summarised in figure 6.4 which displays a model of the quinone binding site of the cytochrome bo_3 complex based on the ESEEM data.

Figure 6.4 The quinone binding site of the cytochrome bo_3 complex based on ^{14}N-ESEEM data.

The quinone is ubiquinone and is shown hydrogen bonded via the carbonyl oxygens to a nitrogen from the polypeptide backbone and to the γ-oxygen of a serine or threonine residue, represented by X.

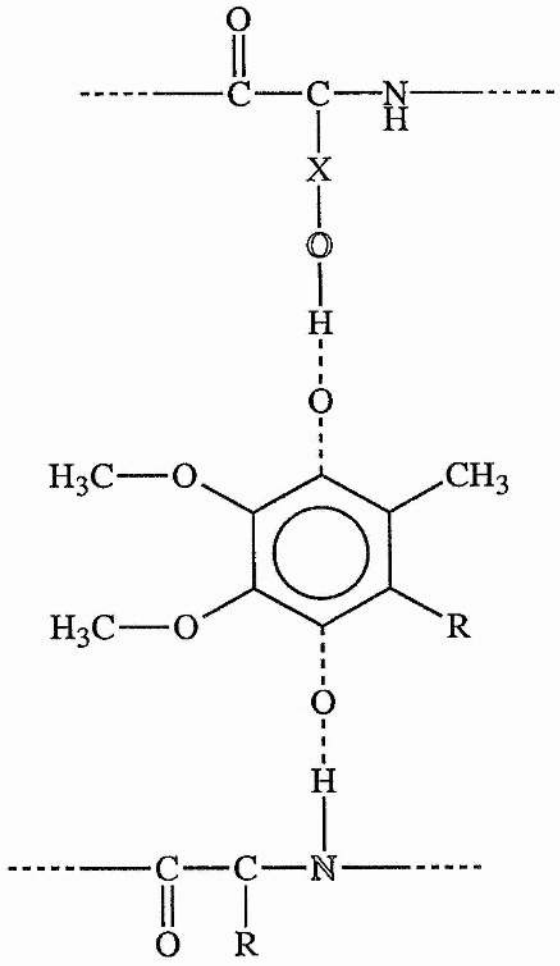

7.0 GENERAL CONCLUSIONS

7.1 Introduction

Quinone binding sites are known to be of potential industrial importance due to them being the site of action of numerous herbicides, pesticides and antibiotics. Despite the sequences of many quinone binding proteins being available in addition to the x-ray crystal structure of two there is to date no general structural motif which can identify a potential quinone binding site.

The aim of this thesis was to further the advancements made in the elucidation of the structure and function relationships of the quinone binding sites associated with the terminal ubiquinol oxidases of *Escherichia coli*, cytochrome bo_3 and cytochrome *bd*. This chapter will summarise only the conclusions already drawn from chapters 3.0 to 6.0.

7.2 The Quinone Binding Site of the Cytochrome bo_3 Complex

The identification of a stable semiquinone intermediate of quinol oxidation associated with the cytochrome bo_3 complex by ESR spectroscopy provided a means by which to study the structure and thermodynamic behaviour of the quinone binding site of cytochrome bo_3 (Ingledew *et al.*, 1995). The ESR spectrum of the semiquinone was unusual due to the presence of partially resolved hyperfine splittings of 0.4mT the source of which was undetermined. Deuterium exchange of the solvent ruled out exchangeable protons as being the major cause of the hyperfine interactions although a slight change in the ESR spectrum of the semiquinone associated with the purified complex did show that

exchangeable protons were present at the site. No change in the ESR spectrum was noted on deuterium exchange of the membrane-bound complex which suggests that the site is not readily accessible to the aqueous medium. Labelling the enzyme with ^{15}N had no effect on the ESR spectrum. The semiquinone form of menaquinone could be stabilised by the complex as could that of plastoquinone and duroquinone. A slight change in the ESR spectrum of the menasemiquinone radical merely reflects the differences in the structures of benzoquinones and napthoquinones.

The ENDOR spectra of the cytochrome *bo*$_3$ semiquinone radicals, whether they were derived from benzoquinones or napthoquinones all showed large hyperfine couplings due to the methyl groups, β-CH_2 groups and protons hydrogen bonded to the carbonyl oxygens when compared to the 'in vitro' radicals. Each quinone type gave comparable hyperfine coupling constants which suggests that the binding of quinones to the site is independent of the chemical structure of those quinones. It is the large hyperfine coupling of the methyl group which gives the ESR spectrum its unusual line shape. The origin of the larger hfc's cannot be accounted for by a simple redistribution of charge. They are most likely due to a shortening of the hydrogen bonding distance between interacting amino acid residues of the protein and the carbonyl oxygens of the quinone indicated by the increased H-bond hfc. This would increase the polarisation of the carbonyl carbon and force more spin density onto the quinone ring thereby causing the large hyperfine couplings of the methyl and β-CH_2 groups.

The hydrogen bond hfc's do not show an orientation dependence, displaying both $A_\perp$ and $A_\parallel$ components on the

corresponding ENDOR spectrum. This means that the hydrogen bonds do not lie in the plane of or perpendicular to the quinone ring but at an angle in between (i.e. 0 to 90°). The observation of only one β-CH_2 hfc suggests that these protons are equivalent and must be at an angle of 60° about the plane of the quinone ring.

ESEEM spectroscopy of the cytochrome bo_3 ubisemiquinone radical showed that one of the carbonyl oxygens of the quinone ring is hydrogen bonded to a peptide backbone nitrogen of the complex. The other presumably is hydrogen bonded to an oxygen atom possibly in the side chain of a serine or threonine residue.

The identification of two quinone binding peptides both located in the cyoA fragment of the complex could contain the amino acid residues which hydrogen bond to the semiquinone (R.B. Gennis, personal communication). The residue which contains the H-bonding nitrogen atom could be any one of 27 amino acids contained in these peptides. There is however only one serine residue in these peptides which is highly conserved in the quinol oxidases, ser169. This is also close to trp136 which is known to affect quinol oxidation when mutated to an alanine. The semiquinone stabilised by this mutant was shown in this study to have a normal ESR spectrum but to have unusual redox behaviour. Trp136 is likely to be involved in electron transfer from the quinone binding site in a similar way to trp M252 of the photosynthetic reaction centre of *Rb. sphaeroides* . Figure 7.1(a) and (b) shows the positions of the two quinone binding peptides, trp136 and ser169 in the crystal structure of the cyoA fragment. The corresponding residues in the crystal of bovine heart cytochrome *c* oxidase are shown in figure 7.1(c) and (d). These

Figure 7.1 The proposed location of the quinone binding site of the cytochrome *bo*$_3$ complex.

(a) The location of quinone binding peptides, 1 (residues 167 to 178) and 2 (residues 254 to 270), shown in magenta and green respectively, with trp136 and ser169, in the crystal structure of the cyoA fragment. (b) as (a) rotated 90° in the x-direction. For reference the engineered Cu_A site is shown.

(c) The corresponding residues in the crystal structure of bovine heart cytochrome *c* oxidase. Subunit I, subunit II, trp104 and asp158 are shown in blue, red, cyan and green respectively. (d) as (c) rotated 90° in the x-direction.

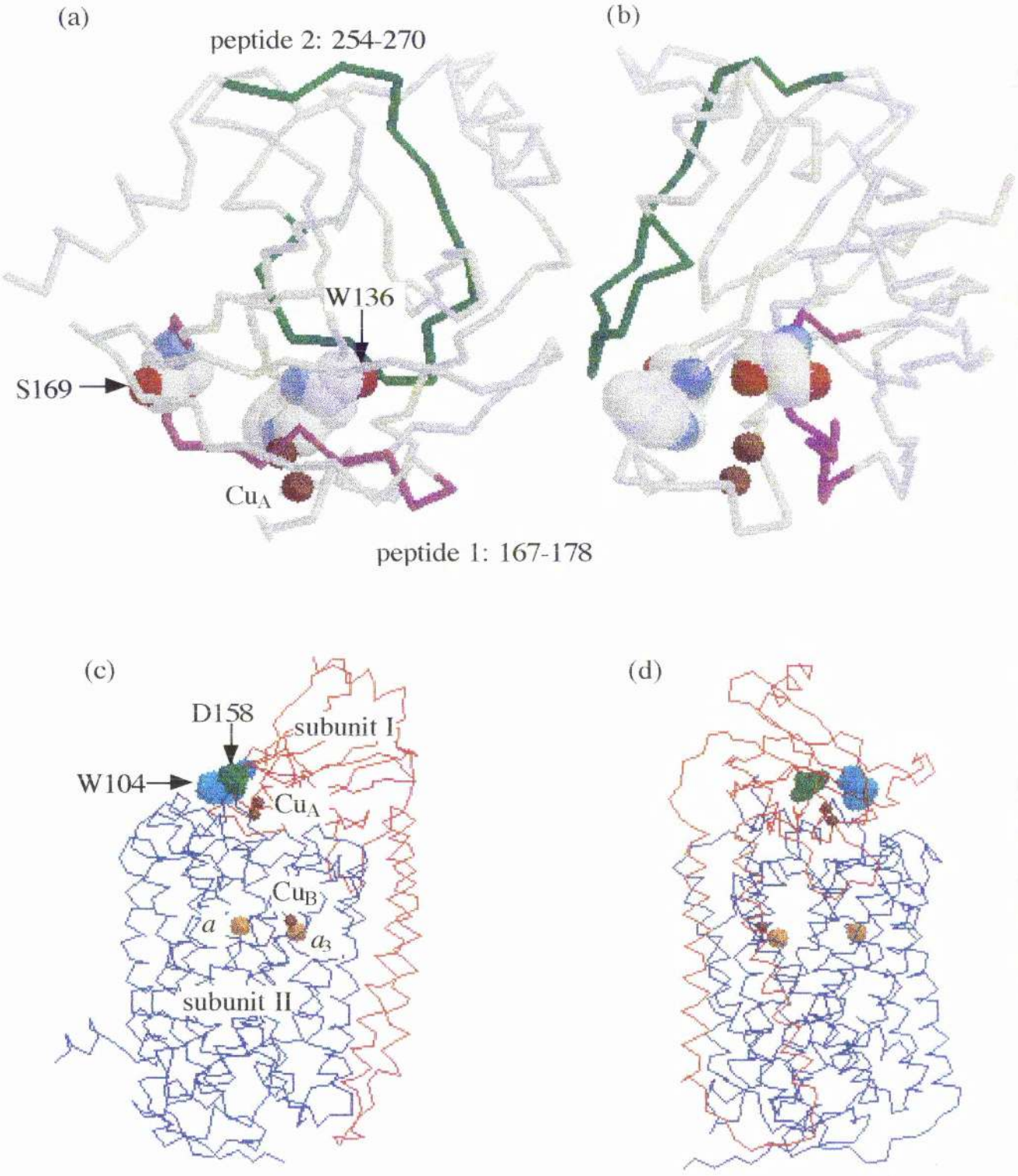
(a)
peptide 2: 254-270
W136
S169
Cu_A
(b)
peptide 1: 167-178
(c)
D158
subunit I
W104
Cu_A
Cu_B
a
a_3
subunit II
(d)

residues, trp104 and asp158, are on the interface between subunits I and II close to the low spin haem, the likely acceptor of electrons from the quinone binding site. This region is therefore a potential location of the cytochrome bo_3 quinone binding site. Ser169 would be a good target for further site directed mutagenesis studies.

The ESR spectrum of the ubiquinol-8 semiquinone from by the membrane-bound complex showed no change when compared to those of shorter chain length, suggesting that chain length is not important in the positioning or recognition of the head group in the site. The potentiometric behaviour of this semiquinone was similar to that of the purified complex suggesting a $2H^+/2e^-$ reaction over the pH range studied and is consistent with electron transfer to the low spin haem *b*. Deviations in the values of E_1 and E_2 with resultant changes in the maximum site occupancy can be accounted for by slight changes in the manner of quinone binding in the purified complex.

The data presented here does not indicate the presence of a second quinone binding site recently proposed by Sato-Watanabe *et al.*, 1994. A preparation of the purified complex with a quinone molecule bound produces a semiquinone radical indistinguishable from that described earlier and this semiquinone can be displaced on the addition of the potent inhibitor of quinol oxidation in cytochrome bo_3, tridecylstigmatellin. Sato-Watanabe *et al.*, 1995b reported that this semiquinone is derived from the second binding site that is distinct from the site of quinol oxidation and mediates electron transfer in a similar way to Q_A of the photosynthetic reaction centres. No semiquinone would be observed at the quinol

oxidation site. Quinol oxidation of this type catalysed by cytochrome bo_3 cannot proceed without the stabilisation of a semiquinone intermediate due to thermodynamic considerations. Only one semiquinone was observed in this study and this is most likely at the site of quinol oxidation.

7.3 The Quinone Binding Site of the Cytochrome *bd* Complex

The semiquinone associated with the cytochrome *bd* complex was characterised using ESR spectroscopy in both the membrane-bound and purified complex. The ESR spectrum of the radical had a linewidth of approximately 0.9mT which is consistent with those reported for other semiquinone species. Formation of the semiquinone is inhibited by the addition of aurachin D and HOQNO. The complex could stabilise menasemiquinone and ubisemiquinone intermediates. Both showed hyperfine structure but this was greater in the menasemiquinone intermediate. Deuterium exchange of the complex caused a slight change in the ESR spectrum of the ubisemiquinone sample. This indicates the presence of exchangeable protons in the site, similar to those identified in the quinone binding site of the cytochrome bo_3 complex. The ESR spectrum of the semiquinone sample derived from membrane-bound cytochrome *bd* also showed hyperfine structure. Both menaquinone-8 and ubiquinone-8 are expected to be present in this sample and so the ESR spectrum appeared to show a mixture of both semiquinone forms. ENDOR spectroscopy of this sample also showed that two semiquinone forms were present both. Two large methyl group hfc's were evident in the ENDOR spectrum, the largest originating from the menasemiquinone radical and the other

from the ubisemiquinone. From this it is concluded that the quinone binding site is causing a large distortion in the electronic structure of the menasemiquinone, possibly through the shortening of the quinone carbonyl oxygen to protein hydrogen bonds, in a similar manner to those at the quinone binding site of cytochrome bo_3. Cytochrome *bd* appears to bind the ubisemiquinone slightly differently and this results in smaller methyl group hfc's.

The redox behaviour of the ubisemiquinone radical associated with the purified complex is consistent with a $2H^+/2e^-$ oxidation reaction over the pH range studied. The semiquinone is more stable at higher pH's where the anionic form of the semiquinone predominates. The data can be fitted by assuming only one quinone binding site and there is no indication, spectrally or thermodynamically, of other quinone binding sites. The potentials of the half-couples for both menaquinol and ubiquinol oxidation will enable the transfer of electrons to the low spin haem *b*. If a branched electron transfer pathway operates in the *E.coli* cytochrome *bd* as is proposed for that of *A.vinelandii* stabilisation of the semiquinone would still be required.

7.4 A Comparison of the Quinone Binding Sites of Cytochrome bo_3 and Cytochrome *bd*

Although cytochrome bo_3 and cytochrome *bd* are structurally unrelated they share many common features in the mechanism of quinol oxidation. The structure of the two sites may well be similar with serine or threonine residues being involved in hydrogen bonding to the bound quinone. Both enzymes are effective stabilisers of the semiquinone state and allow efficient electron

transfer to proceed in two one electron steps to a low spin *b*-haem. The major difference between the two is the binding of menaquinone to each respective site. Cytochrome bo_3 does not appear to discriminate between ubiquinone and menaquinone. It binds both the oxidised and reduced forms equally well with the electronic structure of the semiquinones being greatly distorted to a similar extent as shown by ESR. Cytochrome *bd* binds menaquinol more tightly than menaquinone but the E_{m7} of the ubiquinone/quinol couple is not altered. The ESR spectrum of menasemiquinone shows more hyperfine structure than that of ubisemiquinone. Such differences in binding are most likely related to the low aeration conditions which favour cytochrome *bd* expression. Levels of menaquinone are maximal under anaerobosis and by altering the E_{m7} of the quinone/quinol couple cytochrome *bd* makes electron transfer from menasemiquinone to the haem b_{558} more favourable.

9.0 BIBLIOGRAPHY

Bibliography

Allen, J.P., Feher, G., Yeates, T.O., Komiya, H. & Rees, D.C. (1987a) Proc. Nat. Acad. Sci. 84, 5730-5734

Allen, J.P., Feher, G., Yeates, T.O., Komiya, H. & Rees, D.C. (1987b) Proc. Nat. Acad. Sci. 84, 6162-6166

Albert, I., Leibl, W., Ewald, G., Michel, H. & Rutherford, A.W. (1994) Biochemistry 33, 11355-11363

Anraku, Y. & Gennis, R.B. (1987) Trends Biochem. Sci. 12, 262-266

Astashkin, A.V., Kawamori, A., Kodera, Y., Kuroiwa, S. and Akabori, K. (1995) J. Phys. Chem. 102, 5583-5588

Au, D. C.-T. & Gennis, R.B. (1987) J. Bacteriol. 169, 3237-3242

Bäckström, D., Norling, B., Ehrenberg., A. & Ernster, L. (1970) Biochim. Biophys. Acta. 197, 108-111

Bosch, M.K., Gast, P., Hoff, A.J., Spoyalov, A.P. & Tsvetkov, Yu.D. (1995) Chem. Phys. Lett. 239, 306-312

Borisov, V.B. (1996) Biochemistry (Moscow) 61, 565-574

Brandt, U. & Trumpower, B. (1994) Crit. Rev. Biochem. Mol. Biol. 29, 165-197

Burghaus, O., Plato, M., Rohrer, M. & Möbius, K., MacMillan, F. & Lubitz, W. (1993) J. Phys. Chem. 97, 7639-7647

Calhoun, M.W., Lemieux, L.J., Garcia-Horsman, J.A., Thomas, J.W., Alben, J.O., Gennis, R.B. (1995) FEBS Lett. 368, 523-525

Bibliography

Calhoun, M.W., Newton, G. & Gennis, R.B. (1991) J.Bacteriol. 173, 1569-1570

Calhoun, M.W., Thomas, J.W. & Gennis, R.B. (1994) Trends. Biochem. Sci. 19, 325-330

Cecchini, G., Sices, H., Schröder, I. & Gunsalus, R.P. (1995) J. Bacteriol. 177, 4587-4592

Chepuri, V., Lemieux, L., Au, D.C.-T., & Gennis, R.B. (1990) J. Biol. Chem. 265, 11185-11192

Chepuri, V., Lemieux, L., Hill, J., Alben, J.O. & Gennis, R.B. (1990) Biochim. Biophys. Acta. 1018, 124-127

Chepuri, V. & Gennis, R.B. (1990) J. Biol. Chem. 265, 12978-12986

Chung, T. (1989) Proc. Nat. Acad. Sci. 86, 4367-4372

Cohen, G.N. & Rickenberg, H.W. (1956) Ann. Inst. Pasteur 91, 693-720

Cotter, P.A., Chepuri, V., Gennis, R.B. & Gunsalus, R.P. (1990) J. Bacteriol. 172, 6333-6338

Cotter , P.A. & Gunsalus, R.P. (1992) FEMS. Microbiol. Lett. 91, 31-36

Crofts, A.R., Hacker, B., Barquera, Yun, C.-H. & Gennis, R.B. (1992) Biochim. Biophys. Acta. 1101, 162-165

D'Mello, R., Hill, S. & Poole, R.K. (1995) J.Bacteriol. 177, 867-870

Bibliography

D'Mello, R., Hill, S. & Poole, R.K. (1996) Microbiology 142, 755-763

Degli-Esposti, M., Carelli, V., Ghelli, A., Ratta, M., Crimi, M., Sangiorgi, S., Montagna, P., Lenaz, G., Lugaresi, E. & Cortelli, P. (1994) FEBS Lett. 353, 375-379

De Vries, S., Berden, J.A. & Slater, E.C. (1980) FEBS Lett. 122, 143-148

De Vries, S., Albracht, S.P.J., Berden, J.A. & Slater, E.C. (1982) J. Biol. Chem 256, 11996-11998

Deisenhofer, J., Epp, O., Miki, K., Huber, R. & Michel, H. (1985) Nature 318, 618-624

Deisenhofer, J. & Michel, H. (1989a) EMBO J. 8, 2149-2170

Deisenhofer, J. & Michel, H. (1989b) Science 245, 1463-1473

Deligiannakis, Y., Boussac, A. & Rutherford, A.W. (1995) Biochemistry 34, 16030-16038

Deng, W.P. & Nickoloff, J.A. (1992) Anal. Biochem. 81, 200-212

Devereux, J., Haeberli, P. and Smithies, O. (1984) Nucleic Acids Res. 12, 387-395

Dikanov, S.A., Tsvetkov, Y.D., Bowman, M.K. & Astashkin, A.V. (1982) Chem. Phys. Lett 90, 149-151

Dikanov, S.A. & Tsvetkov, Y.D. (1992) Electron spin echo envelope modulation (ESEEM) spectroscopy, CRC Press, Boca Raton

Bibliography

Ding, H., Daldal, F. & Dutton, P.L. (1995B) Biochemistry 34, 15997-16003

Ding, H., Robertson, D.E., Daldal, F. & Dutton, P.L. (1992) Biochemistry 31, 3144-3158

Ding, H., Moser, C.C, Robertson, D.E., Tokito, M.K., Daldal, F. & Dutton, P.L. (1995A) Biochemistry, 34, 15979-15996

Dorio, M.M., & Freed, J. H., Eds. (1979) Multiple Electron Resonance Spectroscopy, Plenum Press, New York.

Dueweke, T.J. & Gennis, R.B. (1990) J. Biol. Chem. 265, 4273-4277

Dueweke, T.J. & Gennis, R.B. (1991) Biochemistry 30, 3401-3406

Dutton, P.L. (1978) Meths. Enymol. 54, 411-435

Ernster, L. & Dallner, G. (1995) Biochim. Biophys. Acta. 1271, 195-204

Fang, H., Lin, R.-J. & Gennis, R.B. (1989) 264, J. Biol.Chem 8026-8032

Feher, G., Allen, J.P., Okamura, M.Y. & Rees, D.C. (1989) Nature 339, 111-116

Feng, Y., Wand, A.J. & Sligar, S.G. (1991) Biochemistry 30, 7711-7717

Flanagan, H.L. & Singel, D.J. (1987) J. Chem. Phys., 87, 5606-5610

Bibliography

Garcia-Horsman, J.A., Barquera, B., Rumbley, J., Ma, J. & Gennis, R.B (1994) J.Bacteriol. 176, 5587-5600

Garcia-Horsman, J.A., Puustinen, A., Gennis, R.B., Wikström, M. (1995) Biochemistry 34, 4428-4433

Gennis, R.B. (1991) Biochim. Biophys. Acta 1058, 21-24

Georgiou, C.D., Deuweke, T.J. & Gennis, R.B. (1988) J. Biol. Chem. 263, 13130-13137

Georgiou, C.D., Deuweke, T.J. & Gennis, R.B. (1988) J. Bactriol. 170, 961-966

Georgiou, C.D., Fang, H. & Gennis, R.B.(1987) J.Bacteriol. 169, 2107-2112

Ghaim, J.B., Greiner, D.P., Meares, C.F. & Gennis, R.B. (1995) Biochemistry 34, 11311-11315

Glasoe, P.K. & Long, L.A. (1960) J. Phys. Chem. 64, 188-190

Gohke, U., Warne, A. & Saraste, M. (1997) EMBO J. 16, 1181-1188

Gray, K.A., Dutton, P.L., Daldal, F. (1994) Biochemistry 33, 723-733

Green, G.N., Fang, H., Lin, R.-J., Newton, G., Mather, M., Georgiou, C.D. & Gennis, R.B. (1988) J. Biol. Chem. 263, 13138-13143

Green, G.N., Kranz, J.E. & Gennis, R.B. (1984) Gene 32, 99-106

Bibliography

Green, G.N., Lorence, R.M. & Gennis, R.B. (1986) Biochemistry 25, 2309-2314

Hacker, B., Barquera, B., Crofts, A.R. & Gennis, R.B. (1993) Biochemistry 32, 4403-4410

Hales, B.J. & Case, E.E. (1981) Biochim. Biophys. Acta. 637, 291-302

Hamilton, J.A., Cox, G.B., Looney, G.B. & Gibson, F. (1970) Biochem. J., 116, 319-320

Heathcote, P., Moënne-Loccoz, P., Rigby, S.E.J. & Evans, M.C.W. (1996) 35, 6644-6650

Hicks, D. B., Plass, R.J. & Quirk, P.G. (1991) J. Bacteriol. 173, 5010-5016

Higgins, D.G., Bleasby, A.J. & Fuchs, R. (1992) Comp. Applic. Biol. 8, 189-191

Hill, J.J., Alben, J.O., & Gennis, R.B. (1993) Proc. Natl. Acad. Sci. 90, 5863-5867

Hoefnagel, M.H.N., Wiskich, J.T., Madgwick, S.A., Patterson, Z., Oettmeier, W. & Rich, P.R. (1996) Eur. J. Biochem. 233, 533-537

Ingledew, W.J. & Bacon, M. (1991) Biochem. Soc. Trans. 19, 613-616

Ingledew, W.J. & Ohnishi, T (1977) Biochem. J. 164, 617-620

Ingledew, W.J., Ohnishi, T. & Salerno, J.C. (1995) Eur. J. Biochem. 227, 903-908

Bibliography

Ingledew, W.J. & Poole, R.K. (1984) Microbiol. Rev. 49, 222-271

Ingledew, W.J., Rothery, R.A., Gennis, R.B. & Salerno, J.C. (1992) Biochem. J. 282, 255-259

Iwata, S., Ostermeier, C., Ludwig, B. & Michel, H. (1995) Nature 376, 660-669

Iuchi, S. & Lin, E.C.C., (1988) Proc. Nat. Acad. Sci. 85, 1888-1892

Jünemann, S. & Wrigglesworth, J.M. (1995) FEBS Lett. 345, 198-202

Kaysser, T.M., Ghaim, J.B., Georgiou, C. & Gennis, R.B. (1995) Biochemistry 34, 13491-13501

Kaysser, T.M. (1993) Ph.D. Thesis; University of Illinois at Urbana-Champaign, USA

Kelly, M.J.S., Poole, R.K., Yates, M.G. & Kennedy, C. (1990) J.Bacteriol. 172, 6010-6019

Kita, K., Konishi, K. and Anraku, Y. (1984A) J. Biol. Chem. 259, 3368-3374

Kita, K., Konishi, K. and Anraku, Y. (1984B) J. Biol. Chem. 259, 3375-3381

Kolonay, J.F., Farhad, M., Gennis, R.B., Kaysser, T.M. & Maier, R.J. (1994) J.Bacteriol. 176, 4177-4181

Komiya, H., Yeates, T.O., Rees, D.C., Allen, J.P. & Feher, G. (1988) Proc. Natl. Acad. Sci. 85, 9012-9016

Bibliography

Kostyrko, V.A., Semeykina, A.L., Skulachev, V.P., Smirnova, I.A., Vaghina, M.L. & Verkhovskaya, M.L. (1991) Eur. J. Biochem. 198, 527-534

Kotlyar, A.B., Sled, V.D., Burbaev, D.Sh., Moroz, J.A. & Vinogradov, A.D. (1990) FEBS Lett. 347, 22-26

Krab, K. & Wikström, M.(1980) Biochem. J. 259, 637-639

Kranz, R.G. & Gennis, R.B. (1983) J. Biol. Chem. 258, 10614-10621

Kranz, R.G. & Gennis, R.B. (1984) J. Biol. Chem. 259, 7998-8003

Kranz, R.G. & Gennis, R.B. (1985) J. Bacteriol. 161, 709-713

Kröger, A. & Klingenberg, M. (1973) Eur. J. Biochem. 39, 313-323

Kröger, A. (1978) Methods Enzymol. 53, 579-591

Kunze, B., Höfle, G., & Reichenbach, H. (1987) J. Antibiot. 40, 258-265

Kurreck, H., Kirste, B., & Lubitz, W., (1988) Electron Nuclear Double Resonance Spectroscopy of Radicals in Solution; Applied to Organic and Biological Chemistry., VCH Publishers, Weinheim, Germany.

Lam, E (1984) FEBS Lett. 172, 255-260

Lemieux, L.J., Calhoun, M.W., Thomas, J.W., Ingledew, W.J. & Gennis, R.B. (1992) J. Biol. Chem. 267, 2105-2113

Bibliography

Lorence, R.M., Carter, K., Gennis, R.B., Matsushita, K. & Kaback, H.R. (1988) J. Biol. Chem. 263, 5271-5276

Lorence, R.M., Koland, J.G. & Gennis, R.B. (1986) Biochemistry 25, 2314-2321

Lorence, R.M., Miller, M.J., Borochov, A., Faima-Weinberg, R. & Gennis, R.B. (1984) Biochim. Biophys. Acta. 790, 148-153

Lowry, O.H., Rosenbrough, N.J., Farr, A.L. & Randall, R.J. (1951) J. Biol.Chem. 193, 265-275

MacMillan, F., Lendzian, F., Renger, G. & Lubitz, W. (1995) Biuochemistry 34, 8144-8156

Ma, J. (1995) PhD thesis; University of Illinois at Urbana-Champaign, USA

Maniatis, T., Fritsh, E.F. & Sambrook, J., (1982) Molecular Cloning: A Laboratory Manual, Cold Spring Harbor Laboratory, Cold Spring Harbor, NY, USA.

Mather, M.W., Yu, L., Yu, C.-A. (1995) J. Biol. Chem. 270, 28668-28675

Matsushita, K., Patel, L. & Kaback, H.R. (1984) Biochemistry 23, 4703-4714

McConnell, H.M. (1956) J. Phys. Chem 24, 764-765

Meunier, B., Madgwick, S.A., Reil, E., Oettmeier, W. & Rich, P.R. (1995) Biochemistry 34, 1076-1083

Miller, M.J., Hermodson, M. & Gennis, R.B. (1988) J. Biol. Chem. 263, 5235-5240

Mims, W.B., (1972a) Phys. Rev, B5, 2409

Mims, W.B., (1972b) Phys. Rev, B6, 3543

Minagawa, J., Mogi, T., Gennis, R.B. & Anraku, Y. (1992) J. Biol. Chem. 267, 2096-2104

Minghetti, K.C. & Gennis, R.B. (1988) Biochim. Biophys. Res. Com. 155, 243-248

Mitchell, P., (1975) FEBS Lett. 59, 137-139

Mitchell, P. (1976) J. Theor. Biol. 62, 327-367

Miyoshi-Akiyama, T., Hayashi & Unemoto, T. (1993) Biochim. Biophys. Acta. 1141 283-287

Mogi, T., Nakamura, H. & Anraku, Y. (1994) J. Biochem. 116, 471-477

Moody, A.J., Rumbley, J.N., Gennis, R.B., Ingledew, W.J., Rich, P.R. (1993) Biochim. Biophys. Acta.1141, 321-329

Moshiri, F., Chawala, A. & Maier, R.J. (1991) J. Bacteriol. 173, 6230-6241

Moser, C.C., Keske, J.M., Warncke, K., Farid, R.S. & Dutton, P.L. (1992) Nature 355, 796-802

Musser, S.M., Stowell, M.H.B. & Chan, S.I. (1993) FEBS Lett, 327, 131-136

Nakamura, H., Yamato, I., Anraku, Y., Lemieux, L., Gennis, R.B.

(1990) J. Biol. Chem 265, 11193-11197

Newton, G. & Gennis, R.B (1991) Biochim. Biophys. Acta. 1089, 8-12

Newton, G., Yun, C.-H. & Gennis, R.B.(1991) Mol. Microbiol. 5, 2511-2518

O'Malley, P.J. & Babcock, G.T. (1984) J. Chem. Phys. 80, 3912-3913

O'Malley, P.J. & Babcock, G.T. (1986) J. Am. Chem. Soc. 108, 3995-4001

van der Oost, J., Lappalainen, P., Musacchio, A., Warne, A., Lemieux, L., Rumbley, J., Gennis, R.B., Aasa, R., Pascher, T., Malmstrom, B.G., & Saraste, M. (1992) EMBO J. 11, 3209-3217

van der Oost, J., de Boer, A. P.N., de Gier, J.-W.L., Zumft, W.G., Stouthamer, A.H. & Spanning, R.J.M. (1994) FEMS Microbiol. Lett. 121, 1-10

van der Oost, J., Musacchio, A., Pauptit, Ceska, T.A., Wierenga, R.K. & Saraste, M. (1993) J. Mol. Biol. 229, 794-796

Ostermeier, C., Iwata, S. & Michel, H. (1996) Curr. Op. Struct. Biol. 7, 460-466

Poole, R.K & Ingledew, W.J. (1987) *In Escherichia coli* and *Salmonella typhimurium* Cellular and Molecular Biology. (Neirdardt, F.C. ed.) pp. 170-200. American Soc. of Microbiology

Poole, R.K. (1988) *In* Bacterial Energy Transductioin. (Anthony, C., ed.), pp. 231-291. Academic Press

Poole, R.K., Williams, H.D., Downie, J.A. & Gibson, F. (1989) J.Gen.Microbiol. 135, 1865-1874

Puustinen, A., Verkhovsky, M.I, Morgan, J.E., Belevich, N.P. & Wikström, M. (1996) Proc. Natl. Acad. Sci., 93, 1545-1548

Reid, G.A. & Ingledew, W.J. (1980) FEBS Lett. 109, 1-4

Rice, C.W. & Hempfling, W.P. (1978) J. Bacteriol. 134, 115-124

Rich, P.R., (1982) Faraday Discuss. Chem. Soc. 74, 349-364

Rich, P.R. (1996) Pestic. Sci. 47, 287-296

Rigby, S.E.J., Nugent, J.H.A. & O'Malley, P.J. (1994) Biochemistry 33, 1734-1742

Rigby, S.E.J, .Heathcote, P., Evans, M.C.W. & Nugent, J.H.A (1995) Biochemistry 34, 12075-12081

Rigby, S.E.J., Evans, M.C.W. & Heathcote, P. (1996) Biochemistry 35, 6651-6656

Rist, G.H. & Hyde, J.S. (1968) J. Chem. Phys. 49, 2449-2451

Robertson, D.E., Prince, R.C., Bowyer, J.R., Matsuura, K., Dutton, P.L. & Ohnishi, T. (1984) J. Biol. Chem. 259, 1758-1763

Rumbley, J.N. (1995) Ph.D. thesis; University of Illinois at Urbana-Champaign, USA

Saiki, K., Mogi, T. & Anraku, Y. (1992) Biocem. Biophys. Res. Comm. 189, 1491-1497

Saiki, K., Mogi, T., Ogura, K. & Anraku, Y. (1993) J. Biol. Chem. 268, 26041-26045

Saiki, K., Mogi, T., Hori, H., Tsubaki, M. & Anraku, Y. (1993) J. Biol. Chem. 268, 26927-26934

Saiki, K., Nakamura, H., Mogi, T. & Anraku, Y. (1996) J. Biol. Chem. 271, 15336-15340

Sakamoto, K., Miyoshi, H., Takegami, K., Mogi, T., Anraku, Y. & Iwamura, H. (1996) J. Biol. Chem. 271, 29897-29902

Sakamoto, J., Matsumoto, A., Oobuchi, K., Sone, N. (1996) FEMS. Microbiol. Lett. 143, 151-158

Salerno, J.C. & Ingledew, W.J. (1991) Eur. J. Biochem 198, 789-792

Salerno, J.C. & Ohnishi, T. (1980) Biochem. J. 192, 769-781

Salerno, J.C., Osgood, M., Liu, Y., Taylor, H., & Scholes, C.P. (1990) Biochemistry 29, 6987-6883

Samoilova, R.I., Gritsan, N.P., Hoff, A.J., van Liemt, W.B.S., Lugtenburg, J., Spoyalov, A.P. & Tsvetkov, Y.D. (1995) J. Chem. Soc. Perkin Trans. 2, 2063-2068

Samoilova, R.I., van Liemt, W., Steggerda, W.F., Lugtenburg, J., Hoff, A.J., Spoyalov, A.P., Tyryshkin, A.M., Gritzan, N.P. & Tsvetkov, Y.D. (1994) J. Chem. Soc. Perkin Trans 2, 609-614

Saraste, M. (1990) Q. Rev. Biophys. 23, 331-366

Saribas, A.S., Ding, H., Dutton, P.L. & Daldal, F. (1995) Biochemistry 34, 16004-16012

Sato-Watanabe, M., Mogi, T., Miyoshi, H., Iwamura, H., Matsushita, K., Adachi, O. & Anraku, Y. (1994) J. Biol. Chem. 269, 28899-28907

Sato-Watanabe, M., Mogi, T., Ogura, T., Kitagawa, T., Miyoshi, H., Iwamura, H.& Anraku, A. (1994b) J. Biol. Chem. 269, 28908-28912

Sato-Watanabe, M., Itoh, S., Mogi, T., Matsuura, K., Miyoshi, H. & Anraku, Y. (1995) FEBS Lett. 374, 265-269

Seidow, J.N., Power, S., De la Roas, F.F. & Palmer, G. (1978) J. Biol. Chem. 253, 2384-2392

Spinner, F., Cheesman, M.R., Thompson, A.J., Kaysser, T., Gennis, R.B., Peng, Q., & Peterson, J. (1995) Biochem .J. 308, 641-644

Stone, A.J. (1963) Mol. Phys. 6, 509-515

Sturr, M.G., Krulwich, T.A. & Hicks, D.B. (1996) J. Bacteriol. 176, 1742-1749

Sun, J., Osborne, J.P., Kahlow, M.A., Kaysser, T.M., Gennis, R.B. & Loehr, T.M. (1995) Biochemistry 34, 12144-12151

Sun, J., Kahlow, M.A., Kaysser, T.M., Osborne, J.P., Hill, J.J., Rohlfs, R.J., Hille, R., Gennis, R.B. & Loehr, T.M. (1996) Biochemistry 35, 2403-2412

Surpin, M.A., Moshiri, F., Murphy, A.M. & Maier, R.J. (1994) Gene 143, 73-77

Suzuki, H. & King, T.E., (1983) J. Biol. Chem. 258, 352-358

Svensson-Ek, M., Thomas, J.W., Gennis, R.B., Nilsson, T. & Brzezinski, P. (1996) Biochemistry 35, 13673-13680

Tseng, C-P., Albrecht, J. & Gunsalus, R.P. (1996) J. Bacteriol. 178, 1094-1098

Tsubaki, M., Mogi, T., Anraku, Y. & Hori, H. (1993) Biochemistry 32, 6065-6072

Tsubaki, M., Uno, T., Hori, H., Mogi, T., Nishimura, Y. & Anraku, Y. (1993) FEBS Lett. 335, 13-17

Tsukihara, T., Aoyama, H., Yamashita, E., Tomizaki, T., Yamaguchi, H., Shinzawa-Itoh, K., Nakashima, R., Yaono, R. & Yoshikawa, S. (1995) Science 269, 1069-1074

Tsukihara, T., Aoyama, H., Yamashita, E., Tomizaki, T., Yamaguchi, H., Shinzawa-Itoh, K., Nakashima, R., Yaono, R. & Yoshikawa, S. (1996) Science 272, 1136-1144

Unden, G. & Cole, S.T. (1983) FEMS Microbiol. Lett. 20, 181-185

Warnke, K., Gunner, M.R., Braun, B.S., Gu, L., Yu, C.-A., Bruce, M., Dutton, P.L. (1994) Biochemistry, 33, 7831-7841

Weiss, H., Freidrich, T., Hofaus, G. & Preis, D. (1991) Eur. J. Biochem. 197, 563-576

Welter, R., Gu, L.-Q., Yu, C.-A., Rumbley, J. & Gennis, R.B. (1994) J. Biol. Chem. 269, 28834-28838

Westenberg, D.J., Gunsalus, R.P., Ackrell, B.A.C. & Cecchini, G. (1990) J. Biol. Chem. 265, 19560-19567

Westenberg, D.J., Gunsalus, R.P., Ackrell, B.A.C., Sices, H. & Cecchini, G. (1993) J. Biol. Chem. 268, 815-822

Wilmanns, M., Lappalainen, P., Kelly, M., Sauereriksson, E. & Saraste, M. (1995) Proc. Nat. Acad. Sci. 92, 11955-11959

Wittung, P., Källebring, B. & Malmström, B.G. (1994) FEBS Lett. 349, 286-288

Yang, F-D., Yu, L., Yu, C-A., Lorence, R.M. & Gennis, R.B. (1986) J. Biol. Chem. 261, 14987-14990

Yankovskaya, V., Salbin, S.O., Ramsay, R.R., Singer, T.P., Ackrell, B.A.C., Cecchini, G. & Miyoshi, H. (1996) J. Biol. Chem. 271, 21020-21024

Yu, L., Yang, F-D. and Yu, C-A. (1985) J. Biol. Chem. 260, 963-973